The role of the deubiquitinating enzyme USP19 in the regulation of energy homeostasis

Erin Shier Coyne

Department of Biochemistry

Faculty of Medicine

McGill University

Montreal, Quebec, Canada

December 2017

A thesis submitted to McGill University in partial fulfillment of the requirements of the degree of Doctor of Philosophy

Abstract

The regulation of energy homeostasis is vital for the survival of an organism. Any dysregulation in energy storage or mobilization can lead to disease states such as obesity or wasting. At the physiological level, the regulation of energy homeostasis is coordinated by the concerted action of many secreted hormones including insulin and glucocorticoids. At the molecular level, many of these processes are regulated by the ubiquitin system. USP19 is a deubiquitinating enzyme that was first characterized as being upregulated in muscle during muscle wasting. These studies of USP19 in muscle prompted us to study the role of USP19 in the regulation of energy homeostasis. To understand the role of USP19 in these processes, we used a knock-out (KO) mouse model and assessed the loss of function phenotype in a condition of negative energy balance (fasting) and a condition of positive energy balance (high-fat feeding).

In this thesis, we found that USP19 inactivation resulted in mice that were protected from fasting-induced muscle loss as a result of increased rates of protein synthesis. Additionally, we showed that inactivation of USP19 resulted in enhanced insulin sensitivity in the whole organism and increased signaling in the muscle. We also observed that loss of USP19 resulted in decreased gluconeogenesis in the liver. Finally, we found that inactivation of USP19 resulted in decreased glucocorticoid signaling and that the decreased levels of the glucocorticoid receptor in the KO muscle were responsible for the protective effects on muscle atrophy.

To further characterize the role of USP19 in the regulation of energy homeostasis, we studied the role of USP19 in adipose tissue development. We found that the inactivation of USP19 resulted in mice that had significantly less fat mass due to fewer and smaller adipocytes and that cells lacking USP19 showed impaired capacity for adipogenesis. Additionally, when USP19 KO mice were fed a high-fat diet, they gained less weight, were more active, and were protected from the development of diabetes and accumulation of fat in the liver. Finally, we showed that USP19 might also be important for the function of human adipose tissue as USP19 mRNA expression was positively correlated to adipogenic gene expression in human visceral adipose tissue.

Finally, we identified the glucocorticoid receptor (GR) as a target substrate of USP19 that may regulate the above described metabolic processes. We found that GR protein levels were lower in muscle, liver and adipose tissue of USP19 KO mice while mRNA levels were similar. Additionally, GR was more ubiquitinated and more rapidly degraded in USP19 KO cells, and the over expression of USP19 increased the level of GR suggesting that USP19 regulates the protein levels of GR. Taken together, these studies on USP19 in skeletal muscle, adipose tissue, and liver have identified GR as a novel candidate substrate of USP19 and have positioned USP19 as a novel regulator of energy homeostasis through the regulation of insulin and glucocorticoid signaling.

Résumé

La régulation de la balance énergétique est vitale pour la survie de tous les organismes. Tout déséquilibre dans le stockage ou la mobilisation énergétique peut engendrer des maladies comme le diabète ou la dégénérescence musculaire. Au niveau physiologique, la régulation de la balance énergétique est coordonnée par l'action concertée de plusieurs hormones sécrétées telles que l'insuline et les glucocorticoïdes. Au niveau moléculaire, plusieurs de ces processus sont contrôlés par le système de régulation ubiquitine-dépendant. USP19 est une enzyme de déubiquitination qui a été caractérisée en premier lieu comme étant régulée à la hausse dans les muscles en état d'atrophie. Ces résultats nous ont mené à étudier le rôle de USP19 dans la régulation de la balance énergétique. Afin de comprendre le rôle de USP19 dans ces processus, nous avons utilisé un modèle de souris KO (knock-out) pour évaluer le phénotype d'une perte de fonction de USP19 dans des conditions de balance énergétique négative (jeûne alimentaire) ou positive (alimentation riche en gras).

Dans le cadre de cette thèse, nous avons découvert que l'inactivation de USP19 dans les souris a pour conséquence de protéger les muscles de celles-ci contre l'atrophie liée au jeûne alimentaire et ce en augmentant le taux de synthèse protéique dans ces muscles. De plus, nous avons démontré que l'inactivation de USP19 résulte aussi en une augmentation globale de la sensibilité à l'insuline ainsi qu'une augmentation de la signalisation dans les muscles. Nous avons également observé que la perte de fonction de USP19 mène aussi à une diminution de la

néoglucogénèse dans le foie. Finalement, nous avons découvert que l'inactivation de USP19 entraîne une diminution de la signalisation des glucocorticoïdes et que cette réduction dans les niveaux du récepteur des glucocorticoïdes dans les muscles de souris KO est responsable de l'effet protecteur dans une situation d'atrophie musculaire.

Afin de mieux caractériser le rôle de USP19 dans l'homéostasie énergétique, nous avons étudié sa fonction dans le développement du tissu adipeux. Nous avons observé que les souris ayant le gène USP19 inactivé ont significativement moins de masse adipeuse, causé par une diminution du nombre et de la taille des adipocytes. Aussi, des cellules inactivées pour USP19 ont démontré une pertubation au niveau de l'adipogénèse. De plus, lorsque des souris USP19 KO sont nourries avec une alimentation riche en gras, elles accumulent moins de poids corporel, sont plus actives et elles sont protégées contre le développement du diabète et contre une accumulation de gras dans le foie. Finalement, nous avons démontré que USP19 peut également avoir une fonction importante dans le tissue adipeux humain puisque nous avons observé une corrélation de l'expression de l'ARNm de USP19 avec l'expression de gènes adipogéniques dans des tissus de gras viscéral humain.

En conclusion, nous avons identifié le récepteur de glucocorticoïdes (GR) comme étant un substrat cible de USP19 qui pourrait agir dans la régulation des processus métaboliques décrits plus haut. Nous avons découvert que les niveaux protéiques de GR sont diminués dans les muscles, le foie et le tissue adipeux des souris USP19 KO alors que les niveaux d'ARN de GR demeurent

inchangés. De plus, dans les cellules USP19 KO, l'ubiquitination de GR est augmentée et sa dégradation est plus rapide. Par ailleurs, dans des cellules surexprimant USP19, les niveaux protéiques de GR sont augmentés suggérant ainsi que USP19 est capable de moduler les niveaux protéiques de GR. En résumé, ces études sur USP19 dans les muscles squelletiques, le foie et le tissu adipeux ont finalement identifié GR comme un nouveau substrat de USP19 et nous permet de qualifier USP19 comme étant un nouveau régulateur de la balance énergétique via la régulation de la signalisation de l'insuline et des glucocorticoïdes.

Acknowledgements

First, I would like to thank all of the individuals who have supported me throughout my PhD studies. I'm especially thankful to my supervisor, Dr. Simon Wing, for taking me into his lab and training me to become a curious, thoughtful, and independent scientist. He has been an excellent teacher and mentor and his passion for science has been truly inspiring.

I must also thank my Research Advisory Committee members, Dr. Barry I. Posner and Dr. Imed Gallouzi, whose advice and guidance were invaluable to furthering my project and my development as a scientist. Thank you to McGill Faculty of Medicine, Research Institute of McGill University Health Centre, and the Department of Biochemistry for supporting my studies at the PhD level.

Next, I want to thank all of the Wing Lab members, past and present, who have supported me, laughed with me, and cried with me throughout this degree. A special thank you to Nathalie Bédard for teaching me so much and always being available to turn up my transfers, help me find something in the lab and answer my questions. Thank you to Marie Plourde for maintaining the mouse colonies and always making me laugh with your loud sneezes. A special thank you to my lab mates, turned close friends, Nimara Asbah and Rohini Bose without whom grad school would have been very different. Finally thank you to Benjamin Wiles, Ellis Fok, Kai Sheng, SiHan Li, Kate Gong, and the numerous summer students that have come and gone. I will fondly remember our many chocolate therapy sessions.

Similarly, I must acknowledge the fantastic group of people in the Polypeptide Laboratory (PPL). Many thanks to Mary Lapenna and Michel Paré for all their administrative support and guidance over the years. Thank you to the PIs in the PPL - Dr. Posner, Dr. Wing, Dr. Larose, Dr. Laporte and Dr. Rocheleau. The environment of openness, curiosity, and passion for science that you have cultivated in this group is very special. A great big thank you to all of the student members of the PPL. From the weekend trips to the inter-lab competitions, there was never a shortage of laughter and fun. I'm especially grateful for my closest PPL friends - Rohini, Nimara, Kim, Fiona, Icten, Ljiljana, Sahil, George, and (honourary members) Ali and Kat. I couldn't have survived grad school without my PPL family.

Lastly, thank you to my friends and family. A special thank you to my life-long best friend, Jacquie, who is very interested in what I do in the lab and is a constant source of support and motivation. Finally, to my parents, Marina and Michael, and my little sister Meghan, thank you for continuously supporting me through this entire process. Thank you for raising me to be the strong, independent woman that I am today and thank you for always encouraging me to follow my dreams. This is for you.

Preface

This thesis is presented in the traditional format in accordance with the guidelines of Library and Archives Canada. This thesis includes a literature review and introductory chapter, followed by materials and methods, three independent but inter-related results chapters (each with a brief preface and discussion) and finally a general discussion. Although each chapter is written independently of published journal articles, some of the work presented in this thesis has been published or submitted for publication.

Publications arising from work presented in this thesis:

1. **Erin S. Coyne**, Nathalie Bédard, Samer Jammoul, Kezhuo Zhang, Linda Wykes, Robert S. Sladek, Cynthia Stretch, Thomas Jagoe, Barry I. Posner and Simon S. Wing. Inactivation of the USP19 deubiquitinating enzyme prevents muscle wasting by modulating insulin and glucocorticoid signaling. (Chapter 3) *In revision 2017*

2. **Erin S. Coyne**, Nathalie Bédard, Ying Jia Gong, and Simon S. Wing. The deubiquitinating enzyme USP19 modulates adipogenesis and potentiates high fat diet induced obesity. (Chapter 4) *In revision 2017*

3. **Erin S. Coyne**, SiHan Li, Simon S. Wing USP19 regulates the levels of the glucocorticoid receptor. (Chapter 5) *Manuscript in preparation*

4. Phillipe A. Bilodeau*, **Erin S. Coyne*** and Simon S. Wing. The ubiquitin proteasome system in atrophying skeletal muscle: Roles and regulation. 2016 Am J Physiol Cell Physiol 311(3):C392-403 (Chapter 1)

5. **Erin S. Coyne** and Simon S. Wing. The business of deubiquitination - location, location, location. 2016 F100Res Faculty Rev-163 eCollection. (Chapter 1)

Publications arising from other projects:

1. Nathalie Bédard, Samer Jammoul, Tamara Moore, Linda Wykes, Patricia L. Hallauer, Kenneth E. Hastings, Cynthia Stretch, Vickie Baracos, Stephanie Chevalier, Marie Plourde, **Erin Coyne**, Simon S. Wing. Inactivation of the ubiquitin-specific protease 19 deubiquitinating enzyme protects against muscle wasting. 2015 FASEB J 29(9):3998-98.

2. Benjamin Wiles*, Miao Miao*, **Erin Coyne**, Louise Larose, Andrey V. Cybulsky, Simon S. Wing. USP19 deubiquitinating enzyme inhibits muscle cell differentiation by suppressing unfolded protein response signaling. 2015 Mol Biol Cell 26(5):913-23

*Equal Contributors

Contributions of Authors:

Chapter 3:

N.B. performed the initial fasting experiments and electroporation studies (Figures 3.1, 3.2, 3.7) and E.S.C. performed the data analysis. L.W. performed the fractional synthesis rate assays (Figure 3.2 D). S.J., K.Z., R.S.S., and T.J. performed the hypothesis generating microarray analysis. C.S. performed the correlation analysis on human muscle samples (Figure 3.6 C and Table 3.1). Helpful discussions were provided by B.I.P. E.S.C. performed all other experiments and data analysis.

Chapter 4:

Y.J.G. performed the quantification of adipocyte area (Figure 4.1 D). E.S.C performed all other experiments and data analysis with technical assistance from N.B.

Chapter 5:

E.S.C performed and analyzed all experiments described.

Table of Contents

List of Figures

Chapter 1:

Chapter 3:

Chapter 4:

List of Tables

List of Abbreviations

4EBP1	eIF4E binding protein 1
ACTH	adrenocorticotropic hormone
Ang II	angiotensin 2
ANOVA	analysis of variance
ATLG	adipocyte triglyceride lipase
ATP	adensosine triphosphate
BMI	body mass index
BMP	bone morphogenetic protein
BrdU	bromodeoxyuridine
BSA	bovine serum albumin
C/EBP	CCAAT/enhancer binding protein
cAMP	cyclic adenosine monophosphate
cDNA	complementary deoxyribonucleic acid
CHIP	carboxy terminus of Hsp70 interacting protein
CHX	cyclohexamide
cIAP	cellular inhibitor of apoptosis protein
CoA	coenzyme A
COPD	chronic obstructive pulmonary disease
CRH	corticotropin-releasing hormone
CS	CHORD/Sgt1
CSA	cross-sectional area
CTL	control
DAG	diacylglycerol
Ddit4	DNA damage inducible transcript 4
Dex	dexamethasone
DGAT	diacylglycerol acyl transferase
DMEM	Dulbecco's modified Eagle's medium
DNA	deoxyribonucleic acid
DUB	deubiquitinating enzyme
E1	ubiquitin activating enzyme
E2	ubiquitin conjugating enzyme
E3	ubiquitin ligase
EDL	extensor digitorum longus
EGTA	ethylene glycol tetraacetic acid
ER	endoplasmic reticulum
ERAD	endoplasmic reticulum associated degradation
ERK	extracellular signal-regulated kinase
FABP4	fatty acid binding protein 4
FAS	fatty acid synthase
FBPase	fructose 1,6- bisphosphatase
FBS	fetal bovine serum
FKBP51	FK506 binding protein 51

FoxO1	forkhead box protein O1
G6Pase	glucose 6-phosphatase
GC	glucocoriticoids
GLUT1	glucose transporter 1
GPAT3	glycerol-3-phosphate acyl transferase 3
GR	glucocorticoid receptor
GR	glucocorticoid receptor
GRE	glucocorticoid response element
GSK3	glycogen synthase kinase 3
GTT	glucose tolerance test
HDAC	histone deacetylase
HECT	homologous to the E6AP carboxyl terminus
HEK	human embryonic kidney cells
HEPES	4-(2-hydroxyethyl)-1-piperazineethanesulfonic acid
HFD	high fat diet
HOMA	homeostatic model assessment
Hop	Hsc70/Hsp90 organizing protein
HPA	hypothalamic pituitary adrenal
HSL	hormone sensitive lipase
Hsp40	heat shock protein 40
Hsp70	heat shock protein 70
Hsp90	heat shock protein 90
IGF-1	insulin-like growth factor 1
IgG	immunoglobulin G
IKK	IκB kinase
IL-6	interleukin 6
IMCL	intramyocellular lipid
IRS	insulin receptor substrate
ITT	insulin tolerance test
IUCPQ	Institut Universitaire de Cardiologie et de Pneumologie de Quebec
JAMM	Jab1/Mpn/Mov34
kDa	kilo Dalton
KLF	Krüppel-like factor
KO	knock-out
LPL	lipoprotein lipase
Lys	lysine
MAG	monoacyl glycerol
MAPK	mitogen activated protein kinase
MAPS	misfolded associated protein secretion
MARCH6	membrane associated ring-CH-type finger 6
Mg	magnesium
MGL	monoacylglycerol lipase
miRNA	micro ribonucleic acid
MJD	Machado-Joseph Disease
MRI	magnetic resonance imaging
mRNA	messenger ribonucleic acid

mTOR	mammalian target of rapamycin
MuRF-1	muscle ring finger protein 1
MYND	myeloid, nervy and DEAF-1
ND	normal diet
NEFA	non-esterified fatty acid
NEMO	NFκB essential modulator
NF-κB	nuclear factor kappa-light-chain-enhancer of activated B cells
OTU	ovarian tumor
PCNA	proliferating cell nuclear antigen
PDK1	3-phosphoinsositide-dependent protein kinase 1
PEPCK	phosphoenolpyruvate carboxy kinase
PGC1-α	peroxisome proliferator-activated receptor gamma co-activator 1 alpha
PI3K	phosphoinositide 3-kinase
PKB	protein kinase B
polyQ	poly glutamine
PPARγ	peroxisome proliferator-activated receptor gamma
PPI	peptidyl-prolyl isomerase
PTEN	phosphatase and tensin homolog
PTT	pyruvate tolerance test
RBR	RING-between-RING
REDD1	regulated in development and DNA damage response 1
RER	respiratory exchange ratio
RING	really interesting new gene
RIP	receptor interacting protein
RIPA	radioimmunoprecipitation assay
RPS27A	ribosomal protein S27a
S6K	S6 kinase
SCF	Skp, Cullin, F-box containing complex
SDS	sodium dodecyl sulfate
SDS-PAGE	sodium dodecyl sulfate polyacrylamide gel electrophoresis
Sgt1	supressor of G2 allele of skp1
SIAH	seven in absentia homolog
siRNA	small interfering ribonucleic acid
SIRT1	sirtuin 1
SREBP	sterol regulatory element-binding protein
Stat3	signal transducer and activator of transcription 3
STZ	streptozotocin
SUMO	small ubiquitin-like modifier
SVF	stromal vascular fraction
TA	tibialis anterior
TAG	triacylglycerol
TAK	Tat-associated kinase
TBS-T	tris buffered saline tween
TCA	tricarboxylic acid
TGF-β	transforming growth factor beta
TNF-α	tumor necrosis factor alpha

TPR	tetratricopeptide
TWEAK	TNF-related weak inducer of apoptosis
Ub	ubiquitin
UBA1	ubiquitin-like modifier activating enzyme 1
UBA52	ubiquitin A 52
UBA6	ubiquitin-like modifier activating enzyme 6
UBB	ubiquitin B
UBC	ubiquitin C
UBL	ubiquitin-like
UCH	C-terminal hydrolases
UCP1	uncoupling protein 1
UDP	uridine diphosphate
UPR	unfolded protein response
USP	ubiquitin-specific protease
VLDL	very low-density lipoprotein
WT	wildtype

CHAPTER 1

INTRODUCTION

1.1 Energy Homeostasis

The first law of thermodynamics applies to the body as it does to the universe - energy can neither be created nor destroyed, only changed in form. The body is an instrument for taking in chemical energy and converting it into other forms, such as heat or mechanical work. Thus, according to the law of conservation of energy, the amount of energy taken into the system must be equal to the amount of energy expended and stored. Food intake, energy expenditure, and energy storage are homeostatically regulated through a complex, multi-input, multi-organ system that is critical for the prolonged survival of the organism.

1.1.1 Energy Balance

Energy stores are determined by the balance between energy intake and energy expenditure. The components of *energy intake* include the three major macronutrients – carbohydrates, fats, and proteins. Although the majority of the energy in these molecules is absorbed, it is important to note that a proportion of energy intake is lost in the feces and urine due to incomplete absorption. Thus, net energy intake is lower than absolute intake. The components of *energy expenditure* include - resting energy expenditure, energy expenditure associated with digesting and processing foods, and energy expenditure during activity (1).

1.1.2 Major Macronutrients

The three major macronutrients, carbohydrates, fats, and proteins, can be stored in times of excess and mobilized during times of scarcity. These macronutrients will be oxidized or stored depending on the energy demands of the organism. The physiological storage capacity for each nutrient is different, and the majority of energy is stored in the form of fat while only a small proportion is stored as carbohydrate (**Figure 1.1**).

1.1.2.1 Carbohydrates

Carbohydrates are organic compounds consisting of carbon, oxygen and hydrogen atoms. They can be classified into four groups based on the number of carbohydrate monomers they contain. These include the monosaccharides, disaccharides, oligosaccharides, and polysaccharides. Mono and disaccharides are considered simples sugars, oligosaccharides, are covalently linked to other molecules through the process of glycosylation, and polysaccharides serve as carbohydrate storage molecules (e.g., starch and glycogen).

Depending on the diet, carbohydrates often represent a major source of dietary energy, but the storage capacity for carbohydrates is quite small compared to proteins and fats. Human glycogen stores comprise only 500-1000 g for a 70 kg man. Thus, the normal daily intake of carbohydrates is usually 50-100% of the total glycogen stores. This results in a rapid turnover of

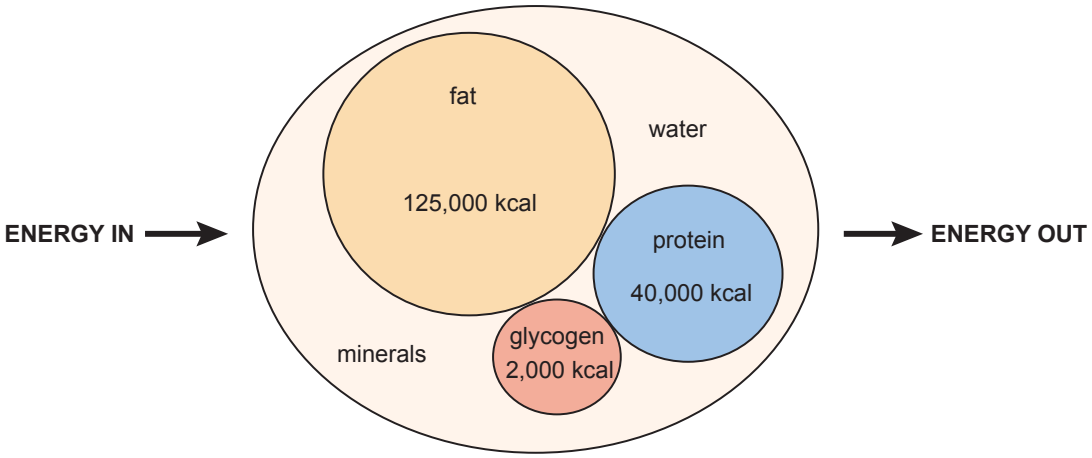

Figure 1.1: Storage of macronutrients

The three macronutrients (carbohydrates, fats and proteins) are stored in the body and mobilized in times of energy deficit. For a 70 kg man, roughly 125, 000 kcal of energy is stored in the form of fat while 40,000 kcal and 2,000 kcal are stored in the form of proteins and carbohydrates respectively.

carbohydrate stores in the body (2). Importantly, the major locations of glycogen storage are in muscle and liver.

1.1.2.2 Fats

Fats are organic compounds that consist of a glycerol molecule with three fatty acids conjugated through ester linkages. Fats are characterized by the number of carbons in the acyl chain, as well as the nature of the bond between carbons. Saturated fats have no double bonds, and thus are saturated with hydrogen molecules, while unsaturated fats have at least one double bond that can be *cis* or *trans* in nature. In addition to fats, other lipid-based molecules exist in the food supply including non-esterified fatty acids, phospholipids, sphingolipids, and cholesterol (3).

Fat is the most energy dense of the major macronutrients as one gram of fat contains 37 kJ (8.8 kcal) of energy, compared to 17 kJ (4 kcal) per gram of protein or carbohydrate. Most of the energy stored in the body is stored in the form of fat even though daily fat intake represents less than 1% of total fat stores (2). Fat storage provides an important energy buffer for the body that can be mobilized in times of scarcity. The main depot for fat storage is in adipocytes which can be found in various locations throughout the body including in the abdominal cavity, under the skin, and within the cells of certain organs (4).

1.1.2.3 Proteins

Amino acids, the building blocks of proteins, are organic compounds with characteristic amine and carboxyl groups along with a side chain R group that is specific to each amino acid. There are roughly 500 naturally occurring amino acids, but only 20 appear in the genetic code. Of those 20 amino acids, 9 are essential meaning that the body cannot synthesize them from other precursors and thus, they must be obtained from dietary sources. Amino acids can be conjugated together by peptide bonds during protein synthesis to generate long polypeptide chains and proteins that have specific functions in the cell.

Generally, about 15-20% of dietary energy comes from protein but protein intake represents less than 1% of total protein stores (2). This makes it difficult for protein stores to grow by increasing dietary protein intake alone. However, protein stores will grow in response to exogenous stimuli, such as hormones and exercise (5,6). The largest depot of protein storage in the body is the skeletal muscle.

1.1.3 Key Tissues for the Storage of Macronutrients

Many tissues in the body are involved in the regulation of energy homeostasis and these tissues respond to the energy requirements of the organism in both the absorptive and post-absorptive states. The brain is the central regulator of these processes as the co-ordinated regulation of food intake and energy expenditure occurs in the hypothalamus (7). The gut is also an important

regulator of energy homeostasis as chemoreceptors and mechanoreceptors in the gastrointestinal tract send signals about food intake to the brain (8). Importantly, there are three key tissues involved in the storage and mobilization of the major macronutrients and those are skeletal muscle, adipose tissue, and liver.

1.1.3.1 Skeletal Muscle

Skeletal muscle comprises nearly half of all body mass and serves as an important tissue for locomotion. It is the largest protein reservoir in the body and is the major site for insulin-stimulated glucose disposal. The functional unit of skeletal muscle is the sarcomere which is composed of thin actin filaments and thick myosin filaments that are interlinked in an anti-parallel fashion and connected through flexible linker proteins such as titin and α-actinin (9). The alternating thick and thin filaments give muscle its characteristic striated pattern. Multiple sarcomeres are linearly connected into myofibrils, and many myofibrils are bundled to compose the myofiber. Importantly, myofibers have different properties depending on the myosin isoform expressed. In rodents, myosin heavy chain has four major isoforms: MHCI, MHCIIa, MHCIIb, MHCIIx giving rise to different fiber types (10,11), while in humans there are only three: MHCI, MHCIIa, MHCIIb (12). Interestingly, the MHCIIb isoform in humans is homologous to MHCIIx and not MHCIIb in rodents (12). Muscles may express only a single fiber type such as in the rat where the EDL and soleus muscles are mainly composed of Type II and Type I fibers, respectively. Most commonly, muscles will be composed of a heterogeneous mix of fiber types (13-15).

Importantly, the metabolic activity of these fiber types is different. Type II fibers are known as fast twitch fibers and are more glycolytic in nature whereas Type I fibers are known as slow twitch and a more oxidative in nature. Fast-twitch, glycolytic fibers have a high level of force production but fatigue rapidly, while slow-twitch, oxidative fibers have a lower level of force production but are resistant to fatigue. In addition to the functional role of muscle in locomotion, skeletal muscle will also store and mobilize carbohydrates, amino acids, and lipids.

1.1.3.1.1 Carbohydrate Storage

Due to the high energy requirements of skeletal muscle contraction, muscle needs an adequate supply of fuel to meet these demands. Skeletal muscle is capable of storing, and then rapidly mobilizing glycogen for these purposes. Type II, fast-twitch fibers, will use glycogen as a primary fuel source, while type I, slow-twitch fibers will preferentially use triglycerides (16-19).

For skeletal muscle to store glycogen, glucose is first taken in from the circulation through the GLUT1 or GLUT4 transporters. GLUT1 is constitutively expressed at the plasma membrane and maintains basal glucose uptake, while GLUT4 is maintained in storage vesicles in the cytosol until insulin stimulation or exercise causes its translocation to the plasma membrane to rapidly increase glucose uptake from the circulation (20). The glucose is then phosphorylated to glucose-6-phosphate by hexokinases to ensure it remains in the cell. Glucose-6-phosphate can feed into metabolic pathways in the cell such as glycolysis and can also be stored as glycogen. Glycogen is a branched chain polymer of glucose that permits its efficient storage. For storage into glycogen

polymers, glucose-6-phosphate is isomerized to glucose-1-phosphate then converted into UDP-glucose. Glycogen is then synthesized by the coordinated action of several enzymes, including the critical enzyme glycogen synthase, using UDP-glucose as a substrate (21). Importantly, prolonged exercise training can promote storage of glycogen in skeletal muscle (22,23).

Glycogen will be broken down into glucose monomers during muscle contractions. This is a process known as glycogenolysis and it takes place in the cytoplasm as well as in lysosomes. Two enzymes are required for the efficient degradation of the glycogen polymer including glycogen phosphorylase and a glycogen debranching enzyme. In the lysosome glycogen break down is accomplished by α-glucosidase (21). Glycogenolysis produces glucose-1-phosphate which must be isomerized into glucose-6-phosphate for use in the cell. Importantly, muscle lacks the enzyme glucose 6-phosphatase, and thus the glucose-6-phosphate that is produced cannot be released into the circulation and must be used in muscle. As with many metabolic processes, the key enzymes involved in glycogen synthesis and degradation are allosterically modulated as well as regulated by hormonal signals (24).

1.1.3.1.2 Muscle Protein

Muscle is the largest reservoir of protein in the body. As such, most of the energy stored as protein is stored in muscle. Skeletal muscle protein turnover occurs naturally at a slow rate as older proteins are degraded while new ones are synthesized. Muscle protein degradation also occurs in conditions of negative energy balance to provide metabolic substrates (amino acids) for

uses in other tissues of the body (25). The maintenance of muscle protein content is a balance between protein degradation and protein synthesis rates. Muscle hypertrophy occurs when the rates of protein synthesis exceed the rates of protein degradation and atrophy occurs when the rates of protein degradation exceed the rates of synthesis.

Muscle protein turnover is regulated by a variety of metabolic stimuli, both anabolic and catabolic in nature (**Figure 1.2**). The key anabolic signals that regulate muscle protein turnover are insulin/insulin-like growth factor 1 (IGF-1), androgens and bone morphogenic proteins (BMPs). Signaling through the Akt-mTOR pathway increases the rates of protein synthesis and allows for muscle growth (26). There are also many catabolic signals that regulate muscle protein turnover by activating the two key proteolytic systems in muscle – the ubiquitin proteasome system and the autophagy-lysosomal system. Many of these catabolic signals activate the FoxO family of transcription factors that serve to upregulate important proteolytic genes. Catabolic mediators of muscle protein turnover include the pro-inflammatory stimuli TNFα, TNF-related weak inducer of apoptosis (TWEAK) and interleukin-6 (IL-6) which act through NF-κB or Stat3 to upregulate important proteolytic genes (27,28). Additionally, steroid hormones such as estradiol and glucocorticoids will act to upregulate proteolytic genes and inhibit the PI3K-Akt-mTOR pathway (29-31). Finally, myostatin, a TGF-β family member, and angiotensin II (AngII) serve to decrease muscle mass through the inhibition of Akt (32-34).

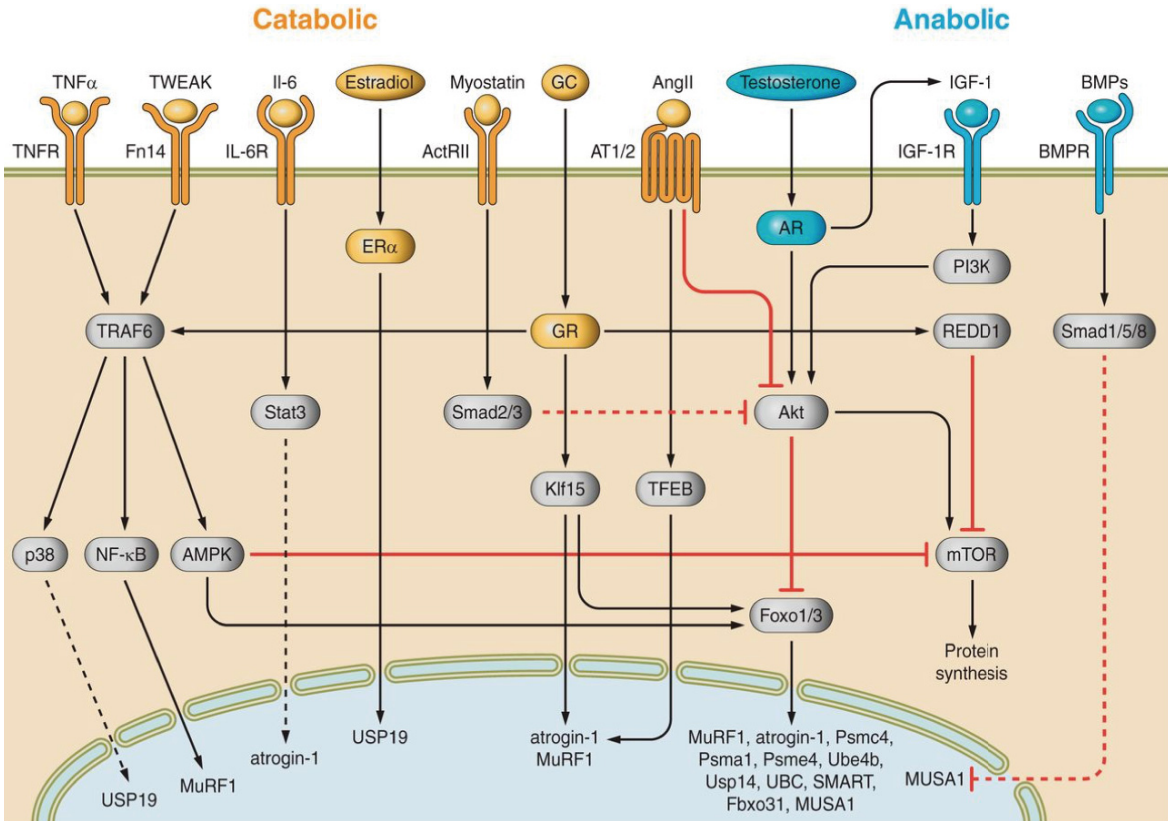

Figure 1.2: Catabolic and anabolic signaling in skeletal muscle

Catabolic and anabolic signals that regulate skeletal muscle protein turnover and activation of ubiquitin proteasome system. Catabolic signals are in orange and anabolic signals are in blue. Dotted lines represent indirect effects through undefined mediators. Many pathways converge on the Akt mTOR pathway. Adapted from Bilodeau, Coyne, and Wing 2016 (35).

1.1.3.1.3 Fat storage

The observation that muscle is also able to store fat was published 50 years ago (36). Intramyocellular lipids (IMCL) can be used as a fuel source for muscle during physical activity but this lipid accumulation can also be pathological as in the case of obesity. High IMCL is associated with the development of insulin resistance but the exact mechanism behind this association is unclear. It is possible that increased IMCL results in increased levels of diacylglycerol which can activate protein kinase C which in turn can block the activity of the insulin receptor (37) or that increased levels of ceramides (derivatives of fatty acids) inhibit insulin signaling (38). Paradoxically, highly trained endurance athletes also have high levels of IMCL with no associated insulin resistance. This repartitioning of lipids into skeletal muscle after exercise likely provides a substrate for energy metabolism rather than contributing to insulin resistance (39,40).

1.3.2 Adipose Tissue

Adipose tissue is an important tissue for the maintenance of energy homeostasis by acting as an energy storage depot, an insulation barrier and by secreting many important hormones called adipokines. Adipose tissue is composed mainly of adipocytes, but other cell types exist within the tissue including fibroblasts, endothelial cells, pre-adipocytes and immune cells (41). The adipocyte is a highly plastic cell capable of rapid expansion as it stores lipids in the form of triacylglycerol (TAG). There are two broad categories of adipose tissue: brown and white. In addition to lipid

storage capabilities, brown adipose tissue is also capable of non-shivering thermogenesis as a result of high mitochondrial content and the tissue-specific expression of uncoupling protein-1 (UCP1) which uncouples oxidative phosphorylation from ATP synthesis generating heat as a by-product (42). White adipose tissue is specialized in the storage and mobilization of lipids to accommodate the energy demands of the organism. In addition to its function as a storage depot, white adipose tissue also serves an important endocrine function to regulate many metabolic processes including energy intake and expenditure as well as insulin sensitivity (43). Importantly, there are different adipose tissue depots in the body that have different metabolic characteristics. Recent reports suggest that abdominal or visceral adipose tissue is highly associated with metabolic dysfunction, while other adipose tissue depots are not (44).

1.1.3.2.1 Adipose Tissue Development

Adipogenesis occurs in both the prenatal and postnatal states, with the bulk of lipid accumulation happening postnatally. Recent lineage tracing studies in mice have shown that different fat depots develop at different times with the gonadal fat developing postnatally, while subcutaneous fat develops during the embryonic period (45). Adipogenesis is the process of differentiation from a pre-adipocyte into a mature, functional adipocyte. The transcriptional regulators of adipogenesis are well characterized. Peroxisome proliferator-activated receptor (PPAR)γ is the master transcriptional regulator of the adipogenic program (46). A deficiency of PPARγ results in the failure to mount the adipogenic program (47) while overexpression is

sufficient to induce adipogenic differentiation (48). Other important transcriptional regulators include CCAAT/enhancer binding proteins (C/EBP), Krüppel Like Factors (KLF) and Sterol regulatory element binding protein (SREBP). C/EBPδ and β are upregulated by glucocorticoids and cAMP and will upregulate the expression of KLF5 and C/EBPα. Insulin will upregulate the expression of SREBP1c, which will activate PPARγ. This transcriptional cascade is induced by hormonal regulators and hinges on the activation of PPARγ and C/EBPα which will drive the expression of genes important for adipocyte function such as fatty acid binding protein 4 (FABP4), adiponectin and leptin, lipoprotein lipase and the lipid droplet protein perilipin to allow for the accumulation of TAG (49) (**Figure 1.3**).

1.1.3.2.2 Triacylglycerol Storage

One of the main functions of the adipose tissue is to act as a storage reservoir for fat. Feeding will stimulate lipogenesis and fat storage while fasting will stimulate lipolysis and the breakdown of the fat for use as an energy source in other tissues (**Figure 1.4**). Lipogenesis can be broken down into *de novo* fatty acid synthesis and triacylglycerol (TAG) synthesis. Under normal conditions, *de novo* fatty acid synthesis occurs mainly in the liver (50-52), however, adipose tissue is also capable of *de novo* lipogenesis or fatty acid synthesis in response to high levels of glucose or other carbohydrates although the majority of the lipid stored in adipose tissue is obtained from dietary fat (53). TAG synthesis begins when TAGs from the circulation arrive at the adipose tissue in chylomicrons and very low-density lipoproteins (VLDL). First, the TAG from the chylomicron

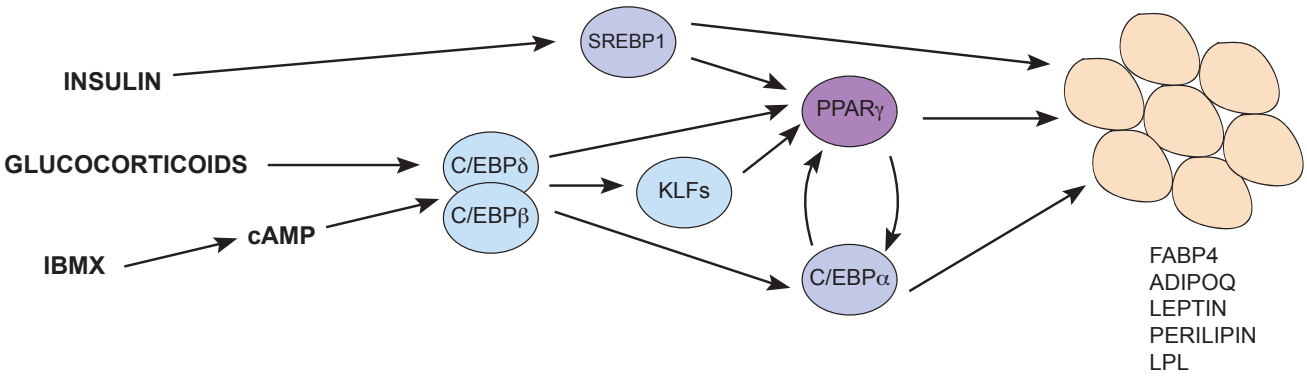

Figure 1.3: Transcriptional regulation of adipogenesis

Adipogenesis is induced *in vitro* by external signals including insulin and glucocorticoids and IBMX which serves to increase the intracellular levels of cAMP. These signals induce the upregulation of transcription factors such as C/EBPβ and C/EBPδ and SREBP1, which in turn induce the expression of additional transcription factors such as KLF family members. This transcriptional cascade drives the upregulation of the transcription factors C/EBPα as well as the master regulator of adipogenesis, PPARγ who exist in a positive feedback loop with one another. Both serve to increase the expression of genes important for the function of the adipocyte such as FABP4, ADIPOQ, LEPTIN, PERILIPIN and LPL.

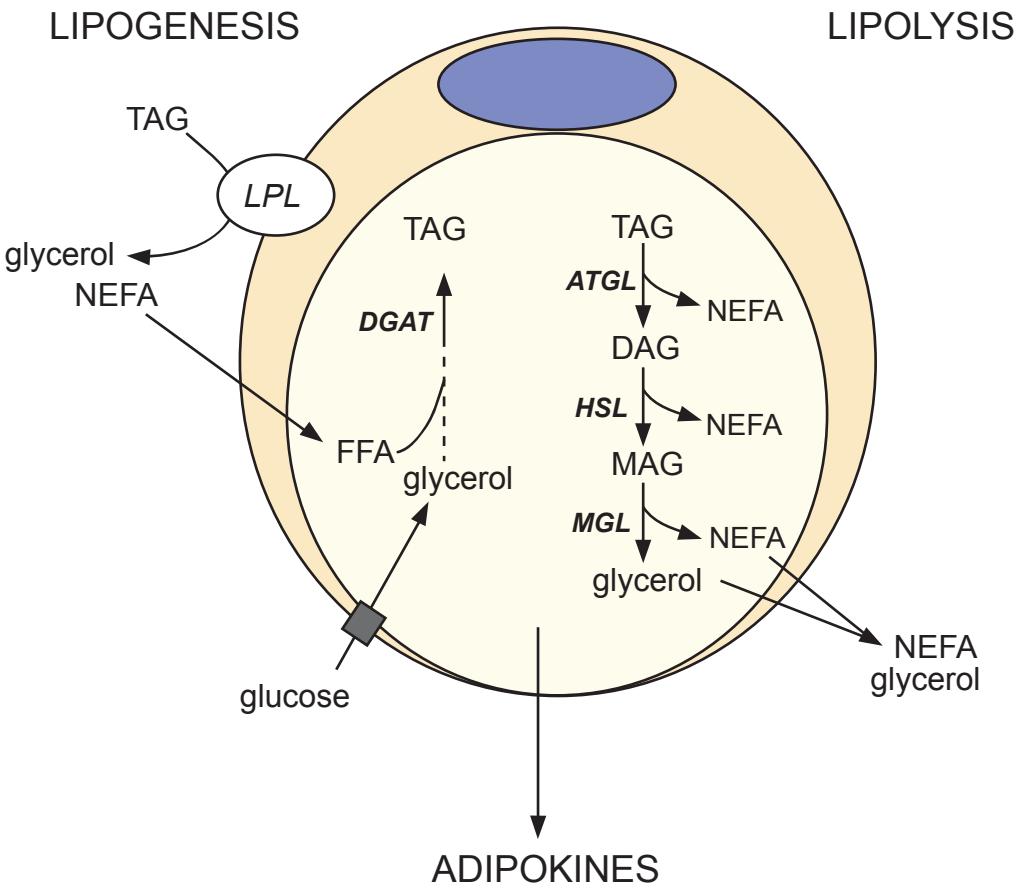

Figure 1.4: Function of the adipocyte

The adipocyte serves to store and mobilize energy in the form of fat. Lipogenesis begins with the hydrolysis of circulating TAG into NEFA which will be taken up by the adipocyte and incorporated into TAG through the sequential action of three acyl transferases including DGAT. Lipolysis occurs in response to lower energy levels and is the hydrolysis of TAG to NEFA and glycerol through the sequential action of three lipases, ATGL, HSL and MGL. Additionally, adipokines, such as adiponectin or leptin, will be secreted from adipocytes to maintain energy homeostasis.

or VLDL must be hydrolyzed into non-esterified fatty acids (NEFA) and glycerol in order to enter the adipocyte. Lipoprotein lipase (LPL), situated on the luminal side of the capillaries in the adipose tissue, is the lipase responsible for this hydrolysis and the efficient entry of the NEFA into the adipocyte (54). The glycerol backbone of the stored TAG does not come from the circulating TAG, rather it is generated as a metabolite from the breakdown of glucose during glycolysis or from glyceroneogenesis in the adipocyte (55). Sequential esterification of the NEFAs to glycerol through the action of the enzymes glycerol-3-phosphate acyltransferase (GPAT), 1-acylglycerol-3-phosphate O-acyltransferase (AGPAT), phosphatidic acid phosphatase (PAP), and diacylglycerol 3-acyltransferase (DGAT), generates the final TAG. The critical enzyme in this process is diacylglycerol acyltransferase (DGAT) which catalyzes the final esterification of NEFA into TAG (56). Importantly, many hormonal signals including insulin stimulate this process.

Lipolysis is a catabolic process that leads to the breakdown of TAG into NEFA and glycerol. This process is induced in low energy conditions such as fasting to mobilize the metabolites for oxidation or use in other tissues (57,58). Lipolysis is the sequential breakdown of TAG into diacylglycerol (DAG), then monoacylglycerol (MAG) and finally glycerol. This is accomplished by three lipases called adipocyte triglyceride lipase (ATGL), hormone-sensitive lipase (HSL) and monoacylglycerol lipase (MGL) (59,60). Lipolysis is inhibited by the hormone insulin and can be stimulated by catecholamines, glucagon, and glucocorticoids.

1.1.3.2.3 Endocrine Function

Adipose tissue secretes a large number of bioactive molecules, collectively known as adipokines, and thus, has a critical endocrine function with the ability to regulate systemic metabolism. The first adipokines that were characterized were leptin (61) and adiponectin (62), both with the ability to regulate energy homeostasis. Leptin does so by acting in the central nervous system to regulate food intake and energy expenditure while also modulating insulin sensitivity in peripheral tissues, while adiponectin promotes systemic insulin sensitivity and also improves glucose metabolism in muscle and liver (63). A large number of adipokines that have been identified to date influence almost every organ system in the body including muscle and liver. Certain adipokines will enhance insulin sensitivity (chimerin, omentin, vaspin, and visfatin) while others will reduce insulin sensitivity (resistin, retinol binding protein 4, TNFα and IL-6) (64).

1.1.3.3 Liver

The liver is an essential metabolic organ and acts as a metabolic hub integrating the metabolism of various tissues including skeletal muscle and adipose tissue. Hepatocytes account for roughly 80% of the cells in the liver and are the cell type in which the majority of metabolic processes occur. In the fed state, macronutrients are digested in the gut, absorbed into the circulation and travel to the liver where they can be stored as glycogen, triacylglycerol, or metabolized and used for protein synthesis. In the fasting state, the main metabolic purpose of the

liver is to increase glucose and metabolite output to maintain normal blood glucose levels and to supply the brain and other tissues with the necessary fuel (65).

1.1.3.3.1 Carbohydrate Metabolism

Glucose is taken up into hepatocytes by the GLUT2 transporter. Glucose will either undergo glycolysis and be oxidized completely or be stored in the form of glycogen. Similar to muscle, glucose is immediately phosphorylated by the specific hexokinase isoform, glucokinase (66). In the post-absorptive state, glycogen is synthesized and stored by the same mechanism as in muscle. The source of the glucose monomers in liver glycogen molecules can come from the diet (direct) or the gluconeogenic production of glucose from pyruvate (indirect) (67). In the fasted state, liver glycogen will go through glycogenolysis to generate glucose monomers. The glucose-6-phosphate that is produced by this process will be dephosphorylated by glucose-6-phosphatase (expressed in the liver and kidney) to generate glucose that can leave the cell and move into the circulation.

In the fasted state, after glycogen stores have been depleted, the liver will turn to gluconeogenesis as a method to produce glucose for output into the circulation. Gluconeogenesis converts pyruvate, lactate, amino acids and glycerol into glucose. These substrates can be generated in the liver, but often they are transported to the liver from other tissues such as skeletal muscle. There are three rate-limiting steps in the process of gluconeogenesis that are regulated by specific enzymes. These steps include the conversion of oxaloacetate to phosphoenolpyruvate by

phosphoenolpyruvate carboxykinase (PEPCK), the conversion of fructose-1,6-bisphosphate to fructose-6-phosphate by fructose 1,6 bisphosphatase (FBPase) and finally, the conversion of glucose-6-phosphate to glucose by glucose 6-phosphatase (G6Pase). Mice with liver-specific KO of Pepck or G6Pase develop hepatic steatosis due to abnormal metabolism of glucose (68,69). Importantly, the flux through gluconeogenesis is regulated by substrate availability as well as the expression levels of the critical enzymes. These enzymes are regulated at the transcriptional level by hormonal signals including insulin and glucocorticoids (70,71).

1.1.3.3.2 Lipid Metabolism

In conditions of excess carbohydrates, the liver will convert glucose into fatty acids through *de novo* lipogenesis. Fatty acid synthesis, catalyzed by fatty acid synthase (FAS), occurs in the cytoplasm using the two-carbon acetyl-CoA as a building block. However, acetyl-CoA is generated in the mitochondrial matrix by the oxidative decarboxylation of pyruvate. Acetyl-CoA cannot readily exit the mitochondrial matrix and so it is reacted with oxaloacetate to generate citrate that can be easily exported. Once in the cytoplasm, citrate is metabolized back into acetyl-CoA and oxaloacetate and fatty acid synthesis can proceed. The remaining oxaloacetate is converted into pyruvate and is imported back into the mitochondrial matrix and the cycle can continue with the generation and export of citrate to generate more cytoplasmic acetyl-CoA for fatty acid synthesis. Cytoplasmic acetyl-CoA will be converted into malonyl-CoA and will be used as the substrate for fatty acid synthesis by fatty acid synthase (FAS). Fatty acids from the

circulation will also travel to the liver where they are used to generate TAG or cholesterol esters for storage or release into the circulation.

In the fasted state, fatty acids will be oxidized as an energy source and will also be used in the formation of ketone bodies. Fatty acid β-oxidation occurs in the mitochondria, in response to low levels of glucose. Fatty acids are sequentially broken down to generate multiple acetyl-CoA molecules that can feed into various metabolic pathways such as the TCA cycle. Other products of fatty acid oxidation are ketone bodies. If acetyl-CoA accumulates in the cell, it will be converted into the ketone bodies acetoacetate, acetone, and D-β-hydroxybutyrate. These ketone bodies are membrane permeable and are therefore used as an energy source by the brain in times of low glucose availability. The brain will convert the ketone bodies back into acetyl-CoA that can then be funneled into other metabolic pathways such as the TCA cycle.

Importantly, all of these processes are regulated by the availability of the substrates and hormones such as insulin and glucocorticoids. In the post-absorptive state, metabolic precursors are abundant and insulin levels are high so *de novo* lipogenesis and TAG synthesis are increased, while the synthesis of ketone bodies is suppressed.

1.1.3.4 Liver, Muscle, Adipose Tissue Cross Talk

The liver is the key player in the co-ordinated regulation of metabolism when it comes to the mobilization of metabolites in the fasted state. Metabolites from muscle and adipose tissues are shuttled to the liver to feed into gluconeogenesis to maintain blood glucose levels (**Figure 1.5**).

In conditions of low energy, metabolites mobilized from muscle include lactate and alanine which are generated from glycolytic pyruvate as well as the breakdown of muscle protein to amino acids. Both alanine and lactate can circulate freely, travel to the liver where they are converted back to pyruvate and feed into the gluconeogenic pathway. These processes of converting pyruvate to lactate or pyruvate to alanine in one tissue and reconverting the metabolite back to pyruvate in another tissue are called the Cori and Cahill cycles, respectively (72,73).

Additionally, in conditions of low energy, the adipose tissue will break down its stored TAG to produce NEFA and glycerol. Glycerol can circulate freely, travel to the liver and act as a gluconeogenic substrate but does not feed into the pathway as pyruvate, but rather further upstream as glyceraldehyde-3-phosphate.

Beyond the shuttling of metabolites between these three organs, hormones secreted from each of these organs can act to regulate the energy metabolism in the other organs. A classic example of this is adiponectin, an adipokine secreted from adipose tissue, which acts on the liver to promote β oxidation and insulin sensitivity (74) and acts on muscle to increase glucose uptake and increase insulin sensitivity (75). Another example is the myokine irisin which is secreted from

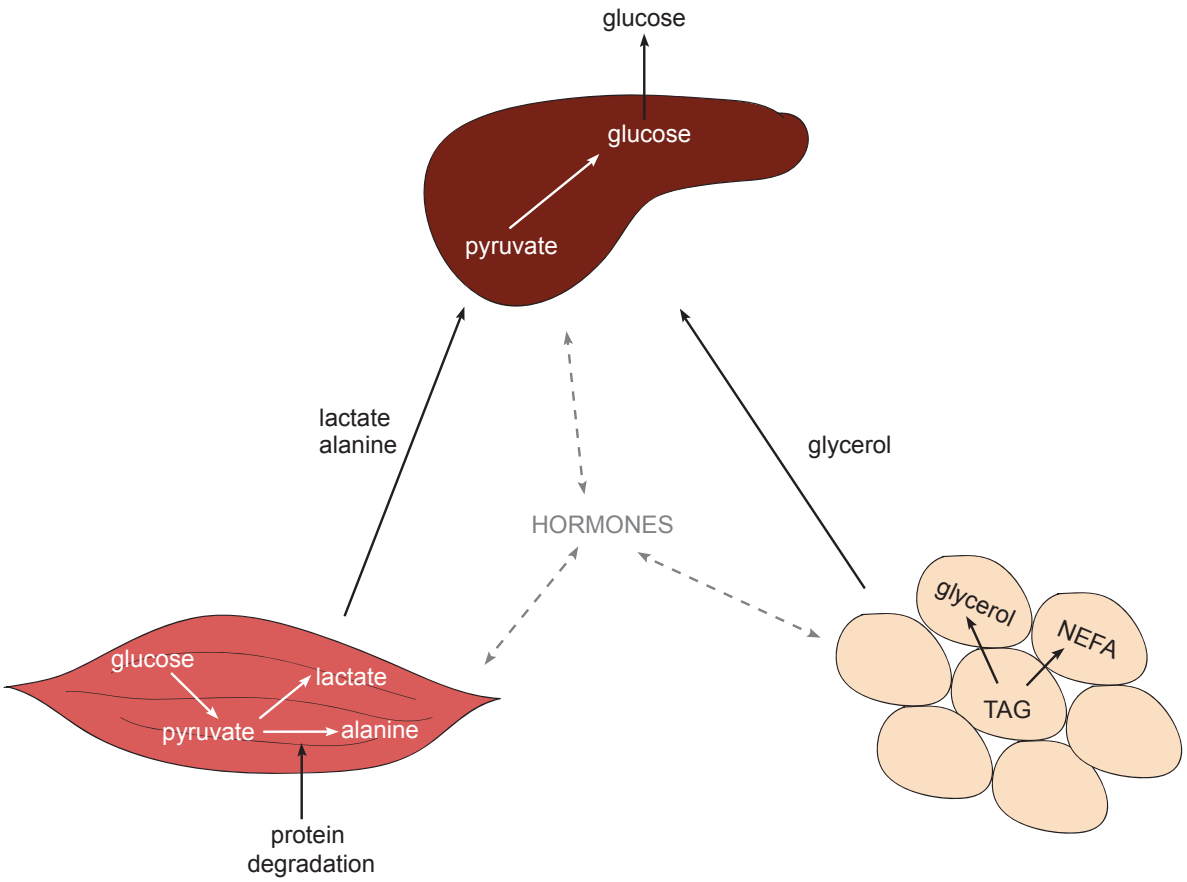

Figure 1.5: Crosstalk between liver, skeletal muscle and adipose tissue

The skeletal muscle and the adipose tissue shuttle metabolites to the liver during periods of energy deficit to provide substrates for gluconeogenesis. In the skeletal muscle, pyruvate is generated as a metabolite of glucose and can be further metabolized to lactate and alanine. Alanine is generated from pyruvate through a transamination reaction, transferring the amino groups from amino acids generated from protein degradation to the pyruvate molecule. In the adipose tissue, TAGs are hydrolyzed to NEFA and glycerol. The glycerol molecule can circulate freely and feed into the gluconeogenic pathway in the liver. Finally, all three tissues are capable of secreting factors that can act on the other tissues to maintain energy homeostasis.

muscle cells and can cause the conversion of white adipose tissue to a more thermogenic beige adipose tissue (76). Finally, circulating liver-derived FGF21 mitigates peripheral insulin resistance and increases brown adipose tissue glucose disposal (77) and the hepatokine LECT2 decreases skeletal muscle insulin sensitivity (78).

1.2 Hormonal Regulation of Energy Homeostasis

The regulation of energy homeostasis is co-ordinately achieved by a variety of hormones that act in both the central nervous system to regulate appetite and energy expenditure, as well as in peripheral tissues to regulate energy storage and mobilization. In the central nervous system, hormones such as insulin, glucagon, leptin, adiponectin, and ghrelin act as energy status signals to regulate appetite and energy expenditure (79-82). In peripheral tissues, hormones such as epinephrine, glucagon, insulin, and glucocorticoids work in concert to regulate blood glucose levels and the storage of macronutrients (83-86). Epinephrine is secreted from the adrenal medulla in response to sympathetic nervous system activation, such as during acute stress or exercise, and will increase plasma glucose levels by increasing hepatic glucose output as well as inhibiting glucose uptake in insulin-dependent tissues. Epinephrine will also increase glycogenolysis in skeletal muscle to increase local glucose availability, and increases in lipolysis in adipose tissue (83,87-89). Glucagon is secreted from the alpha cells of the Islets of Langerhans in the pancreas in response to low plasma glucose levels and high amino acid levels and will increase plasma

glucose levels through increasing levels of glycogenolysis and gluconeogenesis in the liver and increased lipolysis in adipose tissue (90-93). The actions of insulin and glucocorticoids are described in detail below.

1.2.1 Insulin

Insulin is a small peptide hormone that acts as a master regulator of energy metabolism, serves to lower blood glucose, and acts as an anabolic stimulus in muscle, liver and adipose tissue. A deficiency in the production or action of insulin results in abnormally high levels of blood glucose and the development of diabetes mellitus.

1.2.1.1 Biosynthesis

Insulin is produced in response to elevated glucose levels by the β cells of the Islets of Langerhans of the pancreas. Insulin is synthesized from a single mRNA as a single chain preproinsulin peptide, that is subjected to cleavage by a signal peptidase in the endoplasmic reticulum to generate proinsulin (94,95). Proinsulin is then delivered to the trans-Golgi network and cleaved by prohormone convertases followed by processing by carboxypeptidase E to generate mature insulin and C-peptide (96). Mature insulin and C-peptide are packaged into secretory granules and stored in the cytoplasm. When glucose is transported into the β cell by the GLUT2 transporter, it leads to membrane depolarization and a large influx of calcium. This influx of

extracellular calcium is thought to trigger the exocytosis of the insulin secretory granules so that insulin is released into the circulation and can act on peripheral tissues (97).

1.2.1.2 Intracellular Signaling Mechanisms

Insulin acts by binding to the insulin receptor, a receptor tyrosine kinase, to elicit an intracellular signaling cascade that results in the induction of many metabolic programs. The insulin receptor is a tetramer composed of two α and two β subunits linked by disulfide bridges. Upon ligand binding to the extracellular ligand binding domain, there is a conformation change in the intracellular tyrosine kinase domain that activates its tyrosine kinase activity. This allows for auto-phosphorylation of the receptor and the recruitment and phosphorylation of insulin receptor substrate (IRS1 or IRS2) or other phospho-tyrosine binding proteins. IRS1/2 can recruit many downstream effectors, but we will focus only on signaling through the phosphoinositide 3-kinase (PI3K) effector (98). Phosphorylated IRS1/2 will bind PI3K and activate it. Class IA PI3K is a heterodimer composed of a p110 catalytic subunit and a p85 regulatory subunit where the regulatory subunit aids in the activation of the catalytic subunit in the presence of phosphotyrosine residues, but protects the catalytic subunit from degradation and inhibits its activation in quiescent cells (99). Activated PI3K will then convert $PI(4,5)P_2$ to $PI(3,4,5)P_3$ on the membrane. $PI(3,4,5)P_3$ will recruit 3-phosphoinositide-dependent protein kinase1 (PDK1) and activate protein kinase B (PKB or Akt). Akt phosphorylates many (~100) downstream targets by phosphorylation including

FoxO, mTOR and glycogen synthase kinase (GSK3). For the purposes of this thesis, we will only discuss the phosphorylation of FoxO transcription factor and activation of mTOR (**Figure 1.6**).

The FoxO family of transcription factors are important to drive many metabolic processes. The role of FoxO proteins in metabolism and longevity was first characterized in *C. elegans* where DAF16 (the FoxO ortholog in the worm) transduces signals by insulin-like peptides (100,101). Phosphorylation of FoxO proteins by insulin signaling prevents it from translocating to the nucleus. When insulin levels are low, FoxO is not phosphorylated and can translocate to the nucleus to drive the transcription of its target genes which include gluconeogenic enzymes in the liver and proteolytic genes in muscle (102-105). This positions FoxO as an important regulator of metabolism and is especially relevant in muscle as the balance between muscle protein degradation and synthesis is crucial to the maintenance of muscle mass.

mTOR is a conserved serine/threonine kinase that forms two distinct complexes in cells. mTORC1 is composed of mTOR, Raptor, AKTS1, and mLST8 and is involved in the regulation of cell growth and metabolism while mTORC2 is composed of mTOR, Rictor, Sin1 and mLST1 and is involved in cell survival and cytoskeletal processes (106). The major substrates of mTORC1 are eIF4e binding protein (4EBP1) and p70 ribosomal protein S6 kinase (S6K). Activation of the pathway by insulin will allow for mTORC1 to phosphorylate both of these targets resulting in the initiation of protein translation. Thus, mTORC1 activation results in increased protein synthesis and cell growth.

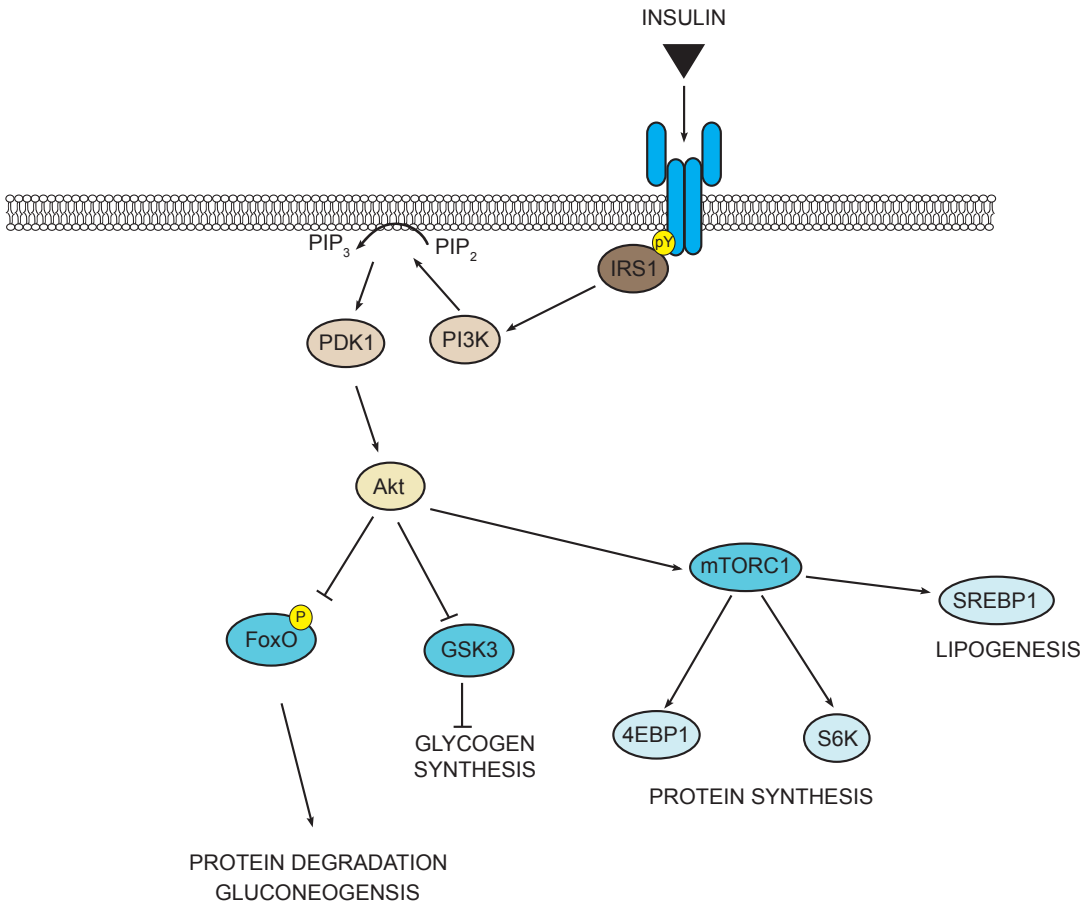

Figure 1.6: Insulin signaling in metabolism

Binding of insulin to the insulin receptor (IR) induces activation of the receptor due to conformational changes that trigger autophosphorylation on tyrosine residues. Activated IR recruits IRS proteins to serve as docking sites for effectors. Interaction of PI3K with IRS proteins leads to its activation and the generation of PIP3 from PIP2. PIP3 recruits PDK1 and Akt to the plasma membrane which results in PDK1 mediated phosphorylation and activation of Akt. Akt will go on to phosphorylate many effector proteins. Phosphorylation of mTORC1 by Akt leads to the phosphorylation of 4EBP1 and S6K, which allows for the initiation of protein synthesis while phosphorylation of SREBP1 will induce lipogenesis in the liver and the adipose tissue. Akt phosphorylation will inhibit the activities of FoxO3 and GSK-3, thereby reducing protein degradation and gluconeogenesis and increasing glycogen synthesis.

Insulin signaling through PI3K is a cascade of phosphorylation events. Thus, much of the pathway is negatively regulated by the action of phosphatases. One of the major negative regulators of this pathway is phosphatase and tensin homolog (PTEN). PTEN dephosphorylates $PI(3,4,5)P_3$ to generate $PI(4,5)P_2$. Expression of PTEN in transgenic mice shows many protective metabolic effects including decreased adiposity and increased insulin sensitivity (107). In addition to negative regulation by dephosphorylation, ubiquitination also serves to regulate this pathway through the ubiquitination and proteolytic degradation of specific targets. There are many ubiquitin ligases that target IRS1/2 for degradation including MG53, Cbl-b, SOCS1/3, and SCF Fbox40, which results in decreased signaling through the pathway (108-113).

1.2.1.3 Target Tissues and Effects

As a master regulator of energy homeostasis insulin acts on muscle, adipose tissue and liver to decrease blood glucose levels and increase the storage of the major macronutrients. It does so by acting through the insulin receptor to activate a variety of downstream effectors that elicit a specific response in each tissue (**Figure 1.7**).

1.2.1.3.1 Insulin Action in Muscle

In skeletal muscle, insulin action increases glucose uptake, glycogen storage, and protein synthesis. Insulin mediates glucose uptake in muscle by increasing the translocation of the GLUT4 glucose transporter to the plasma membrane (114). This influx of glucose into the cell increases the rates of glycolysis. Additionally, insulin increases the activity of glycogen synthase and inhibits

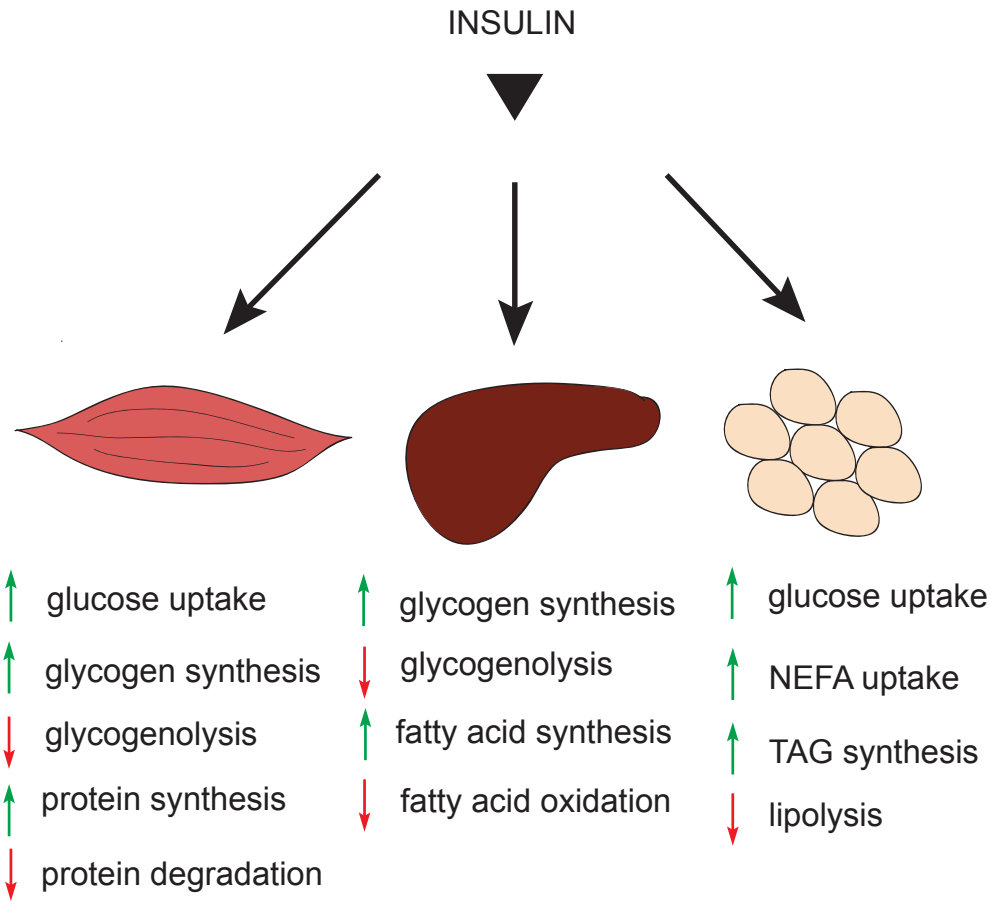

Figure 1.7: Insulin action in tissues

The anabolic hormone insulin will exert effects in the skeletal muscle, liver and adipose tissue to elicit a variety of metabolic responses. In the muscle, insulin will increase glucose uptake and glycogen synthesis as well as decrease glycogenolysis. Additionally, insulin will increase protein synthesis, while preventing protein degradation. In the liver, insulin will increase glycogen synthesis and decrease glycogenolysis and gluconeogenesis as well as increase fatty acid synthesis while decreasing fatty acid oxidation. In the adipose tissue, insulin will increase glucose and NEFA uptake in the adipocytes as well as increase triacylglycerol synthesis while inhibiting lipolysis.

glycogen phosphorylase through the action of glycogen synthase kinase (GSK-3) and protein phosphatase 1 (PP1) (115-117).

In addition to effects on carbohydrate metabolism, insulin is also a potent stimulator of protein anabolism. Insulin signaling activates mTOR and the initiation of protein synthesis via 4EBP1 and S6K. Activation of insulin signaling also inhibits FoxO activity and thus decreases protein catabolism.

1.2.1.3.2 Insulin Action in Adipose Tissue

In the adipose tissue, insulin acts to promote glucose and fatty acid uptake, esterification of fatty acids into triacylglycerol (TAG) as well as inhibit lipolysis. Similar to muscle, adipocytes express the GLUT4 transporter. In response to insulin, GLUT4 is translocated to the plasma membrane to increase glucose uptake. Glucose can then be metabolized and glycerol will be formed as an important precursor for TAG synthesis. Insulin also promotes the uptake of non-esterified fatty acids into the adipocyte and synthesis of TAG through multiple mechanisms including increasing the activity of lipoprotein lipase, fatty acid transport proteins and the upregulation of genes important in TAG synthesis (118-120). Insulin also acts to decrease lipolysis by inhibiting the activity hormone-sensitive lipase (HSL) through the activation of protein kinase A as well as decreasing the levels of adipose triglyceride lipase (ATGL) (120).

1.2.1.3.3 Insulin Action in Liver

In the liver insulin serves to stimulate glycogen synthesis and lipogenesis while suppressing gluconeogenesis. Similarly, as in muscle, insulin stimulates glycogen storage by increasing the activation of glycogen synthase. Insulin also increases the expression of glucokinase which stimulates glucose uptake into the liver, as free glucose is immediately converted to glucose-6-phosphate (66). In the fed state, insulin stimulates hepatic lipogenesis through mTORC1 dependent activation of SREBP1, a critical transcription factor for lipogenesis (121,122). Importantly, insulin potently suppresses hepatic gluconeogenesis through the Akt mediated phosphorylation of the transcription factors FoxO1 and PGC-1α, thereby inhibiting the upregulation of Pepck and G6Pase (123-125). Given the clear role of insulin in hepatic metabolism, it is unsurprising that the development of insulin resistance in the liver leads to pathological conditions such as diabetes and non-alcoholic fatty liver disease.

1.2.2 Glucocorticoids

Glucocorticoids are steroid hormones derived from cholesterol that play an essential role in organismal adaptation to stress. There are both natural glucocorticoids, produced in the body (cortisol in humans and corticosterone in rodents), as well as many synthetic glucocorticoids used in medicine (dexamethasone, prednisone, budesonide, etc.). Synthetic glucocorticoids are much

more potent and often more bioavailable than natural glucocorticoids (126). In the clinic, glucocorticoids are often prescribed for chronic inflammatory conditions and immunosuppression but may also have undesired effects on the regulation of metabolism.

1.2.2.1 Biosynthesis

Glucocorticoid (GC) production is under the tightly controlled regulation of the hypothalamic-pituitary-adrenal (HPA) axis in a circadian and ultradian fashion. GC secretion peaks in anticipation of increasing activity levels (morning for humans) but GCs will also be produced in response to various stress stimuli (127). The secretion of glucocorticoids from the zona fasciculata of the adrenal gland is stimulated by a cascade of hormonal signals originating from the hypothalamus. First, corticotropin-releasing hormone (CRH) is secreted by the hypothalamus to stimulate the production of adrenocorticotropic hormone (ACTH) from the pituitary gland and this ACTH can then act on the adrenal cortex to stimulate the production and release of GC to the bloodstream. GCs in the circulation will act in a negative feedback loop on the hypothalamus and pituitary to decrease the production of CRH and ACTH, thereby stopping the production of GCs from the adrenal gland (128). The local availability of natural glucocorticoids is regulated by Type 2 11-β-hydroxysteroid dehydrogenase which acts to convert active cortisol to the inactive cortisone. The reverse reaction is catalyzed by Type 1 11-β-

hydroxysteroid dehydrogenase. Thus, the regulation of these enzymes has profound effects on the activity of GCs in cells (129).

1.2.2.2 Intracellular Signaling Mechanisms

Glucocorticoids act through the glucocorticoid receptor (GR) (**Figure 1.8**). GR is a nuclear hormone receptor that contains a central DNA-binding domain, an N-terminal transactivation domain, and a C-terminal ligand binding domain. Importantly, the DNA-binding domain and the ligand binding domain contain nuclear localization signals that allow import to the nucleus through an importin-dependent mechanism (130). The DNA-binding domain of GR recognizes and specifically binds glucocorticoid response elements (GRE) on target genes. GREs are short imperfect palindromic sequences of six base pairs long, separated by any three base pairs. There is variation in the sequence which allows for variation of GR transcriptional activity (131).

The canonical effect of GCs is through their regulation of transcription. When ligand binds to GR, it translocates to the nucleus and homodimerizes. There, it can bind to positive GREs or negative GREs to activate or repress transcription (131,132). A negative GRE is an inverted palindromic sequence that upon GR binding will recruit transcriptional repressors such as NCOR and SMRT which will then recruit HDACs to further suppress transcription (133). GR binding to the negative GRE will also prevent its dimerization which may explain the differential effects on transcription (134). GR can also bind indirectly to the DNA via interaction with other proteins and

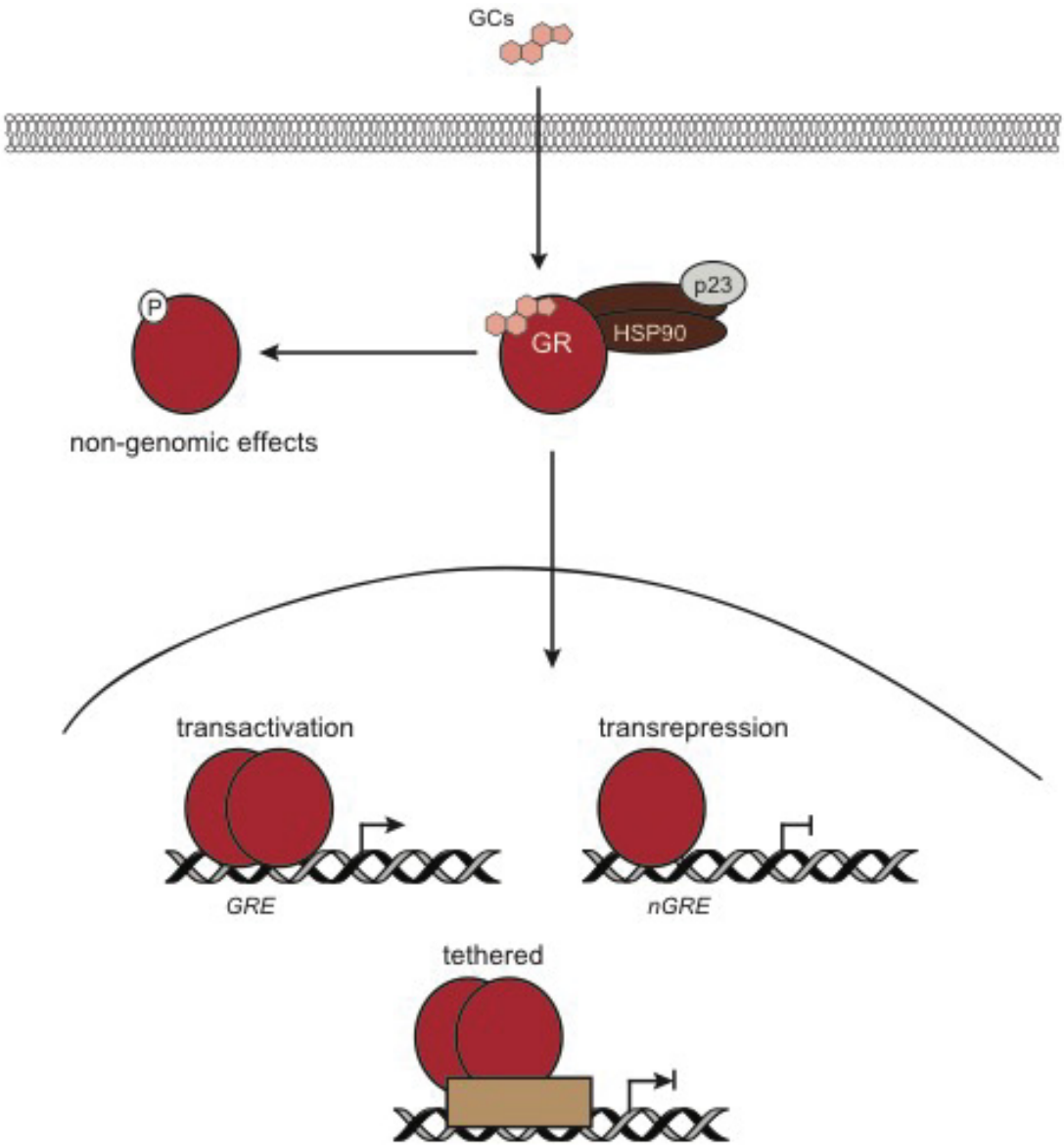

Figure 1.8: Glucocorticoid signaling

Glucocorticoids enter the cell and bind to the glucocorticoid receptor in the cytoplasm. The glucocorticoid receptor is maintained in the cytoplasm in association with molecular chaperones HSP90, HSP70 and co-chaperones such as p23. Upon ligand binding to the receptor, it dissociates from its chaperones, dimerizes, and is transported to the nucleus where it can activate or repress gene transcription. Ligand bound GR can also be phosphorylated to exert effects that are still not well understood. Transactivation – increasing gene expression. Transrepression – repressing gene expression. Tethered – indirect association with DNA through the interaction of other DNA binding proteins to either transactivate or repress gene expression.

can activate or repress transcription. A classic example of this is the interaction between GR and NF-kB (135), where NF-kB binds the DNA and associates with GR to inhibit transcription. The target genes of GR will go on to elicit many cellular responses including anti-inflammatory effects and important metabolic processes.

There are also non-genomic effects of GCs, whereby they exert an immediate effect (within minutes) on the cellular environment. The exact mechanisms of non-genomic GC actions are still poorly understood. They could be explained by the one or more of following: cytoplasmic GR can interact with and alter other cellular signaling pathways, GCs can bind to a membrane-bound GR to exert a non-genomic effect or GCs can intercalate and alter the plasma membrane (136).

In the absence of ligand, the glucocorticoid receptor (GR) is maintained in the cytosol by the chaperones Hsp70 and Hsp90. This ATP-dependent system regulates the folding, ligand binding and turnover of GR and thus is very important for its function as evidenced by studies where the inhibition of Hsp90 causes rapid degradation of GR (137). The important players in the Hsp70/Hsp90-GR chaperone complex include the co-chaperones Hsp40, Hop, p23, and FKBP51. A partially folded GR ligand binding domain will associate with the Hsp70/Hsp40 complex and will be transferred to Hsp90 via interaction of both chaperones with the TPR-domain containing protein Hsc70/Hsp90-organizing protein (Hop). ATP will then bind to the ATP binding pocket in the N-terminal domain of Hsp90 and will proceed through the ATPase cycle of Hsp90. This cycle

also requires the binding of a peptidylprolyl isomerase protein such as FKBP51 as well as the co-chaperone p23, for efficient maturation and the generation of a ligand-binding competent GR. Importantly, a ubiquitin ligase, CHIP that interacts with the Hsp70/Hsp90-GR complex can ubiquitinate and cause the rapid degradation of GR (138).

GR is also regulated by many post-translational modifications including acetylation, phosphorylation, ubiquitination, and SUMOylation. GR can be phosphorylated on several serine residues by various kinases including MAPK and glycogen-synthase kinase-3. The majority of these phosphorylation events occur in a hormone-dependent manner, but can also occur independent of ligand binding (139). The phosphorylation of GR changes its transcriptional activity with some phosphorylation events promoting activity, and others inhibiting it (140,141). GR can also be acetylated on various lysine residues potentially through the action of HDAC2 and this acetylation results in the inability of GR to impair NF-κB signaling (142). Finally, GR can be ubiquitinated and SUMOylated. Lys426 of GR can be ubiquitinated and this causes the rapid proteasomal degradation of GR (143,144). SUMOylation of GR at Lys277, Lys293 or Lys703 also promotes its degradation (145,146).

1.2.2.3 Target Tissues and Effects

Glucocorticoids are recognized as an essential part of the organismal response to stress and serve to rapidly increase blood glucose levels to supply large muscles with the necessary fuel during the acute stress response (colloquially known as the fight or flight response).

Glucocorticoids also have anti-inflammatory properties, but for the purpose of this thesis, we will focus on the metabolic action of glucocorticoids, of which there are many (**Figure 1.9**). The main metabolic function of glucocorticoids is to increase blood glucose levels and this is accomplished through the mobilization of stored macronutrients in muscle, liver, and adipose tissue.

1.2.2.3.1 Glucocorticoid Action in Muscle

Elevated levels of glucocorticoids will act in muscle to increase protein degradation and decrease protein synthesis rates as well as decrease glucose uptake and glycogen synthesis. The glucocorticoid receptor (GR) directly and indirectly activates genes involved in muscle catabolism including the FoxO family of transcription factors and the ubiquitin ligases responsible for the breakdown of the sarcomere such as MuRF1 and atrogin-1 (31,147). Beyond its ability to directly upregulate genes required for protein breakdown, GR also has anti-anabolic functions. GR upregulates genes that can inhibit the insulin/IGF-1 signaling pathways including the regulatory subunit of PI3K (p85α), Ddit4 (REDD1) which will inhibit mTOR and the transcription factor Klf15 which indirectly inhibits mTOR and will also upregulate FoxO and MuRF1 (31,148). Under fed conditions, when insulin levels are high, the actions of glucocorticoids are blunted as the anabolic pathway dominates but upon fasting, when insulin levels are low and glucocorticoids are in excess glucocorticoids will act to increase proteolysis of muscle protein. As a result of glucocorticoid action in muscle, amino acids are mobilized and will travel to the liver to be converted into pyruvate and used in gluconeogenesis to ultimately increase blood glucose levels.

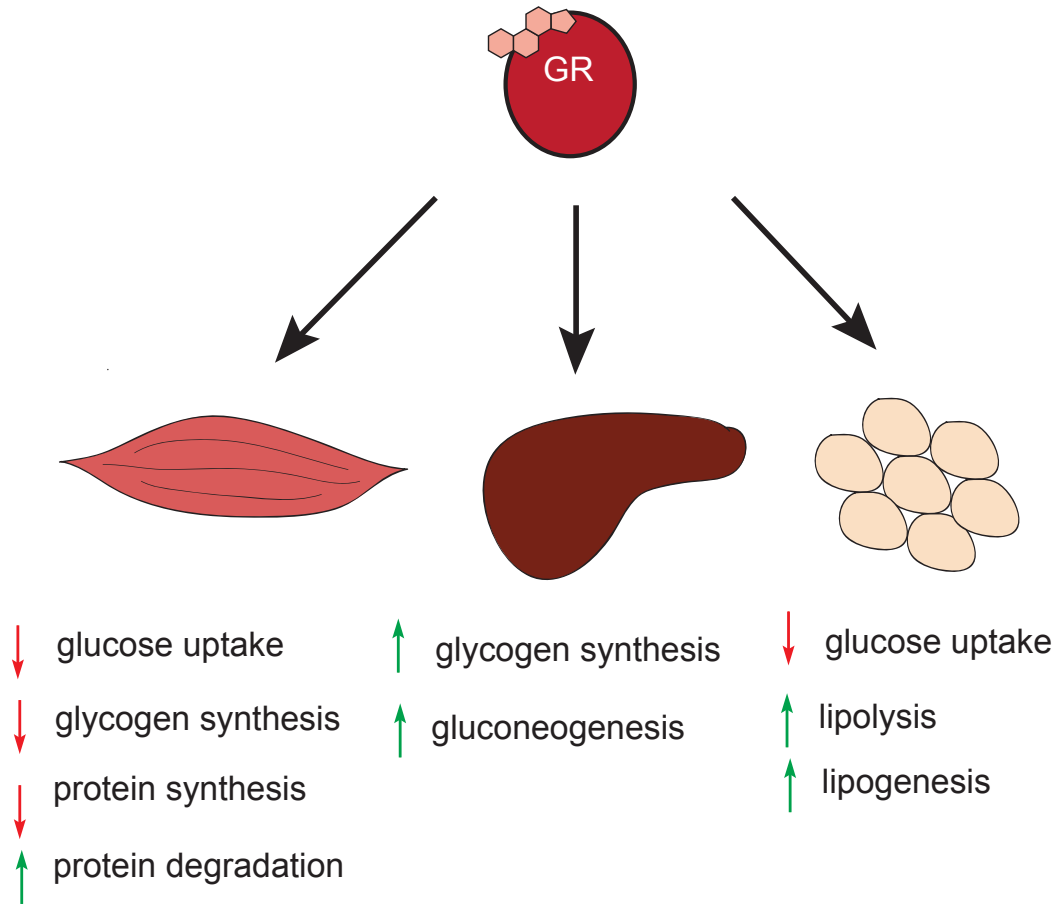

Figure 1.9: Glucocorticoid action in tissues

Glucocorticoids are catabolic hormones that exert effects in the skeletal muscle, liver and adipose tissue to elicit a variety of metabolic responses. In the muscle, glucocorticoids will decrease glucose uptake and glycogen synthesis as well as decrease protein synthesis, while increasing protein degradation. In the liver, glucocorticoids will increase glycogen synthesis and gluconeogenesis. In the adipose tissue, glucocorticoids will decrease glucose uptake as well as increase lipolysis.

1.2.2.3.2 Glucocorticoid Action in Adipose Tissue

In adipose tissue, glucocorticoids have pro-adipogenic and pro-lipolytic functions. GCs will upregulate genes important for adipogenesis including CEBPs, and PPARγ (149,150). Dexamethasone is an important component of the *in vitro* induction cocktail (insulin, dexamethasone, and 3-isobutyl-1methylxanthine) to induce the adipogenic transcriptional cascade and development of mature adipocytes in culture (149,151). GCs will also promote adipose tissue lipolysis as they increase the expression of all three enzymes (ATLG, HSL, and MGL) responsible for the hydrolysis of triacylglycerol (TAG) into non-esterified fatty acids and glycerol (152-154). This is through the direct transcriptional action of GR on the promoters of these genes or through GR upregulation of FoxO family transcription factors (155). GCs also have an effect on adipose tissue lipogenesis, and can increase both *de novo* lipogenesis and TAG synthesis but must act with insulin to do so. They either have a permissive effect on insulin action or enhance the effect of insulin but the mechanisms are still unclear (156-158). It seems counterproductive for a hormone to increase adipogenesis and lipogenesis, while at the same time increasing lipolysis. This inconsistency may be due to the different behaviours of GCs in different adipose tissue depots. GC effects in abdominal depots are more adipogenic in nature, while in peripheral depots they are more lipolytic (159,160).

1.2.2.3.3 Glucocorticoid Action in Liver

Glucocorticoids were first characterized due to their ability to increase blood glucose levels and much of this action occurs in the liver. Glucocorticoid activation of GR increases the expression of gluconeogenic enzymes such as Pepck and G6Pase (161) and the inactivation of GR in hepatocytes, causes fasting hypoglycemia and protection from streptozotocin-induced and obesity-related diabetes (71,162). Glucocorticoids also induce glycogen synthesis in the liver by activating glycogen synthase (163-165). Interestingly, GCs enhance the anabolic effects of insulin on lipogenesis in the liver as they do in the adipose tissue (166).

1.3 Dysfunctional Energy Homeostasis

There are many pathologies associated with dysfunctional energy homeostasis. In this section, the focus will be on two conditions, muscle atrophy and obesity, which are conditions of negative energy balance and positive energy balance, respectively.

1.3.1 Muscle Atrophy

Skeletal muscle is the largest protein reservoir in the body. In times of stress and low energy, catabolic programs are activated and the protein in muscle is degraded to provide amino acid precursors for energy production in other organs such as gluconeogenesis in the liver. Muscle

wasting is associated with many chronic conditions and this wasting significantly reduces patient quality of life and is an independent risk factor for mortality (167-169).

1.3.1.1 Causes

Muscle atrophy occurs in conditions of inactivity (e.g. cast immobilization or bed rest) or denervation (e.g. spinal cord injuries) as well as a systemic response to fasting and diseases such as renal failure, excessive glucocorticoids, and certain cancers as well as during aging (170). No matter the initiating event, muscle atrophy results in a loss of muscle protein content, reduced fiber size, decreased resistance to fatigue and decreased force production (171).

1.3.1.2 Pathophysiology and Mechanisms

The maintenance of muscle mass is a balance between protein degradation and protein synthesis. When that balance is dysregulated, muscles will grow larger (hypertrophy) or become smaller (atrophy). During atrophying conditions, muscle protein synthesis is decreased (172) and muscle proteolysis is increased (173-176). This results in the disassembly of the myofibrils that comprise the functional contractile units of muscle. The net result of this is smaller muscle fibers and a reduction in muscle mass and strength. The mechanisms regulating these processes will be expanded upon in the following sections.

1.3.1.2.1 Protein Synthesis

Anabolic pathways regulate the levels of protein synthesis in muscle. Insulin/IGF-1 stimulated Akt-mTOR signaling is one of the major pathways involved in muscle growth by activating mTOR and inhibiting the action of FoxO transcription factors. Under certain conditions, mTOR can also suppress autophagy and the ubiquitin proteasome system – the major proteolytic pathways involved in muscle atrophy (31,177,178). During atrophying conditions such as fasting, decreased insulin/IGF-1 signaling results in decreased muscle mass as a result of decreased protein synthesis and increased activation of FoxO. Overproduction of IGF-1 or Akt is able to protect mice from muscle loss (179,180).

1.3.1.2.2 Protein Degradation

In order for the protein in muscle to be degraded, the myofibril must be disassembled. In atrophying conditions both the ubiquitin proteasome and autophagy-lysosomal systems are activated to allow for this myofibrillar disassembly and protein breakdown. The many genes that are regulated during muscle atrophy are termed atrogenes (181), of which are many components of the ubiquitin proteasome system. Multiple ubiquitin ligases are upregulated during atrophying conditions including the well characterized ligases MuRF1 and Atrogin-1. The inactivation of either of these ligases results in the protection from muscle wasting although their molecular substrates are not the same (182,183). These ligases are upregulated by a variety of catabolic stimuli that increase the levels of FoxO transcription factors or upregulate the ligases directly. The

activation of autophagy is also important in muscle atrophy, especially in response to nutrient deprivation.

1.3.1.2.3 Signaling

Many signaling pathways, both anabolic and catabolic, are coordinately regulated to modulate muscle atrophy. For the purposes of this thesis, we will only discuss the anabolic insulin/IGF-1 pathway and the catabolic glucocorticoid signaling pathway and how they interact in order to modulate muscle wasting. As described above, insulin/IGF-1 signaling serves to increase protein synthesis as well decrease protein degradation. Many catabolic pathways, including glucocorticoid signaling, converge on the insulin/IGF-1 signaling pathway to negatively regulate it. Glucocorticoid target genes such as Ddit4 (REDD1) and Klf115 both serve to inhibit mTOR through different mechanisms (31). REDD1 acts by sequestering 14-3-3 proteins thereby increasing the activity of TSC1/2 that act to inhibit mTOR (184,185) . Klf15 is a transcription factor that increases the expression of branched-chain aminotransferase 2 (BCAT2) which causes the degradation of branched chain amino acids and results in the negative regulation of mTOR (31). Klf15 also increases the expression of FoxO transcription factors, atrogin-1, and MuRF-1 ligases. Additionally, the GR target gene Pi3kr1 (p85α) is the regulatory subunit of PI3K which, when expressed at high levels, acts as a dominant negative thereby inhibiting PI3K activity and decreasing Akt activation (148,186). Another target gene of glucocorticoid signaling is Cbl-b, a ubiquitin ligase that ubiquitinates IRS-1 which results in decreased insulin/IGF-1 signaling

(148,187). All of these targets of glucocorticoid signaling serve to negatively regulation insulin/IGF-1 signaling, thereby decreasing protein synthesis and increasing protein degradation (**Figure 1.10**).

1.3.1.3 Clinical Outlooks

Currently, there are no approved pharmaceuticals to specifically treat muscle wasting. Clinical trials with selective androgen receptor modulator enobosarm showed improvement in muscle mass with limited improvement in muscle function (188). Additionally, clinical trials with ghrelin agonists, such as anamorelin, resulted in increased quality of life score and muscle mass, but not muscle function (189). The only clinical intervention that shows improvement in both muscle mass and function is exercise (190,191). Exercise as an intervention becomes challenging in populations that have muscle wasting because they are often bed-ridden, critically ill or on chemotherapy. Thus, there is a pressing need to develop novel therapies for patients with muscle wasting.

Current research aims to understand the factors that mediate the maintenance of muscle mass during exercise. These include PGC-1α which promotes mitochondrial biogenesis, JUNB, and SIRT1 (192-194). Pharmaceuticals that can elevate the levels and activity of these proteins may be of therapeutic benefit. Additional studies demonstrate that β_2-adrenoreceptor agonists can

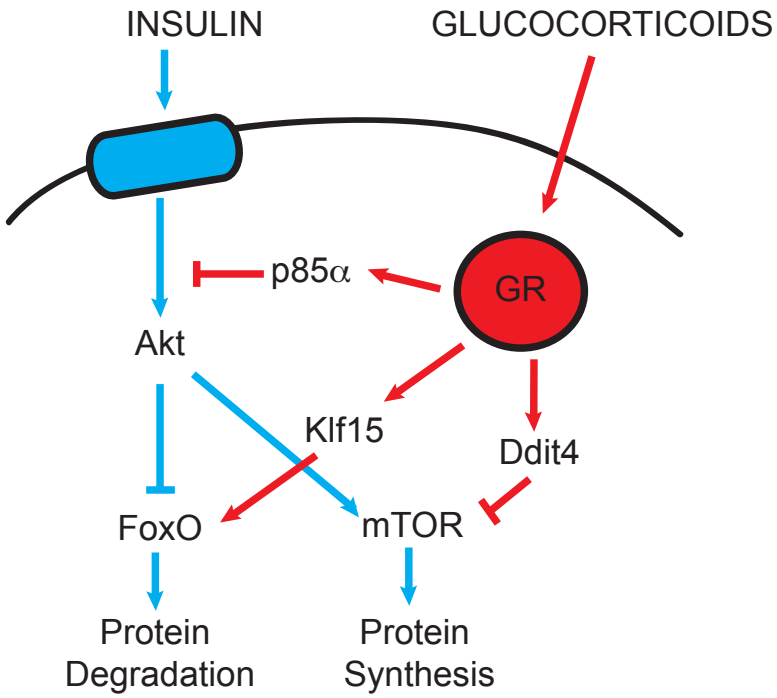

Figure 1.10: Insulin-glucocorticoid signaling cross-talk

Glucocorticoid signaling is antagonistic to insulin signaling in many cell types. Transcriptional target genes of glucocorticoid receptor signaling include p85α the regulatory subunit of PI3K, Klf15, a transcription factor that induces the expression of FoxO transcription factors and Ddit4, a negative regulator of mTOR. In muscle, this results in an increase in protein degradation concomitant with a decrease in protein synthesis in the presence of glucocorticoids as they antagonize the anabolic effects of insulin.

reduce muscle atrophy and thus, these could become promising therapeutics (195,196). There are also several clinical trials in progress or trials that have been completed targeting various signaling pathways including TNFα, IL-6, myostatin/activin, ghrelin receptor and androgen receptor. Many of these trials showed no improvement in muscle mass, or increased muscle mass but no increase in muscle function (197).

1.3.2 Obesity

Obesity is a very costly and burdensome disease. It is estimated that obesity and obesity-related complications cost the Canadian economy somewhere between $4-7 billion annually (198). Obesity is currently defined as a body mass index of equal to or greater than 30 kg/m^2 and is highly associated with several co-morbidities such as insulin resistance, type 2 diabetes, coronary heart disease and certain cancers. The distribution of body fat is also an important factor in obesity. Central obesity, or the accumulation of fat in the abdominal cavity, is highly associated with the many co-morbidities of obesity, while the accumulation of subcutaneous fat, such as in the buttocks or thighs, is less associated with these co-morbidities (199).

1.3.2.1 Causes

Obesity is a disease of positive energy balance. When energy expenditure is less than energy intake, that excess energy is often stored in the form of triacylglycerol (TAG) in the adipose tissue rather than being oxidized as fuel. Obesity is not a single disorder, but a complex condition

determined by interactions between genetics, environment and psychosocial factors. While genetics and heritability are important to a certain degree, the recent rise in obesity is best explained by changing environment and behaviours (200).

1.3.2.2 Pathophysiology and Mechanisms

The excess TAG that is stored in the adipocyte can lead to adipocyte dysfunction. As the adipocyte begins to accumulate lipid it enlarges and undergoes cellular and molecular changes that ultimately affect systemic metabolism. Increased adipose tissue lipolysis results in increased levels of circulating fatty acids and glycerol and this likely promotes insulin resistance and the metabolic complications associated with obesity (201-204). In addition to increased circulating fatty acids, obesity causes increased expression of pro-inflammatory cytokines including TNF-α and IL-6 in adipose tissue (205-207).

Metabolic syndrome is defined as having three or more of the following criteria: high blood pressure, high blood glucose levels, high triglyceride levels, low HDL-cholesterol and large waist circumference. This metabolic syndrome is the result of dramatic physiological changes in systemic metabolism as a result of obesity. Type 2 diabetes is a common complication of obesity that arises from the development of insulin resistance. Many macro and microvascular complications are associated with poorly managed diabetes such as cardiovascular disease, nephropathy, retinopathy and neuropathy (208). Another complication of obesity-related to insulin resistance is the development of non-alcoholic fatty liver disease as excess lipids are deposited in

the liver. Excess lipid in the hepatocytes can lead to inflammation and the development of steatohepatitis and eventually cirrhosis (209-211). Finally, cardiovascular disease is highly associated with obesity. Obesity results in alterations in circulating lipids, blood pressure, coagulation and inflammation which all contribute to the development of cardiovascular disease (212).

Additionally, an association between obesity and mortality have been shown in several large studies. In the prospective Framingham Heart Study, subjects who were obese lived 5.8 (women) or 7.1 (men) fewer years than their non-obese counterparts (213).

1.3.2.3 Clinical Outlooks

Currently, there are clinical interventions that aim to treat obesity and its associated co-morbidities. These include lifestyle interventions, pharmacological therapies or surgical options. In terms of lifestyle interventions, changes to diet and exercise regiments are critical in addition to obesity counseling and support (214,215). There are a variety of anti-obesity medications that will decrease appetite or reduce the absorption of calories. These include, among others, Orlistat, Lorcaserin, and Liraglutide. Orlistat is a pancreatic lipase inhibitor that will prevent the breakdown and absorption of dietary fat (216). Lorcaserin is a selective 5-HT_{2C} serotonin receptor activator that reduces appetite (217). Liraglutide is a GLP-1 analog and promotes a feeling of satiety (218). Most of these medications only lead to a 5-10% weight loss in patients and thus must be combined with other interventions (219). In addition to anti-obesity medications, a variety of pharmaceuticals

can be prescribed to obese patients for the treatment of the co-morbidities such as type 2 diabetes and heart disease (214,215,220). Finally, bariatric surgery is an option for severely obese patients with co-morbid disease when lifestyle interventions are inadequate to achieve a healthy weight (221). Even with all these treatment strategies, a very substantial portion of the population remains obese. It is clear that we need a better understanding of the genetics and physiological effects of obesity to tackle this problem more effectively.

1.4 The Ubiquitin System

The ubiquitin system is a highly co-ordinated system involved in most if not all cellular processes. Importantly, ubiquitination regulates many metabolic processes. In 1978, the laboratory of Avram Hershko characterized a heat-stable polypeptide component of an ATP-dependent proteolytic system in rabbit reticulocytes (222). This heat-stable polypeptide component was identified as ubiquitin, a 76 amino acid protein first characterized in 1975 by Goldstein et al. as a highly conserved polypeptide that induces the differentiation of T cells and B cells (223). An entirely new field of biology emerged from the discoveries linking ubiquitin to proteolysis and the 2004 Nobel Prize in chemistry was awarded to Aaron Ciechanover, Irwin A. Rose, and Avram Hershko for their contributions.

1.4.1 Ubiquitin Conjugation

The seminal work by Ciechanover, Rose, and Hershko identified the main components of ubiquitin conjugation – the E1, E2 and E3 enzymes. These enzymes are responsible for ubiquitin activation, conjugation and conferring substrate specificity, respectively (**Figure 1.11**).

1.4.1.1 Ubiquitin Activation (E1)

There are two ubiquitin-activating enzyme (E1) genes encoded by the human genome: UBA1 and UBA6. To activate ubiquitin, the E1 enzyme binds an ATP-Mg^{2+} and a ubiquitin molecule. A ubiquitin-adenylate intermediate is created through the C-terminal adenylation of ubiquitin. Then, this activated ubiquitin is transferred to a cysteine residue in the catalytic domain of the activating enzyme to generate a thioester bond between the E1 and ubiquitin. The E1-ubiquitin conjugate will then engage an E2 enzyme to continue the ubiquitination cascade (224).

1.4.1.2 Ubiquitin-Conjugating Enzymes (E2)

There are ~40 E2 enzymes in the human genome that transfer ubiquitin or ubiquitin-like proteins to target substrates. The activated ubiquitin is trans-thiolated from the E1 to the active site cysteine of the E2 enzyme to generate a new thioester bond. Interestingly, most of the E2s in a cell exist as E2-ubiquitin conjugates and so are primed to ubiquitinate target substrates (225). The intrinsic reactivity of E2 enzymes is not very high (226). Therefore, E2s require the presence of E3 enzymes to enhance their activity.

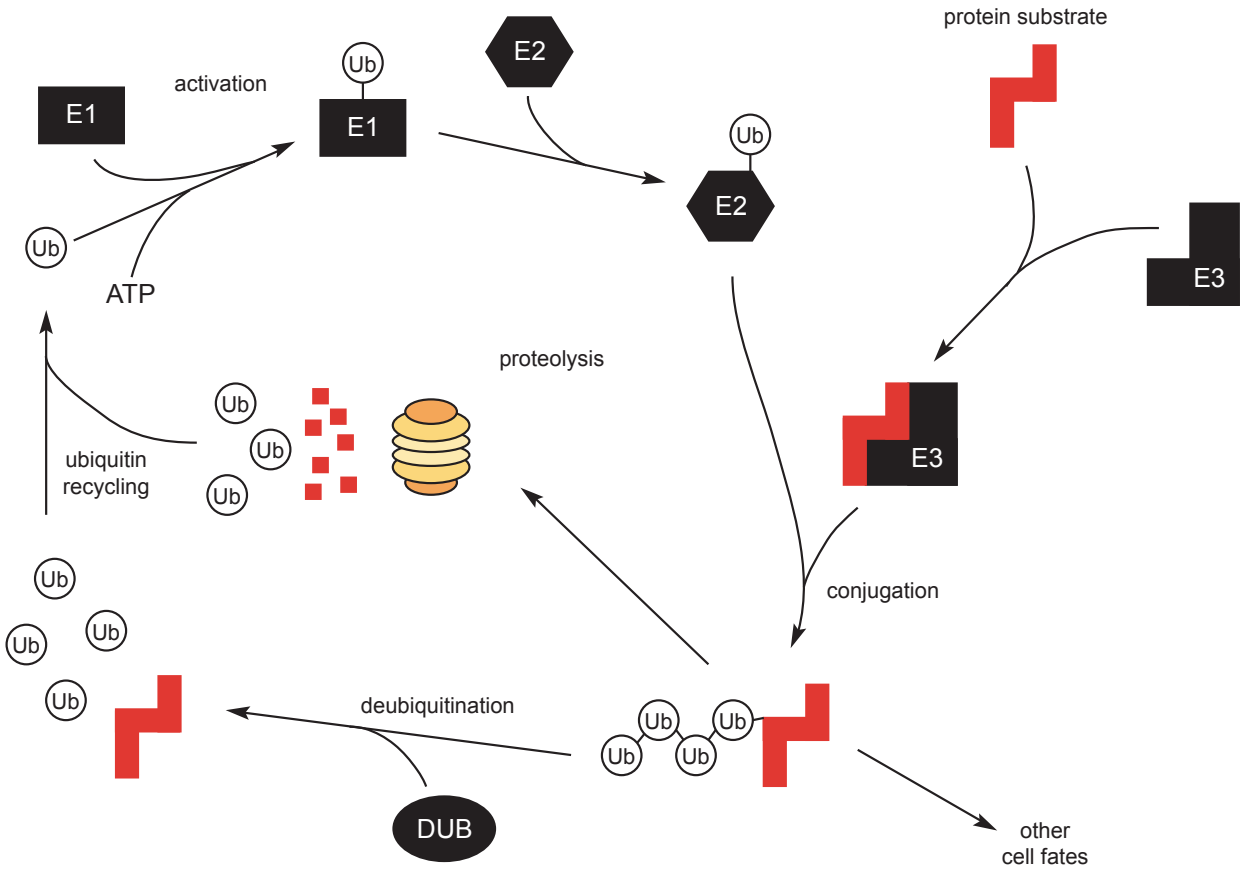

Figure 1.11: The ubiquitin system

Ubiquitin is conjugated to target substrates through the sequential action of three enzymes. First, an E1 ubiquitin activating enzymes activates ubiquitin in an ATP dependent process and transfers it to an E2 ubiquitin conjugating enzyme. Then, in concert with an E3 ubiquitin ligase, ubiquitin is transferred to the target substrate. The ubiquitin itself can be further ubiquitinated to generate a poly-ubiquitin chain and depending on the nature of that chain the protein will be targeted to the 26S proteasome for proteolysis or have other non-proteolytic cell fates. The ubiquitinated substrate can also be deubiquitinated by a class of enzymes called deubiquitinating enzymes (DUBs). Importantly, DUBs generate free ubiquitin that will be recycled into the cellular pool.

1.4.1.3 Ubiquitin Ligases (E3)

There are over 700 E3 ubiquitin ligases encoded in the human genome. The vast majority of these enzymes are RING-type (Really Interesting New Gene) of which there are more than 600 genes. RING finger E3s do not form a catalytic intermediate with ubiquitin. They serve only as a scaffold that brings the target substrate and the E2-ubiquitin conjugate into close proximity for catalysis to occur. RING E3s can be monomeric or be part of multi-protein complexes such as the SCF E3s (227). HECT (homologous to the E6AP carboxyl terminus) domain E3s are another family of E3s of which there are 28. Another smaller class of E3 enzymes called the RBR (RING-between-RING) exist of which there are ~12 (228). In contrast to RING E3s, HECT and RBR E3s require an obligate thioester intermediate between the ubiquitin and the active site cysteine of the E3 ligase (229). Ubiquitin ligases allow for the efficient transfer of ubiquitin to the target protein and confer the substrate specificity of the ubiquitination process.

1.4.2 Fates of Ubiquitinated Proteins

The C-terminal glycine of ubiquitin is generally conjugated to the ε-amino group of a lysine residue of the target substrate, but can also be conjugated to the α-amino group at the N-terminus of the protein, or in rare cases, the thiol group of a cysteine residue or the hydroxyl group of a serine/threonine residue (230). Subsequent ubiquitination events on a lysine on the proximal

ubiquitin lead to the formation of polyubiquitin chains. The nature of these poly-ubiquitin chains will direct the fate of the protein substrate in the cell.

1.4.2.1 Ubiquitin Chain Linkage Types

Ubiquitin has seven internal lysine residues, each capable of being ubiquitinated. Thus, proteins can be polyubiquitinated on lysines Lys6, Lys11, Lys27, Lys29, Lys33, Lys48 and Lys63. In addition to the internal lysine residues, ubiquitin can be conjugated to the N-terminal methionine (Met1) of the preceding ubiquitin (231). The topology of each of these ubiquitin chains is unique (**Table 1.1**). This unique topology allows for the varied fate of each of the targeted proteins based on the recruitment of specific downstream effectors. To make the system even more complex, there may be multiple linkage types within the same polyubiquitin chain generating branched structures or mixed chains (232,233). Much less is known about how these branched ubiquitin structures dictate the fate of the protein in the cell, but it is currently being explored. In addition to polyubiquitination of substrates, many substrates in the cell are mono-ubiquitinated or mono-ubiquitinated on multiple residues (230).

1.4.2.2 Proteolysis

The ubiquitination process is important for both proteasomal and lysosomal degradation pathways. The proteasome has many substrates and it is estimated that half of all cellular proteins can be targeted to the proteasome (234). The 26S proteasome is an ATP-dependent protease that

Table 1.1: Fates of Ubiquitinated Proteins

Ubiquitin Linkage	Nature of Linkage	Chain Topology	Fate of Protein
Lys6	poly-Ub		unclear – proteasomal degradation
Lys11	poly-Ub	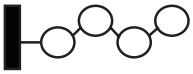	proteasomal degradation
Lys27	poly-Ub	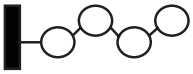	unclear - proteasomal degradation
Lys29	poly-Ub	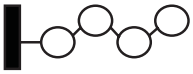	unclear – proteasomal degradation
Lys33	poly-Ub	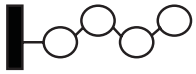	unclear – proteasomal degradation
Lys48	poly-Ub	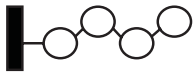	proteasomal degradation
Lys63	poly-Ub	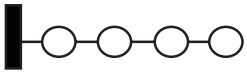	NF-κB signaling, DNA damage response
Met1	poly-Ub linear	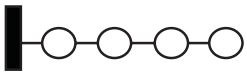	NF-κB signaling, proteasomal degradation
-	mono		endocytosis, protein interaction/localization

serves to degrade ubiquitinated proteins in the cell. It is comprised of a 19S regulatory particle where ubiquitinated substrates dock before they are passed through the 20S core particle where they are hydrolyzed (235). The 20S core particle is a cylindrical structure composed of 4 rings stacked on top of one another with each ring composed of seven distinct subunits (236). The outer most rings contain the α1-7 subunits, while the inner rings contain the β1-7 subunits, 3 of which have proteolytic activity. The 19S regulatory particle can bind to one or both ends of the 20S core structure (237). The 19S regulatory particle contains subunits that have ATPase activity that serve to unfold and translocate the protein into the 20S core. Importantly, it also has associated deubiquitinating enzymes, to remove and recycle the ubiquitin before degradation (238). Lys48 poly-ubiquitin chains are well characterized proteasomal targeting signals. In general, a chain of at least four ubiquitin moieties must be conjugated to the protein in order for it to be recognized by the proteasome (239). Although not as common, other ubiquitin chains can also target proteins to the proteasome for degradation including Lys6, Lys11, Lys27, Lys29, Lys63, Met1 (240-242).

1.4.2.3 Cellular Signaling

Mono-ubiquitination and Lys63 poly-ubiquitination are also involved in many non-proteolytic functions of ubiquitinated proteins. It is well established that cell surface receptors become mono-ubiquitinated upon ligand binding. This ubiquitination functions as a sorting signal that will target the substrate for lysosomal degradation (243). Interestingly, this mono-ubiquitinated receptor can still signal from within the endocytic pathway, but the nature of the

signaling from the ubiquitinated receptor is not fully understood. Ubiquitination is also a very important player in NF-κB signaling. Lys63 poly-ubiquitination of upstream effectors such as IKK, TAK, RIP and NEMO are all required for signaling to proceed. These Lys63 poly-ubiquitinated species likely act as scaffolds to bring the signaling molecules into close proximity (244-246).

1.4.2.4 Protein Interaction, Activity, and Localization

Ubiquitination can regulate other cellular processes such as protein interactions, protein activity and protein localization. A single ubiquitin modification is sufficient to recruit binding partners to certain proteins including the DNA polymerase processivity factor PCNA (247). Lys63 chains can also regulate protein-protein interactions. Lys63 poly-ubiquitin chains can serve as scaffolds and recruit binding partners and this is especially important in the DNA damage response process (248). Not only can ubiquitination serve to recruit binding partners, but it can also inhibit protein-protein interactions (249). Ubiquitination can also modulate protein activity. A classic example of this is the ubiquitin-dependent degradation of the NF-κB inhibitor IκBα (250). Finally, ubiquitination can regulate protein localization. Mono-ubiquitination is a well-characterized signal for internalization of proteins found on the plasma membrane (251). Additionally, the transcription factor p53 can be mono-ubiquitinated on multiple sites, and this causes its export from the nucleus (252).

1.4.3 Deubiquitinating Enzymes (DUBs)

Ubiquitination is a reversible process. This process is catalyzed by a class of enzymes known as deubiquitinating enzymes or deubiquitinases. These enzymes catalyze the cleavage of the peptide or isopeptide bond between ubiquitin and ubiquitin or ubiquitin and substrate. There are ~90 DUBs in the human genome compared to the over 700 ligases (253).

1.4.3.1 DUB Families

DUBs are classified into five families based on the homology of their catalytic domains. Four of these families are cysteine proteases, while the fifth family comprises a group of metalloproteases. The cysteine protease families include the ubiquitin-specific proteases (USP), the C-terminal hydrolases (UCH), ovarian tumor domain (OTU), and the Machado-Joseph Disease (MJD). The mechanism of action of these cysteine proteases is similar to that of plant papains, where the nucleophilic cysteine forms a catalytic triad with an aspartate and a histidine, where the histidine primes the cysteine for nucleophilic attack and the aspartate aligns and polarizes the histidine (254). The metalloprotease family Jab1/Mpn/Mov34 (JAMM) requires the coordination of a zinc ion for catalysis which generates a reactive hydroxyl species due to the abstraction of a hydrogen from a water molecule. This hydroxyl species is then capable of hydrolyzing the peptide bond. The largest of the DUB families is the USP family comprising 56 members while the smallest is the MJD family with 4 members (**Table 1.2**).

Table 1.2: Families of Deubquitinating Enzymes

Family	#	DUB
Ubiquitin C-terminal Hydrolase (UCH)	4	UCHL1 UCHL3 UCHL5 BAP1
Ubiquitin Specific Protease (USP)	56	USP1 USP2 USP3 USP4 USP5 USP6 USP7 USP8 USP9X USP9Y USP10 USP11 USP12 USP13 USP14 USP15 USP16 USP18 USP19 USP20 USP21 USP22 USP24 USP25 USP26 USP27X USP28 USP29 USP30 USP31 USP32 USP33 USP34 USP35 USP36 USP37 USP38 USP39 USP40 USP41 USP42 USP43 USP44 USP45 USP46 USP47 USP48 USP49 USP50 USP51 USP52 USP53 USP54 DUB3 CYLD USPL1
Ovarian Tumor (OTU)	16	OTUB1 OTUB2 OTUD1 OTUD3 OTUD4 OTUD5 OTUD6A OTUD6B OUT YOD1 Otulin A20 Cezanne Cezanne2 TRABID ACPIP1
Machado-Joseph Disease (MJD)	4	Ataxin-3 Ataxn-3-like JosD1 JosD2
JAB1/MPN/ Mov34 (JAMM)	11	PSMD7 PSMD14 EIF3H BRCC36 CSCN5 CSCN6 AMSH AMSH-LP MPND PRPF8 MYSM1

1.4.3.2 DUB Functions

DUBs have various functions within the cell. A critical function of DUBs is to maintain the pool of free ubiquitin. Ubiquitin is encoded in the human genome as four distinct genes: the ubiquitin fusion genes (*UBA52* and *RPS27A*), which encode a single ubiquitin fused to ribosomal proteins L40 and S27A and two poly-ubiquitin genes (*UBB* and *UBC*), which encode 3 and 9 repeats of ubiquitin respectively (255). Therefore, all ubiquitin that is synthesized *de novo* must be cleaved to generate free mono-ubiquitin. The free pool of ubiquitin is also maintained by the recycling of ubiquitin that has already been conjugated to target proteins. This is accomplished by deubiquitinating enzymes, residing at the proteasome or acting in the endocytic-lysosomal system, catalyzing the cleavage of ubiquitin just prior to degradation. DUBs also contribute to the pool of free ubiquitin by cleaving ubiquitin from specific target substrates thereby altering the fate of that substrate and allowing the recycling of the free ubiquitin. Interestingly, DUBs may also be capable of editing ubiquitin chains to direct the fate of substrates (256). DUBs have also been shown to interfere with the conjugation process by binding to the E2 and interfering with ubiquitin transfer (257,258).

1.4.3.3 DUB Regulation

DUBs can be regulated in a number of ways in the cell including at the level of expression, through post-translational modifications, through substrate activation, through allosteric

modulation and subcellular localization. At the level of expression, many DUBs are known to be expressed in certain tissue types or regulated by specific stimuli (259,260). This regulation occurs at the level of transcription, but also at the post-transcriptional level by miRNAs (261). DUBs can also be regulated by cleavage or degradation events resulting in decreased levels of the DUB (262,263). Substrate activation is another way in which DUBs are regulated. The apo-enzyme of specific DUBs is inactive due to the formation of an auto-inhibitory loop that prevents catalysis. Upon substrate (or ubiquitin) binding, the conformation of the DUB changes and relieves the auto-inhibition, thus activating the DUB (264,265). DUBs are also regulated through post-translational modifications and these modifications can regulate the levels and activity of the DUBs. DUBs can be SUMOylated (266), phosphorylated (267,268) and ubiquitinated (269,270). Interestingly, oxidation of the active site cysteine by reactive oxygen species has been shown to inactivate DUBs, and this inactivation can be reversed (271,272). DUB activity can also be regulated allosterically. Binding of other proteins to DUBs has been shown to activate (273,274) and inhibit (275,276) DUB activity. Finally, the subcellular localization of the DUB can play an important role in its regulation. Specific DUBs are known to localize to specific organelles or large intracellular complexes such as the proteasome (277).

1.4.3.4 Ubiquitin-Specific Protease 19

Ubiquitin-specific protease 19 (USP19) is 150 kDa protein from the USP family of DUBs. It is expressed in most tissues including the important metabolic tissues such as the skeletal muscle,

liver and adipose tissue. It was first characterized in 2005 as a DUB that is upregulated in skeletal muscle during a variety of catabolic conditions (278).

1.4.3.4.1 USP19 structure

The crystal structure of USP19 has not been solved, but the structures of other USP family members including USP7, USP14, USP8, USP2, USP21 and USP4 have been published (264,279-283). USP19 is a cysteine protease with a highly conserved catalytic triad comprised of cysteine, histidine and aspartate residues. In addition to the catalytic core, USP19 has a Zn Finger MYND domain and two N-terminal CHORD/Sgt1 (CS/p23) domains. These domains may mediate protein-protein interactions or could suggest a possible chaperone/co-chaperone role for USP19 with HSP90 as these domains have high homology to the HSP90 co-chaperones p23 and Sgt1 (284). An N-terminal SIAH interacting motif has also been characterized in USP19, and indeed SIAH1/2 can interact with USP19 and regulate its stability (285). USP19 also has a ubiquitin-like domain (UBL) within its catalytic core with a currently uncharacterized function. Many DUBs do have UBL domains that allow for substrate recognition, localization or modulation of catalytic activity (286).

USP19 has seven transcript variants, with two major isoforms – one with a C-terminal transmembrane domain that anchors it to the ER-membrane with its catalytic core facing the cytosol and the other generated by alternative splicing of the final exon that lacks the transmembrane domain but contains a C-terminal EEVD motif (**Figure 1.12**). C-terminal EEVD

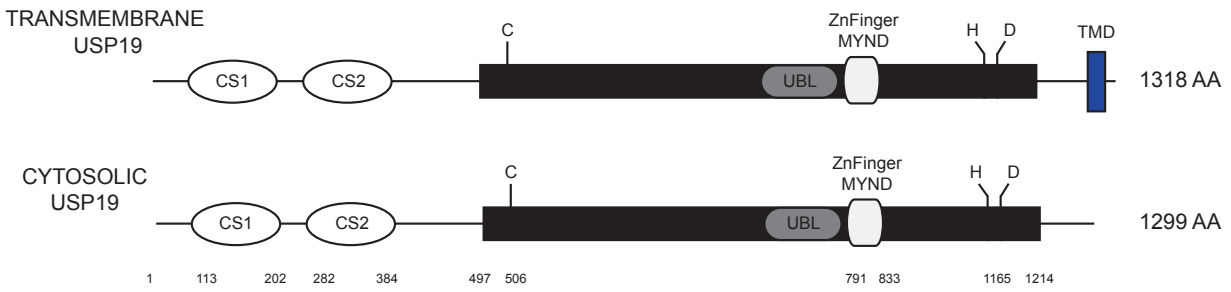

Figure 1.12: Ubiquitin-specific protease 19 (USP19) structural and functional domains

USP19 is a 150 kDa deubiquitinating enzyme with two major isoforms. One of the major isoforms has a C-terminal transmembrane domain (TMD) that anchors it to the endoplasmic reticulum with the catalytic domain and N-terminus of the protein facing the cytosol. The other major isoform lacks the TMD due to alternative splicing of the final exon, but has a C-terminal MEEVD motif. USP19 is part of the ubiquitin-specific protease family of deubiquitinating enzymes and has a conserved catalytic domain with an active site cysteine at position 506 as well as a histidine and aspartate residue that comprise the catalytic triad. USP19 has two N-terminal CS domains that have high homology to Sgt1/p23. Finally, USP19 has a ubiquitin like domain and a Zn Finger myeloid, Nervy and DEAF-1 (MYND) domain within its catalytic domain.

motifs are also found on cellular chaperones such as Hsp90 and Hsp70 and are recognized by tetratricopeptide repeat (TPR) containing co-chaperones (287,288).

1.4.3.4.2 Regulation of USP19

Very little is known about the regulation of USP19. Our laboratory and others have previously shown that USP19 is upregulated at the mRNA level in muscle in various catabolic conditions including fasting, streptozotocin induced diabetes, glucocorticoid treatment, cancer and denervation (278,289). In another study, it was found that USP19 is upregulated in muscle cells after incubation with cigarette smoke extract (a model for COPD) and that this upregulation is mediated through ERK and p38 MAPKs (290). Another study in muscle cells showed that USP19 is upregulated at the transcriptional level by 17β-estradiol through the action of the estrogen receptor α (29). At the post-translational level, one paper has shown that USP19 is ubiquitinated by the ligases SIAH1 and SIAH2 and this ubiquitination can regulate its stability (285).

1.4.3.4.3 Biochemical Functions of USP19

Many substrates of USP19 have been identified that implicate it in a wide variety of cellular processes. This suggests that USP19 likely has condition and tissue-specific roles that need to be further characterized.

USP19 has a major isoform that is localized to the ER-membrane (291). Thus, many studies have assessed the function of USP19 at the ER. A major protein quality control pathway at the ER is endoplasmic reticulum-associated degradation (ERAD). ERAD is initiated in response a variety

of cellular stresses including the unfolded protein response (UPR). USP19 may be involved in ERAD as overexpression of the ER-localized USP19 can rescue model ERAD substrates from proteasomal degradation (291). USP19 also regulates the levels of the ERAD ubiquitin ligase MARCH6 and therefore regulates the ERAD substrates of MARCH6 (292). Another study contradicts these claims by showing that endogenous USP19 is mostly localized to the cytosol where it interacts with HSP90. This study also shows that silencing of endogenous USP19 does not affect ERAD (293). Finally, a study in muscle cells shows that the ER-localized isoform of USP19 inhibits myogenesis by blunting the activation of the UPR (294).

USP19 has also been implicated in the regulation of cell proliferation. Through its deubiquitinating activity, USP19 regulates the levels of KPC1, the ubiquitin ligase for p27(Kip1). p27(Kip1) is a cyclin-dependent kinase inhibitor that regulates the G1/S transition and cells lacking USP19 have significantly slower cell proliferation (295). In addition to regulating cell proliferation, USP19 has been shown to deubiquitinate HDAC1/2 to regulate DNA damage repair and chromosomal stability (296).

USP19 has been shown to directly regulate the levels of certain proteins through its deubiquitinating action. These proteins include the ubiquitin ligases cIAP1/2 (297), HRD1 (298) and the important autophagy protein Beclin-1 (299).

Importantly, USP19 has been shown to interact with the chaperone HSP90 (284,293,300). It is still unclear whether USP19 is acting as a chaperone, co-chaperone or a chaperone associated

deubiquitinase with respect to HSP90. One paper argues that USP19 interacts with HSP90 through its CS/p23 domains to modulate the levels of polyQ expanded proteins through its deubiquitinating activity (300). Another paper suggests that USP19 itself has chaperone activity and can recruit misfolded proteins to the ER for deubiquitination (284).

1.4.3.4.4 Physiological Functions of USP19

Recent work on USP19 suggests that it may play a role in neurodegenerative disorders. In a mouse model of Parkinson's disease, USP19 appeared to be upregulated in the striatum of symptomatic mice (301). In cell models, the cytosolic USP19 isoform has been shown to upregulate the levels of the polyglutamine (polyQ) containing proteins, Ataxin and Huntingtin, potentially enhancing the pathology of these aggregate-prone disease-causing proteins (300). Finally, a recent paper implicates USP19 in a new protein quality control pathway called misfolded associated protein secretion or MAPS. In this paper, the authors identify MAPS as a novel pathway that is activated to handle misfolded proteins in proteasome-inhibited cells. They show that the ER-localized isoform of USP19 recruits misfolded proteins to the ER for deubiquitination, packaging into vesicles, and eventual secretion. Interestingly, the Parkinson's disease protein α-synuclein, which is prone to misfolding and formation of aggregates which are then released and taken up into other neurons resulting in disease propagation, can be secreted from cells by this pathway (284). The majority of this work was done in cell lines, therefore, it must be confirmed

in animal models but does suggest a promising avenue for exploring USP19 as a therapeutic target for treating neurodegenerative disorders.

Beyond a potential role for USP19 in neuronal pathology, the main physiological function of USP19 that has been characterized to date is its involvement in muscle wasting. As described above, muscle wasting involves the upregulation of ubiquitin ligases to assist in the disassembly of the myofibril to generate amino acids as an energy source. It was initially hypothesized that if ligases are upregulated in muscle in catabolic conditions, then there are likely DUBs that are downregulated. To date, no such DUB has been identified (181,302). Instead, certain DUBs are upregulated in catabolic conditions including the proteasomal associated USP14 and the previously uncharacterized USP19 (181,278). USP19 is upregulated in the skeletal muscle of rodents under many catabolic conditions including fasting, STZ induced acute diabetes, dexamethasone, and cancer (278). It has also been shown in muscle cells that USP19 can suppress the expression of the major myofibrillar proteins (303) and that ER-localized USP19 inhibits myogenesis by regulating the unfolded protein response (294). Additionally, USP19 decreases muscle mass through estrogen receptor-dependent mechanisms in female mice (304). All of these observations suggested that USP19 does play a role in regulating muscle mass. Indeed, our laboratory has shown that USP19 null (KO) mice are protected from dexamethasone and denervation-induced muscle wasting (305). Intriguingly, these USP19 KO mice have significantly

less fat mass than their wild-type littermates suggesting a possible role for USP19 in other metabolic tissues beyond the muscle.

1.5 Objectives of this Thesis

1.5.1 Hypothesis

Given the previously characterized roles of ubiquitin-specific protease 19 (USP19) in the catabolic process of muscle wasting and the observation that USP19 null mice had significantly less fat mass than wild-type mice, we wished to extend our studies beyond the role of USP19 in muscle. Inter-organ communication through the action of various secreted factors such as myokines, adipokines, and other hormones integrate their actions to regulate energy homeostasis. Therefore, we wished to characterize the role of USP19 in metabolic tissues such as muscle, liver, and adipose tissue, as well as identify the substrates of USP19 deubiquitinating action. The overarching hypothesis of this thesis is that USP19 is an important regulator of energy homeostasis and that inactivation of USP19 results in mice with an improved metabolic phenotype.

1.5.2 Objectives

The objectives of the work presented in this thesis were as follows -

Use a loss of function mouse model (USP19 KO mice) to characterize:

1. The mechanisms by which USP19 modulates muscle wasting
2. The role of USP19 in adipose tissue development and function
3. Substrates of USP19 that mediate the above metabolic processes

CHAPTER 2

MATERIALS AND METHODS

2.1 Animal Studies

All animal studies were approved by McGill University or the Research Institute of McGill University Health Centre Animal Care Committees and carried out in accordance with the regulations of the Canadian Council for Animal Care.

2.1.1 Breeding and Genotyping

Whole body USP19 KO mice (described previously (305)) were obtained by breeding heterozygous mice to obtain WT and KO mice from the same litter. Genotyping was performed by genomic PCR on tail DNA using oligos for USP19 (forward 5'-GGCTCAAGATGTCTGCAG-3' and reverse 5'-GTTCCTTTCGAGGAAGGG-3') or the geo cassette inserted in the KO mouse (forward 5'-CAGCAACCAGTAACCTCTG-3' and reverse 5'-GACAGTATCGGCCTCAGGAAGATC-3').

2.1.2 Fasting and High Fat Diet

Female mice were food deprived for 48 hours prior to sacrifice. To avoid male cannibalism during fasting, female mice were used. Male mice were fed a high-fat diet for 18 weeks where 60% of calories were from fat (TD.06414 - Harlan Laboratories, Madison, WI). Male mice were chosen for the high fat diet since female mice are more resistant to the development of insulin resistance and glucose intolerance on this diet (306).

2.1.3 Dexamethasone Treatment

Female or male mice were administered 5 mg/kg dexamethasone subcutaneously twice a day for 7 days.

2.1.4 Metabolic Studies

Animals were housed in TSE PhenoMaster (TSE Systems, Germany) metabolic cages for 1 week of acclimatization, followed by 1 week of measurements.

2.1.5 Glucose Homeostasis Tests

Glucose tolerance tests (GTT), insulin tolerance tests (ITT) and pyruvate tolerance tests (PTT) were performed on mice fed a normal diet (ND) or mice fed a high-fat diet (HFD). Mice were fasted for 16 hours overnight (GTT, PTT and fasting insulin) or for 4 hours (ITT). For GTT, ITT and PTT, 2 mg/g glucose, 0.75 U/kg (ND) or 1 U/kg (HFD) crystalline zinc insulin (Humulin R, Lilly) or 2 mg/g sodium pyruvate, respectively, was administered to the mice intraperitoneally. Blood was collected via tail vein puncture, and blood glucose was measured with a glucometer (Roche AccuChek) at the indicated time points. For fasting insulin and leptin, blood was collected from the saphenous vein and allowed to clot. Serum insulin and leptin levels were measured with an insulin singleplex assay kit or the insulin leptin mouse metabolic kit (Meso Scale Discovery).

2.1.6 Insulin Signaling Studies

Mice on a normal diet or on a high fat diet were administered 0.75 U/kg or 1 U/kg, respectively 20 minutes before sacrifice. At sacrifice, the insulin-sensitive tissues (muscle, adipose tissue and liver) were collected.

2.1.7 BrdU Incorporation

Three-week-old mice were injected intraperitoneally with 100 mg/kg bromodeoxyuridine (BrdU) in saline and sacrificed 24 hours later. White adipose tissue was collected.

2.1.8 Electroporation Studies

Under general anesthesia, an incision was made through the skin and subcutaneous fascia of the anterior surface of the leg of the mouse to expose the tibialis anterior muscle. For expression of GR, a plasmid expressing 3X HA and 3X Flag-tagged GR was used. To identify transduced fibers, 5 μg of GFP expressing plasmid was also included. The plasmids (50 μg in 25-30 μl of 0.9% saline) were injected into the tibialis anterior muscle with a 31-gauge needle. One electrode was then placed between the muscle and the underlying bone and the other electrode on top of the muscle. Five pulses were delivered (21 V, 20 msec pulse length and 200 msec pulse interval). After one week of recovery, the mice were treated with dexamethasone (5 mg/kg) subcutaneously twice daily for one week to induce atrophy. At sacrifice, the muscles were frozen in dry-ice chilled isopentane and sectioned and viewed with a fluorescence microscope to identify GFP positive

fibers. The section was then fixed and stained with anti-dystrophin antibody to delineate the borders of the myofibers. Images were processed and analyzed using ImageJ Fiji software.

2.2 Cell Culture

C2C12 myoblast cells were cultured at 37°C with 5% CO_2 in DMEM supplemented with 10% fetal bovine serum (FBS) and 1% penicillin and streptomycin. Cells were transfected with 50 nM non-specific (nsp) siRNA duplexes (5'GUCAGCGUGCAGAUAGAGUUU-3') or USP19 specific siRNA duplexes (5'-ACGACCUGGUUUCGUCUACUGUUGUC-3') using JetPrime reagent (Polyplus Transfections) following the manufacturer's protocol. The following day, cells were induced to differentiate into myotubes with DMEM supplemented with 2% horse serum. After four days of differentiation, cells were serum starved overnight in DMEM with 0.1% BSA. The following day, cells were treated with 10 nM insulin for 5 minutes and then immediately harvested for analysis.

HEK293 or 293T cells were cultured at 37°C with 5% CO_2 in DMEM supplemented with 10% FBS and 1% penicillin and streptomycin. For transfection of USP19 and GR constructs, 0.8 μg of plasmid DNA was transfected into cells in twelve well plates using JetPrime as per the manufacturer's protocol. Cells were treated with 100 μg/μl cycloheximide or vehicle for up to 6 hours. Cells were treated with 25 μM MG132 or vehicle for 6 hours. USP19 KO 293T cells (gift

from Dr. Yihong Ye, NIH) were generated using CRISPR-Cas9 technology with guide RNAs targeting the translational start site of USP19 (284).

2.3 Isolation and Culture of Mouse Primary Cells

Primary cells from USP19 WT and KO mice were isolated from metabolic tissues including muscle, liver and adipose tissue as outlined below.

2.3.1 Primary Muscle Cell Isolation and Culture

Primary myoblasts were isolated from the tibialis anterior (TA) muscle of 4-week old WT and USP19 KO mice by collagenase digestion. Briefly, the TA muscle was dissected and placed in 0.2% collagenase in DMEM and incubated for 1.5 hours at 37°C and 5% CO_2. After digestion, muscle fibers were separated by gentle pipetting with a P200 pipetteman. Isolated fibers were plated in plating media (DMEM supplemented with 10% horse serum, 0.5% chick embryo extract and 1% antibiotic antimycotic) onto polymerized matrigel. After four days of adhering, cells were grown in proliferation media (DMEM supplemented with 20% FBS, 10% horse serum and 1% chick embryo extract with 1% antibiotic-antimycotic). At 70% confluence, cells were trypsinized, counted and plated for experiments at a density of 20, 000 cells per cm^2 on polymerized matrigel. Cells were differentiated in DMEM supplemented with 2% FBS, 10% horse serum, 0.5% chick embryo extract with 1% antibiotic and antimycotic.

2.3.2 Primary Hepatocyte Isolation and Culture

Primary hepatocytes were isolated via portal vein collagenase perfusion. Briefly, mice were anesthetized and a vertical incision was made to open the body cavity. The portal vein was visualized and a catheter was inserted and tied off. First, a HEPES/EGTA/heparin solution was perfused to enhance cell dissociation. Then a collagenase solution (200 U/mL in HEPES buffer) was perfused for 20 minutes or until clear digestion of the liver was obvious. The liver was collected into DMEM/F12 with antibiotics and digested cells were liberated by gentle disruption of the liver. The cells in DMEM were collected and passed through sterile gauze to eliminate undigested tissue. Cells were centrifuged for 5 minutes at 1000 rpm to pellet cells and then resuspended in DMEM supplemented with five times normal antibiotics. Cells were incubated with gentle rocking in this high antibiotic solution for 1 hour. After incubation, cells were centrifuged again and resuspended in plating media (DMEM supplemented with 10% FBS and 1% antibiotic/antimycotic). The following day media was changed for serum free media (DMEM/F12 supplemented with 0.4 mM ornithine, 25 nM selenium, 10 nM ethanolamine and 0.025% lactic acid). For gluconeogenesis assays, cells were treated with 100 nM dexamethasone, 100 uM dibutyryl cAMP, 1 mM pyruvate and 10 mM lactate in glucose-free DMEM for 6 hours.

2.3.4 Stromal Vascular Fraction (SVF) Isolation and Culture

The SVF of the inguinal fat pad from 8-week old mice was isolated as follows: inguinal fat pads were removed from male WT or KO mice and placed in 37°C DMEM/F12 before processing.

Tissue from 3-5 fat pads was minced and digested for 1 hour in a 10 mg/mL collagenase solution, shaking at 37°C. Digested tissue was passed through a 240 μm filter to remove debris and undigested tissue. Cells were centrifuged at 50 g for 5 minutes at room temperature to separate the adipocytes. The infranatant (below the floating adipocyte layer) containing the SVF cells was collected into a new tube. SVF cells were spun at 500 g for 15 minutes. All but 5mL of the media was removed and 10mL of red blood cell lysis buffer (155 mM NH_4Cl, 10 mM $KHCO_3$, 10 mM EDTA) was added, vortexed and incubated at room temperature for 5 minutes. DMEM/F12 was added up to 30 mL. Cells were passed through a 20 μm filter to concentrate the SVF cells. Cells were centrifuged at 500 g for 15 minutes to pellet the SVF. Cells were resuspended in DMEM/F12 supplemented with 10% FBS and 1% antibiotics and plated at a density of $2.4x10^5$ cells in a 6 well plate and grown until confluence for differentiation. Cells were differentiated in a cocktail of 1 μM dexamethasone, 0.5uM IBMX, 200 μM indomethacin and 10 μg/μl insulin for 48hrs. Differentiating cells were maintained in DMEM/F12 with 1 μg/μl insulin.

2.4 Muscle Protein Synthesis

Muscle protein synthesis rates were measured by injecting mice with a flooding dose of deuterated phenylalanine as described previously (305). Mice were sacrificed 30 minutes later and the gastrocnemius muscle was collected and flash frozen in liquid nitrogen. Muscles were processed and fractional synthesis rates were determined as in (307).

2.5 Histological and Immunofluorescence Analysis

Mouse tissues (epididymal adipose tissue and liver) were fixed in 4% paraformaldehyde, embedded in paraffin, sectioned and stained with H&E. Histological analysis was performed on 5 μM sections. Cross-sectional area of adipocytes was measured by tracing the outline of each adipocyte in ImageJ. Five different fields per animals were used and ~50 adipocytes per field were counted. Observer was blinded to genotype during analysis. For immunofluorescence analysis, slides were rehydrated and antigen retrieval was performed. Sections were blocked with 10% goat serum and 1% BSA for 1 hour at room temperature. Slides were incubated with primary antibodies to BrdU and perilipin overnight at 4°C in a humidified chamber. The following day, sections were incubated with the appropriate secondary antibody conjugated to Alexa488 or Texas Red. Five random fields were selected and BrdU positive/perilipin positive cells were counted.

2.6 Human Tissue Analyses

Human adipose tissue was obtained from the biobank at Institut Universitaire de Cardiologie et de Pneumologie de Quebec (IUCPQ), where written informed consent was obtained from the subjects. Female subjects (BMI 35-40 kg/m^2 and 60-69 kg/m^2) were paired for age and date of bariatric surgery. Patients with diabetes were excluded. Study approval was obtained from the Research Ethics Board of the McGill University Health Centre and IUCPQ.

Correlation of gene expression in human muscle tissue was obtained from a cohort of

patients with abdominal cancers at the University of Alberta. This study was approved by the Alberta Cancer Research Ethics Committee, and all patients provided written consent. Biopsies of *rectus abdominis* muscle (0.5–1 g) were taken from the site of the incision at the time of surgery. Muscles were procured at the beginning of the operation by sharp dissection, then immediately snap frozen. Tissues were stored at the Alberta Cancer Research Biorepository/Canadian Breast Cancer Foundation Tumor Bank (Cross Cancer Institute, Edmonton, AB, Canada) and the University of Calgary HPB/GI Tumor Tissue Bank (Calgary, AB, Canada). Processing of tissues and microarray analysis have been previously described in detail (305,308).

2.7 qPCR Analyses

RNA was prepared from cells or tissue by solubilisation in 4M guanidium isothiocyanate followed by phenol-chloroform extraction. For tissue, solubilisation was followed by ultracentrifugation through a cesium chloride cushion prior to phenol chloroform extraction. RNA was quantified using a NanoDrop LITE spectrophotometer (Thermo Fischer Scientific). cDNA was synthesized from 1 μg of RNA using the High Capacity cDNA Reverse Transcriptase Kit (Applied Biosystems). qPCR analysis was done using SYBR-Green Master Mix (Applied Biosystems) on a ViiA7 thermocycler with gene-specific primers **(Table 2.1 and 2.2**). Differences in target gene expression were calculated using the ΔΔCt method.

2.8 Immunoprecipitation

Lysate (500 μg) from cells was subjected to immunoprecipitation with 5 μg of anti-HA antibody. Briefly, Protein G agarose beads were pre-cleared with mouse IgG and lysate for 1 hour at 4°C. The pre-cleared lysate was incubated with antibody overnight at 4°C while rocking. The following day, the lysate with antibody was then incubated with Protein A or G agarose resin for 4 hours to immunoprecipitate the complexes. Finally, the resin was washed three times and protein complexes were eluted from the resin with SDS sample buffer at 95°C and analyzed by SDS-PAGE and Western blot.

2.9 Western Blot Analyses

Tibialis anterior muscles, epididymal white adipose tissue and liver were homogenized in ice cold RIPA buffer with protease and phosphatase inhibitors. The homogenate was spun in a refrigerated centrifuge at 17, 000 x g for 15 minutes to clear the lysates. Cells were lysed in cold RIPA buffer or 2% SDS in 10 mM Tris. Protein concentration was determined by the BCA Micro Protein Assay (Thermo Fischer Scientific). Lysate (10 μg) was subjected to SDS-PAGE and transferred to 0.45 μm nitrocellulose membranes. After blocking with 5% non-fat milk in TBS-T, membranes were probed with primary antibodies **(Table 2.3)** followed by secondary antibodies conjugated to horseradish peroxidase and visualized with chemiluminescence (Clarity ECL,

BioRad). Membranes were visualized with a ChemiDoc Touch (BioRad). Signals were quantified using Image Lab software (BioRad).

2.10 Proximity Ligation Assay

C2C12 myoblasts were plated on an eight-chamber cell culture coated microscope slide (Falcon) at a density of 2,000 per cm^2. After 24 hours in culture, cells were fixed with 4% paraformaldehyde for 15 minutes at room temperature and then permeabilized in 0.1% Triton-X 100. Cells were blocked in the manufacturer's (Sigma) blocking solution for 1 hour in a humidified chamber at 37°C. Primary antibodies (one mouse and one rabbit – **Table 2.3**) for USP19, GR, or HSP90 were incubated with the cells overnight in a humidified chamber at 4°C. Cells were then washed twice in the manufacturer's wash buffer. Cells were incubated for 30 minutes with a DNA ligase in a humidified chamber at 37°C and then washed twice in manufacturer's wash buffer. Finally, cells were incubated with an amplification solution including a polymerase for 100 minutes in a humidified chamber at 37°C. Cells were washed three times and the slides were mounted using a mounting media with DAPI.

2.11 Luciferase Assay

Luciferase assays were performed in 293T CTL or USP19 KO cells that were transfected (as above) with a 3X GRE-Firefly luciferase construct, a Renilla luciferase construct (as a transfection control) and a GR construct. Cells were treated with 1 nM dexamethasone (Sigma)

for up to 12 hours. Luciferase activity was analyzed by the Dual-Luciferase Reporter Assay System (Promega) according to the manufacturer's protocol.

2.12 Microarray Gene Expression Analysis

RNA from muscle of fed and fasted WT and KO mice were reverse transcribed, fluorescently labeled and hybridized with microarrays containing oligonucleotide probes derived from mouse cDNAs (Affymetrix Mouse Gene 1.0 ST). The preparation of probes, the hybridization, and the scanning of the microarrays were performed at the McGill University and Génome Québec Innovation Centre according to the manufacturer's instructions.

Background correction and normalization were performed with the Flexarray software (version 1.6.3) in the R environment (version 3.1.2) with the Bioconductor packages using the robust multiarray average method for ST (RMA for ST) of the affy package. Differential expression analysis of WT fasted vs KO fasted was performed using the significant analysis of microarrays (SAM) in the Flexarray software. The data was encoded in a design matrix and then fitted to a linear model. Genes were filtered for a minimum expression fold difference of approximately 1.4 ($2^{0.5}$), which totaled 110 probesets. All control probesets in the Mouse Gene 1.0 ST chip were excluded from the analysis (from 10338001 to 10344613 included), as they do not represent real RNA transcripts.

Transcription factor motif discovery was performed using Hypergeometric Optimization of Motif EnRichment (HOMER v4.9, which runs in Perl and C++. To identify candidate transcription factors responsible for differential gene expression in WT fasted and KO fasted muscle, the findMotifs.pl method was used, with all 110 probesets used as input (of which 93 unique genes were recognized by HOMER), using the official gene symbol as identifier and the

mm9 mouse genome. Motifs that were within 1000 bp upstream to 500 bp downstream of the transcriptional start site were considered in the analysis. The enrichment score represents the odds ratio of the odds of finding a motif in the promoter of a regulated gene versus a background gene.

2.13 Statistical Analyses

Statistical analysis was carried out using GraphPad Prism 6 (GraphPad Software). Parametric Student's t-test was performed using two-tailed distribution for analysis involving two groups of samples (WT and KO). Two-way ANOVA was used for analysis involving more than one independent variable (genotype and time). One-way ANOVA was used for analysis involving 3 or more conditions. $p<0.05$ was considered significant.

Table 2.1 – Mouse qPCR Primers

Gene	Forward (5'-3')	Reverse (5'-3')
Adipoq	CTCTCCTGTTCCTCTTAATCCT	ACCAAGAAGACCTGCATCTC
Angptl2	CCTGGAGGTTGGACTGTCAT	CAGACCAGTCCTCCATGGTT
Atg4	ATTGCTGTGGGGTTTTTCTG	AACCCCAGGATTTTCAGAGG
Atgl	GGAGACCAAGTGGAACATCTCA	AATAATGTTGGCACCTGCTTCA
Cblb	CAGGCAGAACTCACCAGTCA	CGGGAGTGGTTTGTCTTGTT
Cebpa	CGCAAGAGCCGAGATAAAGC	CGGTCATTGTCACTGGTCAACT
Cebpb	CAAGCTGAGCGACGAGTACA	AGCTGCTCCACCTTCTTCTG
Ces1d	AGAGGAGACCAACCTCAGCA	CTTTGTCCTTCAGCCTCTGG
Cidea	TGCTCTTCTGTATCGCCCAGT	GCCGTGTTAAGGAATCTGCTG
Ddit4	GTGCCCACCTTTCAGTTGAC	GCTGCTCGGAGCTGTAGAGT
Fabp4	TGTGATGCCTTTGTGGGAAC	ATGATCATGTTGGGCTTGGC
Fbxo32	GCAAACACTGCCACATTCTCTC	CTTGAGGGGAAAGTGAGACG
Fkbp5	GACACCAAAGAAAAGCTGACG	CTTCTCTGACAGGCCGTATTC
Foxo3	ACCTTCGTCTCTGAACTCCTTG	CTGTGGCTGAGTGAGTCTGAAG
Gabarap	CATCGTGGAGAAGGCTCCTA	ATACAGCTGGCCCATGGTAG
Gapdh	CACCATCTTCCAGGAGCGAG	CCTTCTCCATGGTGGTGAAG
Gpat3	GGAGGATGAAGTGACCCAGA	CCAGTTTTTGAGGCTGCTGT
Grb10	GTGAACTTCTTCCCGGATCA	TCTTCCAAGACTTGCGTCCT
Hsl	TGTGGCACAGACCTCTAAAT	GGCATATCCGCTCTC
Igfbp1	AGCCCAGAGATGACAGAGGA	GTTGGGCTGCAGCTAATCTC
Il6	GAGGATACCACTCCCAGAG	AAGTGCATCGTTCATACA
Klf15	CCAAACCTATTGGCTCAGGA	AACTCATCTGAGCGGGAAAA
Lcn2	GTCGCTACTGGATCAGAACA	CTTGGTTCTTCCATACAGGGT
Lep	TGTGTCGGTTCCTGTGGCTTT	CTGCGTGTGTGAAATGTCATTG
Lpl	CTGCTGGCGTAGCAGGAAGT	GCTGGAAAGTGCCTCCATTG
Map1lc3b	CACTGCTCTGTCTTGTGTAGGTTG	TCGTTGTGCCTTTATTAGTGCATC
Nampt	CATAGTGGCATCTGCTCATT	GCTATCGCTGACCACAGACA
Nr3c1	AGGCCGCTCAGTGTTTTCTA	TACAGCTTCCACACGTCAGC
Odf3l2	AGTTACTCGCTTTGGCCGTA	GAGGTGTCTGGAGGCTTCTG
Pi3kr1	TGACGAGAAGACGTGGAATG	CCGGTGGCAGTCTTGTTAAT
Pparg	TTTCAAGGGTGCCAGTTTCG	ACTTGAGCAGAGTCACTTGGTC
Ppargc1a	CCCTGCCATTGTTAAGACC	TGCTGCTGTTCCTGTTTTC
Rbp4	GACAAGGCTCGTTTCTCTGG	AAAGGAGGCTACACCCCAGT
Retn	TCATTTCCCCTCCTTAGCCT	CAAGACTGCTGTGCCTTCTG
Tnfa	CATGAGCACAGAAAGCATGATCC	AAGCAGGAATGAGAAGAGGCT
Trim63	ACCTGCTGGTGGAAAACATC	CTTCGTGTTCCTTGCACATC
Ucp1	ACTGCCACACCTCCAGTCATT	CTTTGCCTCACTCAGGATTGG
Usp19	GTAGTTTCATTTGGCGAGAC	CCGATCATGCCTCCGTAGTG

Table 2.2 – Human qPCR primers

Gene	Forward (5'-3')	Reverse (5'-3')
ADIPOQ	CCTAAGGGAGACATCGGTGA	GTAAAGCGAATGGGCATGTT
FABP4	TACTGGGCCAGGAATTTGAC	GTGGAAGTGACGCCTTTCAT
GAPDH	CACCATCTTCCAGGAGCGAG	CCTTCTCCATGGTGGTGAAG
LEP	GGCTTTGGCCCTATCTTTTC	CCAAACCGGTGACTTTCTGT
PPARG	GACCACTCCCACTCCTTTGA	GATGCAGGCTCCACTTTGAT
USP19	GATCGAGCAAACCAGGAGAG	GACCCTGACGATGAAGGAAA

Table 2.3 – List of Antibodies

Antibody	Supplier	Dilution
Western Blot		
pAkt (T308)	Cell Signaling Technology	1:1000
pAkt (S473)	Cell Signaling Technology	1:1000
Akt	Cell Signaling Technology	1:1000
pS6K	Cell Signaling Technology	1:500
S6K	Cell Signaling Technology	1:500
pFoxO1/3	Cell Signaling Technology	1:1000
FoxO1	Cell Signaling Technology	1:1000
p4EBP1	Cell Signaling Technology	1:1000
4EBP1	Cell Signaling Technology	1:1000
IR	Cell Signaling Technology	1:1000
IRS-1	Cell Signaling Technology	1:1000
GR	Santa Cruz Biotechnology	1:1000
γ-tubulin	Sigma Aldrich	1:10,000
USP19	Bethyl Laboratoties	1:1000
PPARg	Santa Cruz Biotechnology	1:1000
Adiponectin	Generous gift T. Combs	1:1000
Immunoprecipitation		
HA	Santa Cruz Biotechnology	1ug per 100ug lysate
Flag	Sigma Aldrich	1ug per 100ug lysate
Immunofluorescence		
Dystrophin	Vector Labs	1:100
BrdU	Roche	1:50
Perilipin	Santa Cruz Biotechology	1:50
GR	Abcam	1:100
GR	Cell Signaling Technology	1:100
USP19	Our Laboratory	1:100
HSP90	SressMarq Biosciences	1:100
Proximity Ligation Assay		
GR	Abcam	1:100 (mouse)
GR	Cell Signaling Technology	1:100 (rabbit)
USP19	Our Laboratory	1:100 (rabbit)
HSP90	SressMarq Biosciences	1:100 (mouse)

CHAPTER 3

RESULTS

Inactivation of USP19 protects against muscle wasting by modulating insulin and glucocorticoid signaling

3.1 - Preface to Chapter 3

In this chapter, we explore the role of USP19 in fasting-induced muscle atrophy. It has been shown that USP19 is required to mount the full muscle wasting response. Indeed, inactivation of USP19 results in mice that are protected from dexamethasone and denervation-induced muscle atrophy (305). To date, the mechanisms by which USP19 mediates these effects on muscle wasting remains unknown. In this chapter, we uncover two pathways (insulin and glucocorticoid signaling) that are modulated by USP19. Modulation of these pathways by loss of USP19 results in protection from muscle wasting induced by fasting as well as an enhanced ability to maintain blood glucose homeostasis by enhancing insulin sensitivity and protein turnover in skeletal muscle and hepatic glucose output from the liver.

3.2 - Results

3.2.1 - USP19 KO mice are protected from fasting induced muscle loss

Upon fasting, both WT and USP19 KO mice lost weight progressively with time with near identical kinetics (**Figure 3.1 A**). To explore whether specific tissues might respond differently, we measured the changes in mass of the key tissues involved in the metabolic response to fasting. Upon fasting, there was similar atrophy in fat, liver, kidney, and heart in WT and KO mice. In terms of relative muscle loss, the KO mice lost significantly less muscle upon fasting in the tibialis anterior muscle, with a trend towards less muscle loss in the gastrocnemius muscle (**Figure 3.1 B**). Interestingly, in the fed state, the liver kidney and heart are significantly smaller in the KO mice (**Figure 3.1 C**). This observation suggested that there may be a protective effect in muscle due to the loss of USP19. To explore this further, we measured the grip strength of these mice and KO mice showed improved grip strength, a sign of greater muscle functionality (**Figure 3.1 D**). In addition to less atrophy and increased strength, USP19 KO mice had increased average muscle fiber cross-sectional area in the fasted condition (**Figure 3.1 E**) as well as an observable shift to larger fiber sizes in the fiber size distribution (**Figure 3.1 F**). Taken together, USP19 KO mice show a protection from fasting induced muscle atrophy.

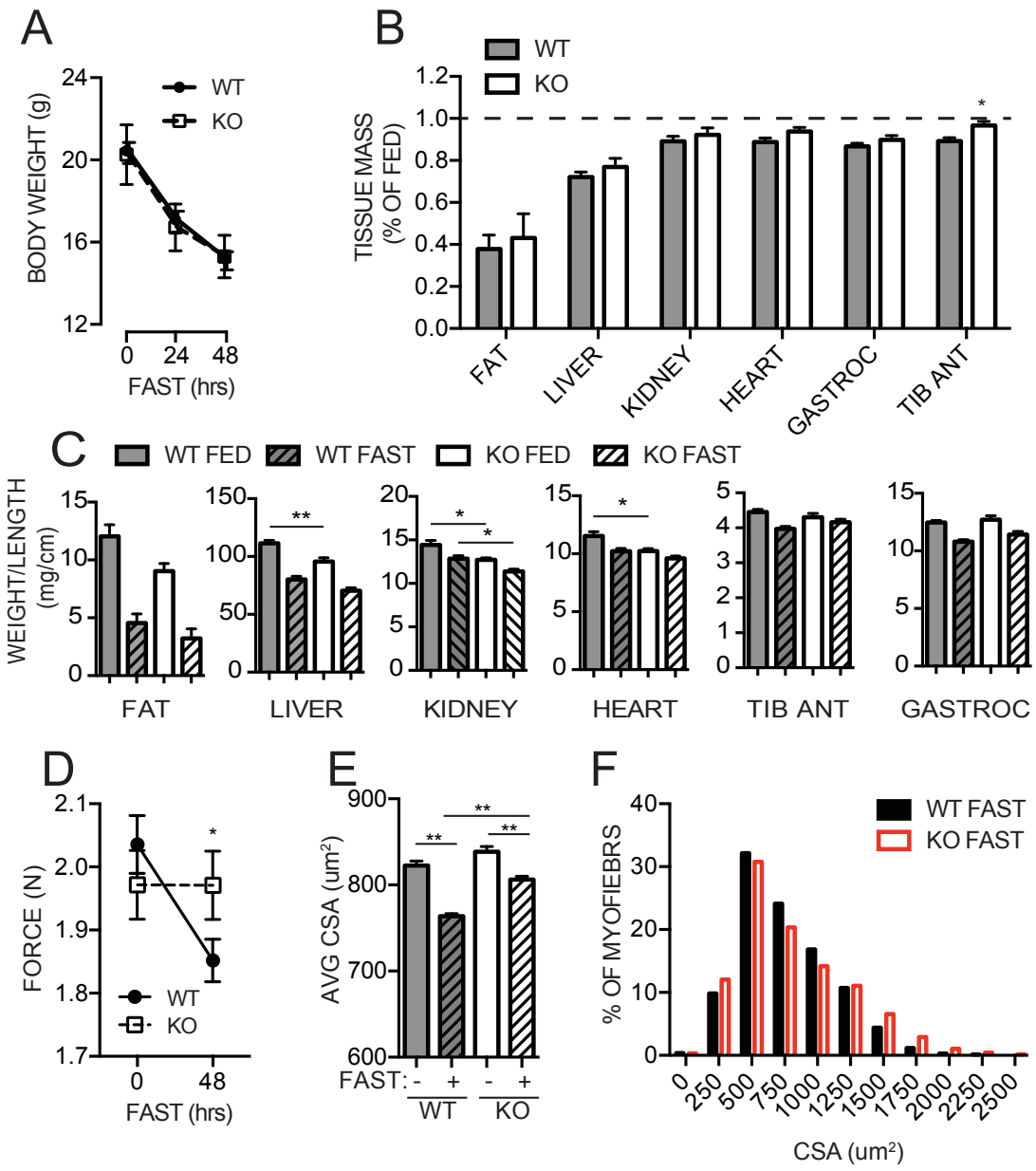

Figure 3.1 Inactivation of USP19 protects against muscle wasting induced by fasting

USP19 WT and KO female mice were fed or food deprived for up to 48hrs. (A) Body weight change of the mice at 0, 24, and 48 hours of food deprivation. Important metabolic tissues were collected and weighed at sacrifice and normalized to body length. (B) Relative loss of tissue mass in WT and USP19 KO mice upon fasting. n=15-23 (C) Normalized tissue weight in the fed and fasted state. (D) Grip strength of the hindlimb was measured at 0 and 48 hours of food deprivation. (E) Average cross-sectional area of tibialis anterior muscle fibers in WT and KO mice (F) Fiber size distribution in WT and KO mice. n=12,000-13,000 fibers. *p<0.05, **p<0.01

3.2.2 – USP19 KO mice show similar levels of atrophy related gene expression but increases in levels of protein synthesis in muscle

The loss of protein in the skeletal muscle during atrophy is due to a combination of increased protein degradation and decreased protein synthesis. It is not practical to measure protein degradation *in vivo* so to assess why USP19 KO mice lost less muscle mass upon fasting we assessed the upregulation of the proteolytic pathways involved in muscle wasting. First, we looked at the expression levels of the critical ubiquitin ligases (MurF1 and Atrogin-1) that mediate the degradation of muscle protein. As previously described, MuRF1 and Atrogin-1 are induced upon fasting (181,183,302), but we found no difference in the upregulation of these genes between WT and KO mice (**Figure 3.2 A**). Another proteolytic pathway that is highly upregulated upon fasting is the autophagy-lysosomal pathway. We assessed the lipidation of LC3 upon fasting and found no differences between WT and KO mice (**Figure 3.2 B**). Additionally, we assessed the gene expression of a variety of autophagy related proteins including Map1lc3a (LC3), Atg4 and Gabarap and found no differences between WT and KO mice (**Figure 3.2 C**). Taken together, these results suggest that the muscles of USP19 KO mice are not spared from atrophy because of decreased protein degradation.

Since there were no differences in the upregulation of the proteolytic pathways in our KO mice, we examined whether there were any differences in muscle protein synthesis that could

explain the decrease in muscle loss seen in the KO mice. As expected, we observed decreased levels of protein synthesis upon fasting. However, the KO mice had higher levels of muscle protein synthesis in both the sarcoplasmic and the myofibrillar fractions (**Figure 3.2 D**) compared to WT mice upon fasting. These results suggest that USP19 KO mice lose less muscle upon fasting due to the ability to maintain an increased level of protein synthesis.

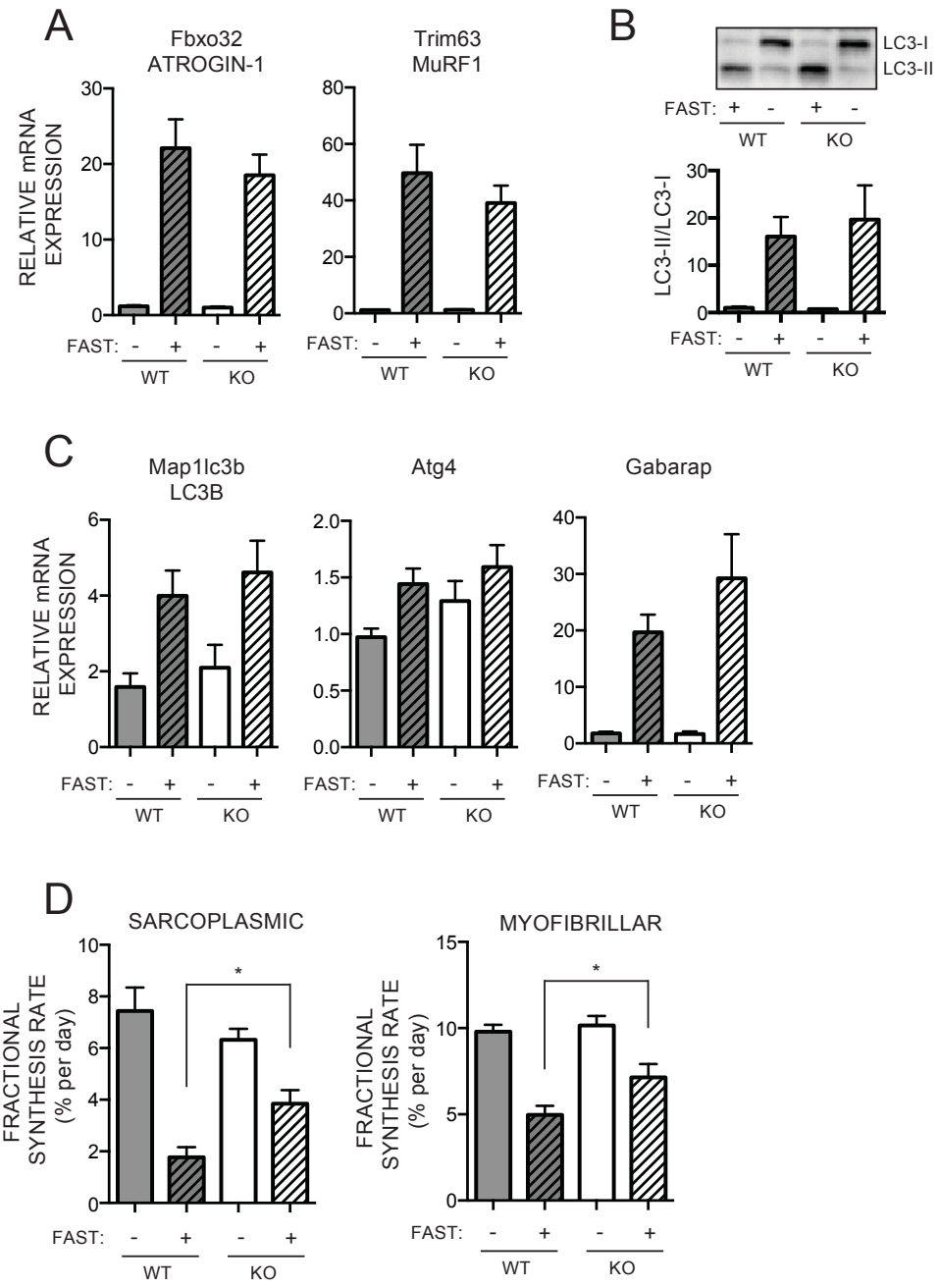

Figure 3.2 USP19 KO mice show no differences in atrophy related gene expression but show increases in levels of protein synthesis

(A) mRNA expression of ubiquitin ligases involved in muscle atrophy. (B) Western blot and quantification of the fasting induced conversion of LC3-I to its lipidated form LC3-II (C) mRNA expression of autophagy-lysosomal system genes involved in muscle atrophy n=21-30. (D) Fractional synthesis rates of the sarcoplasmic and myofibrillar protein fractions n=6-7. *p<0.05

3.2.3 – USP19 KO mice show enhanced insulin signaling in the muscle

In the previous section, we showed that USP19 KO mice had increased levels of muscle protein synthesis upon fasting. This suggested that USP19 might be modulating an anabolic pathway. Because fasting is an insulinopenic state, we first assessed insulin-stimulated Akt-mTOR signaling in the skeletal muscle. We observed that USP19 KO mice had increased levels of phosphorylated Akt on both the threonine 308 and serine 473 residues after insulin stimulation. Downstream of Akt we observed significantly increased levels of phosphorylated $p70^{S6K}$, but no increases in the phosphorylation of 4EBP1 or Foxo1/3 (**Figure 3.3 A and 3.3 B**). We next asked whether this effect on insulin signaling in the muscle was cell autonomous. Because we are working with a global KO mouse, it is possible that factors modulated by USP19 extrinsic to the muscle are mediating the effects on insulin signaling. To test the cell-autonomous effects of USP19 on muscle insulin signaling, we used a muscle cell line (C2C12) where USP19 is silenced. In C2C12 cells, where USP19 has been silenced, there was a 20% increase in levels of phosphorylated Akt after insulin stimulation (**Figure 3.3 C and 3.3 D**). Taken together, these data suggest that USP19 modulates the anabolic insulin-Akt-mTOR signaling axis in skeletal muscle and that this is a cell-autonomous effect.

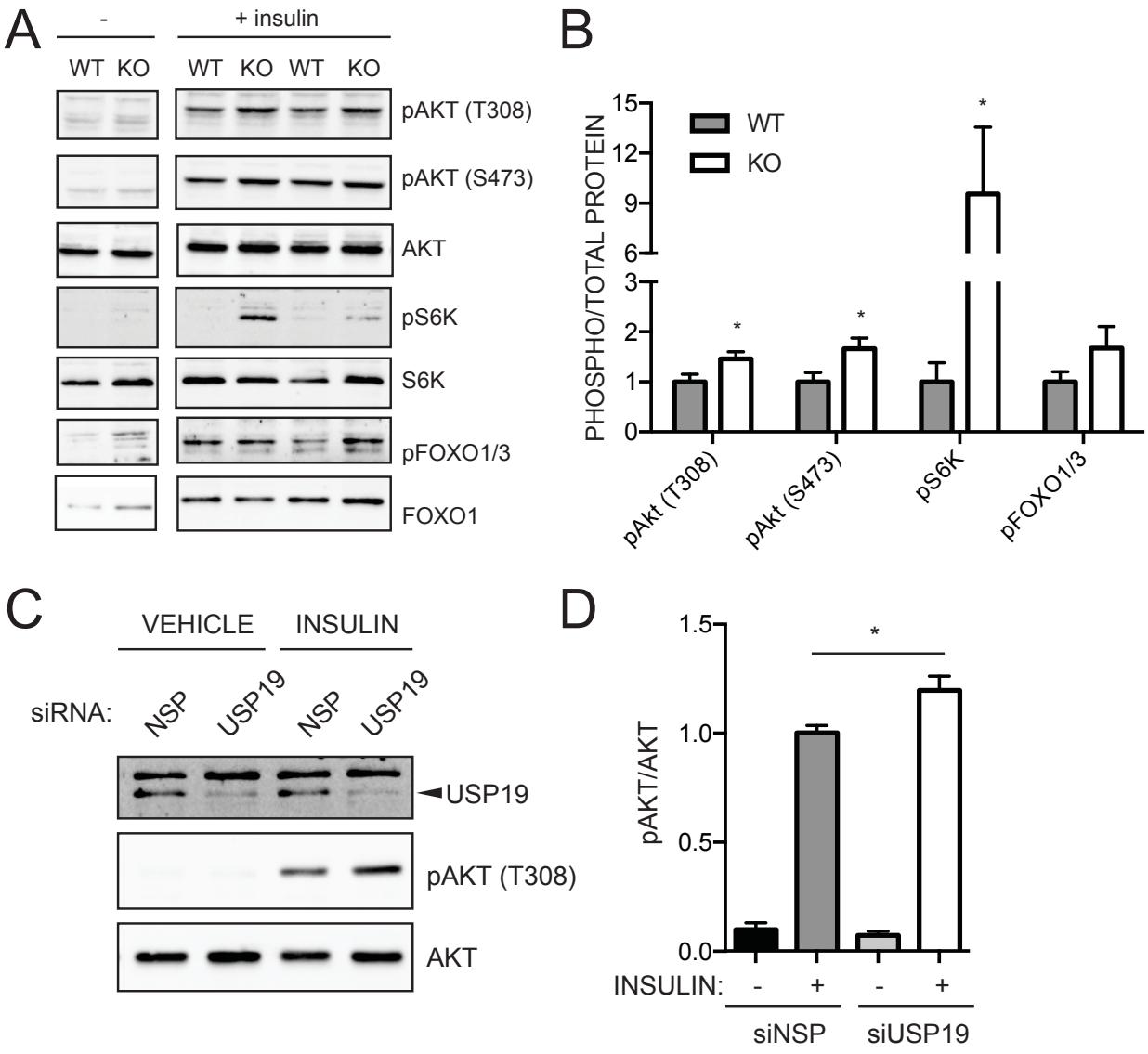

Figure 3.3: USP19 KO mice have enhanced insulin signaling in the muscle

(A) WT and USP19 KO mice were administered 0.75 U/kg insulin or vehicle before sacrifice. Components of the insulin signaling pathway were analyzed by western blot. (B) Quantification of phosphorylated components of the insulin signaling pathway normalized to total levels of the specific protein. (C) C2C12 myotubes were treated with 1 nM insulin for 5 minutes. Activation of Akt was measured by western blot of phosphoAkt T308. (D) Quantification of pAkt T308 relative to total Akt levels. n=9 *p<0.05

3.2.4 – USP19 KO mice are more insulin sensitive and glucose tolerant than WT mice

Since USP19 KO mice have enhanced insulin signaling in skeletal muscle, we next asked whether this enhanced signaling at a cellular level translated into a physiological effect on insulin sensitivity at the organismal level. To test this, we performed an insulin tolerance test (ITT) where mice were administered insulin and their blood glucose was monitored over time. USP19 KO mice showed dramatically improved blood glucose lowering compared to WT mice suggesting that they are indeed, more insulin sensitive (**Figure 3.4 A**). If the KO mice are more insulin sensitive, this suggests that they might be more glucose tolerant and able to clear glucose from their circulation more effectively. To test this, we performed a glucose tolerance test (GTT) where glucose is administered to the mice and their blood glucose monitored over time. Indeed, USP19 KO mice showed improved glucose clearance during the GTT (**Figure 3.4 B**). As a final indicator of insulin sensitivity, we measured the fasting insulin and fasting glucose levels in these mice. USP19 KO mice have significantly lower fasting insulin levels compared to WT mice (**Figure 3.4 C**), while maintaining similar fasting blood glucose levels (**Figure 3.4 D**). This suggests that USP19 KO mice can maintain their blood glucose levels with significantly less insulin, an indication that they are more insulin sensitive. Taken together, these results show that USP19 KO mice are more insulin sensitive and glucose tolerant than WT mice and are better able to maintain blood glucose homeostasis.

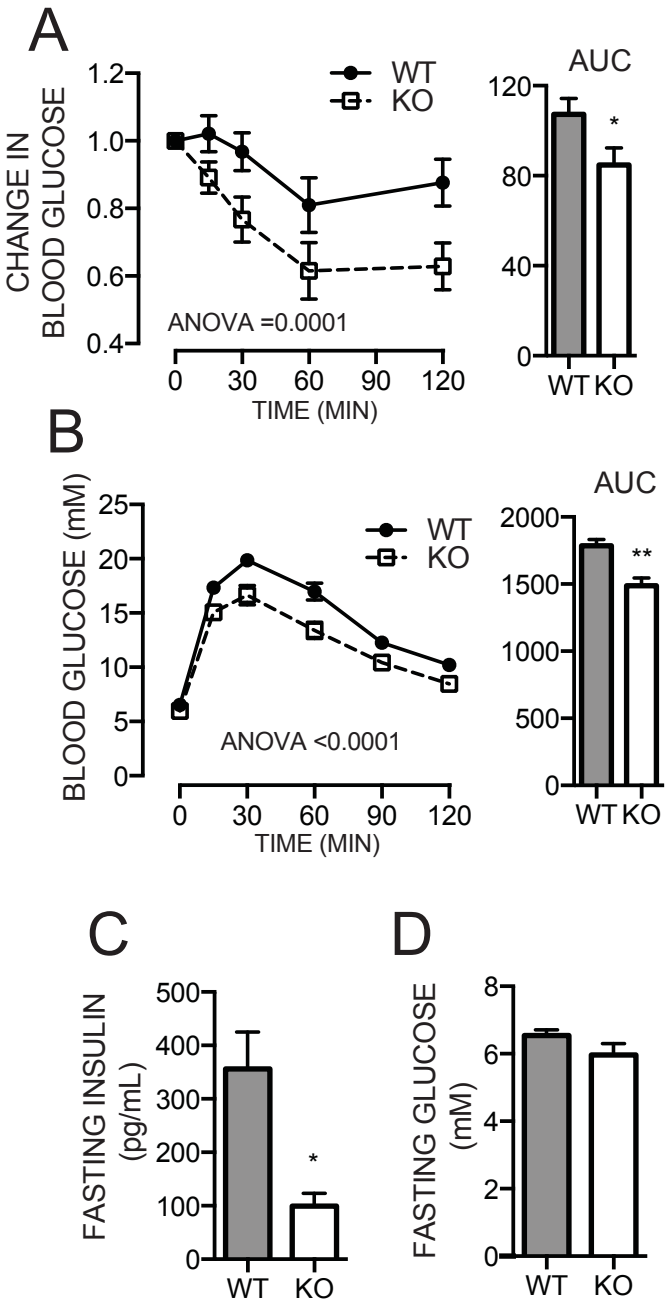

Figure 3.4: USP19 inactivation results in mice that are more insulin sensitive and glucose tolerant

(A) Insulin tolerance test and (B) glucose tolerance test in male mice and areas under the curve. (C) Fasting insulin and (D) fasting glucose levels. Shown are means ± SEM. n=10-24 *p<0.05 **p<0.01

3.2.5 – USP19 KO mice have decreased hepatic glucose output

Given the significant increase in insulin sensitivity and glucose tolerance in the KO mice and knowing the important contribution of the liver to the maintenance of blood glucose homeostasis, we next looked at hepatic glucose output in the KO mice. In the fasting condition, the liver breaks down glycogen stores and produces glucose *de novo* through gluconeogenesis to maintain blood glucose in the normal physiological range. Administration of pyruvate (a substrate for gluconeogenesis) will promote hepatic glucose output that is reflected by increased glucose levels in the circulation. USP19 KO mice showed lower levels of hepatic glucose output compared to WT mice during the PTT (**Figure 3.5 A**). To explore the mechanisms of USP19 regulation of hepatic glucose output, we looked at the expression of the critical enzymes involved in gluconeogenesis, Pepck and G6pase. We found that Pepck mRNA levels were lower in the livers of KO mice who had been fasted, but there were no differences in G6pase levels (**Figure 3.5 B**). Next, we asked whether the upregulation of the expression of these enzymes was different when we induce gluconeogenesis. To test this, we isolated primary hepatocytes from WT and KO mice and induced gluconeogenesis in culture. Upon treatment with dexamethasone and dibutyrul cyclic AMP (a gluconeogenic stimulus) in addition to lactate and pyruvate (gluconeogenic substrates), cells dramatically upregulated Pepck and G6pase (**Figure 3.5 C and 3.5 D**). However, in the KO cells, the upregulation of Pepck was blunted (**Figure 3.5 C**). Taken together, these results suggest

that USP19 KO mice have a defect in hepatic glucose output, at least in part due to lower levels of the gluconeogenic enzyme Pepck.

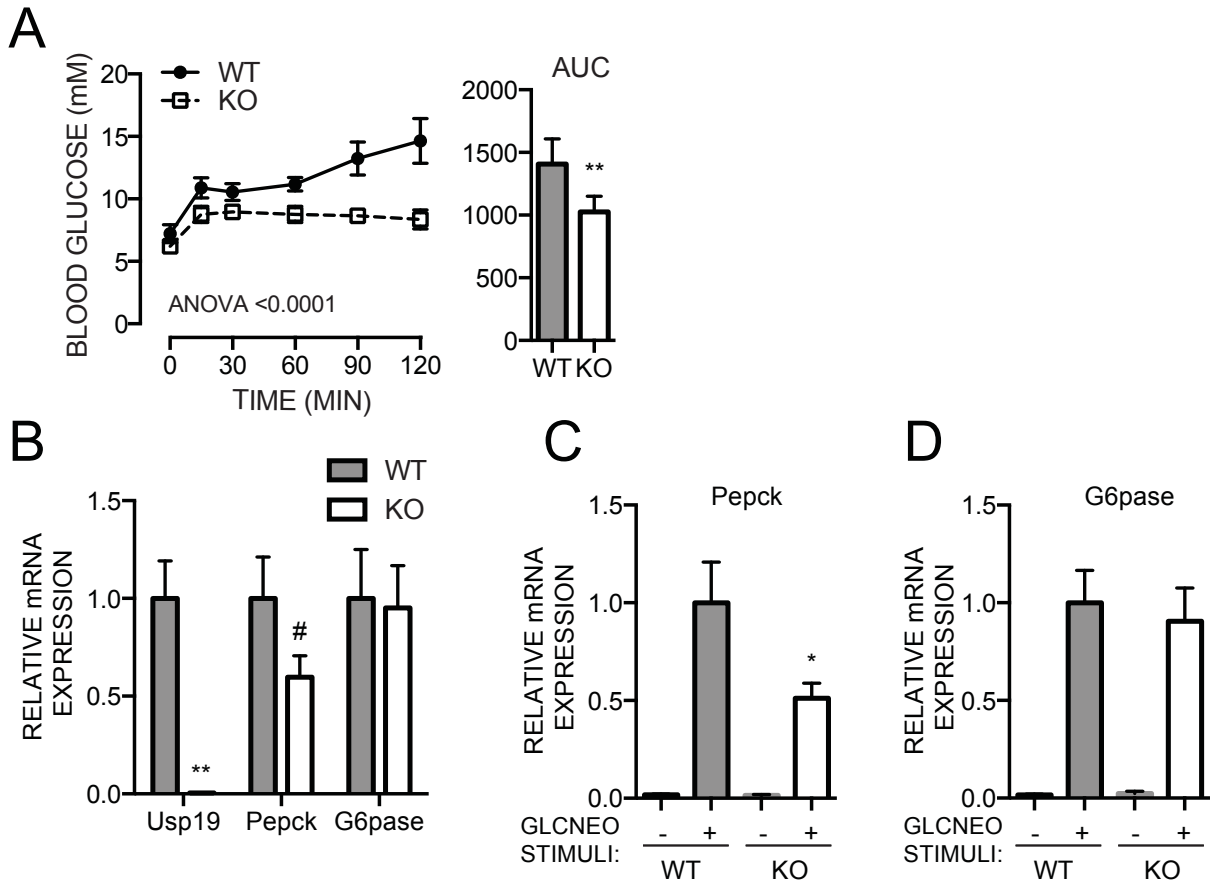

Figure 3.5: USP19 inactivation results in mice that have lower hepatic glucose output

(A) Pyruvate tolerance test and area under the curve in male mice. (B) mRNA expression of the critical gluconeogenic enzymes after 48 hours of fasting. (C, D) mRNA levels of Pepck and G6pase during a gluconeogenesis assay in primary hepatocytes. Shown are means +SEM. n=6-9 *p<0.05, **p<0.01, #p=0.16.

3.2.6 – USP19 inactivation results in decreased glucocorticoid signaling

In the previous sections, we showed that USP19 modulates glucose homeostasis. Specifically, USP19 modulates insulin signaling in the skeletal muscle, thereby promoting whole-body insulin sensitivity as well as modulating hepatic glucose output. Next, we asked what pathways might be modulating these physiological effects. To address this, we performed a microarray analysis on the muscles from fasted WT and USP19 KO mice. Following normalization, approximately 24,000 genes were found to have a significant level of expression in the skeletal muscles. Amongst these genes, 110 were found to be differentially expressed by more than 1.4-fold in WT and KO fasted mice while many fewer genes were differentially expressed in WT and KO fed mice. To try to identify a signaling pathway that might be modulated by USP19, we evaluated whether the promoters of these differentially expressed genes were enriched with binding sites for specific transcription factors. Interestingly, the presence of binding motifs for 11 transcription factors – MafA, Irf2, Mef2b, Mef2c, Mef2d, Pax7, Pparg, Srebp1a, PR, Smad2/3 and glucocorticoid receptor (GR) were found to be enriched in the differentially expressed genes (**Figure 3.6 A**). GR signaling is known to induce muscle wasting, negatively regulate insulin signaling and regulate hepatic glucose output (309,310) and thus, was of interest to us. We confirmed the observation that GR signaling is differentially regulated in KO muscle by analyzing the expression of a subset of GR target genes in the muscle of fasted mice. The analyzed genes were identified from our microarray analysis or known to negatively regulate insulin signaling and

validated as GR targets in a ChIP-seq experiment in C2C12 muscle cells (148). Of the 12 genes analyzed, 7 were significantly down-regulated in the USP19 KO mice upon fasting (**Figure 3.6 B**). Next, we asked whether these genes were also differentially regulated during dexamethasone administration which directly activates GR signaling. Indeed, upon dexamethasone treatment 8 of the genes were significantly decreased in KO muscle (**Figure 3.6 C**). To explore whether this regulation may be relevant in human skeletal muscle, we examined whether the expression of these GR target genes correlates with that of USP19 in muscle samples obtained from patients undergoing surgery for gastrointestinal cancer, a common cause of muscle atrophy. Indeed, mRNA levels of 9 of the 12 genes were significantly correlated to levels of USP19 mRNA (**Figure 3.6 D and Table 3.1**).

Table 3.1: Correlation between USP19 and GR target gene expression in *rectus abdominis* muscle of patients with abdominal cancers

Gene Name	*Accession Number*	*Probe*	*r*	*p-value (two-tailed)*	*Significant?*
LCN2	NM_005564	A_23_P169437	-0.06	0.4697	-
ODF3L2	NM_182577	A_23_P316850	0.32	0.0002	Yes
CES1	NM_001266	A_23_P206733	0.08	0.3455	-
IGFBP1	NM_000596	A_23_P42868	-0.08	0.3691	-
CBLB	NM_170662	A_23_P29830	0.29	0.0006	Yes
GRB10	NM_001001555	A_23_P122863	0.38	<0.0001	Yes
PI3KR1	NM_181523	A_23_P144980	0.24	0.0055	Yes
DDIT4	NM_019058	A_23_P104318	0.24	0.0053	Yes
KLF15	NM_014079	A_23_P40805	0.39	<0.0001	Yes
FOXO3	NM_001455	A_32_P102062	0.59	<0.0001	Yes
FKBP5	NM_004117	A_23_P111206	0.37	<0.0001	Yes
CEBPB	NM_005194	A_23_P411296	0.66	<0.0001	Yes

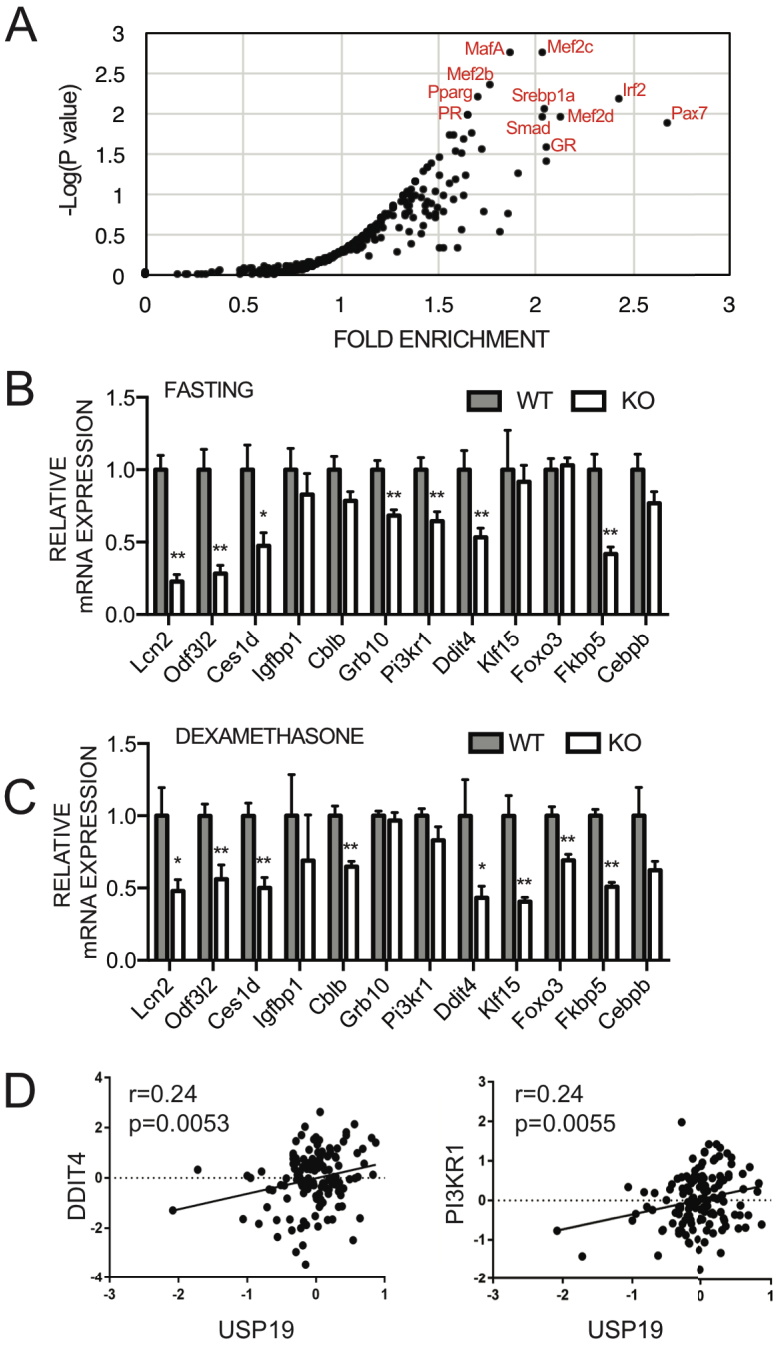

Figure 3.6: USP19 regulates glucocorticoid receptor signaling (A) HOMER analysis revealed transcription factor motifs in the promoters of differentially regulated genes in WT and KO mice upon fasting identified by microarray. One of the transcription factors identified was the glucocorticoid receptor (GR) (B) Glucocorticoid receptor target gene expression in the TA muscle after 48 hours of fasting. (C) Glucocorticoid target gene expression in the TA muscle after one week of dexamethasone treatment (5 mg/kg/day). Presented are means + SEM. n=10-23. *p<0.05, **p<0.01 (D) Correlation between USP19 mRNA and GR target gene (DDIT4 and PI3KR1) mRNA levels (arbitrary units) in human muscle biopsies from patients with abdominal cancers.

3.2.7 – Restoring levels of GR in KO muscle reverses the muscle sparing phenotype

Since USP19 modulates glucocorticoid signaling, we next asked how USP19 might be mediating this process. We first looked at the levels of the glucocorticoid receptor (GR) in the muscle. USP19 KO mice have 50% lower levels of GR protein in the muscle but similar levels of GR mRNA (**Figure 3.7 A and 3.7 B**). This suggested to us that GR might be a substrate of USP19 deubiquitinating action because in the absence of a deubiquitinating enzyme, a substrate should be more ubiquitinated and therefore more degraded. This will be explored in greater detail in Chapter 5. Finally, we asked whether regulation of GR by USP19 is mediating the effects on muscle wasting. To address this, we tested if restoring the levels of GR in KO muscle could reverse the protection from muscle atrophy that we observed in the KO mice. To test this, we electroporated a GR plasmid or an empty vector (EV) into the muscle of KO mice and asked whether there were differences in muscle atrophy in response to dexamethasone treatment. A plasmid expressing GFP was also included to identify transduced fibers. We observed that KO muscle had significantly larger fibers compared to WT muscle, but KO muscle where GR has been restored had significantly smaller muscle fibers (**Figure 3.7 C-E**). Taken together, this suggests that USP19 is mediating its effects on muscle wasting through the regulation of the GR and glucocorticoid signaling.

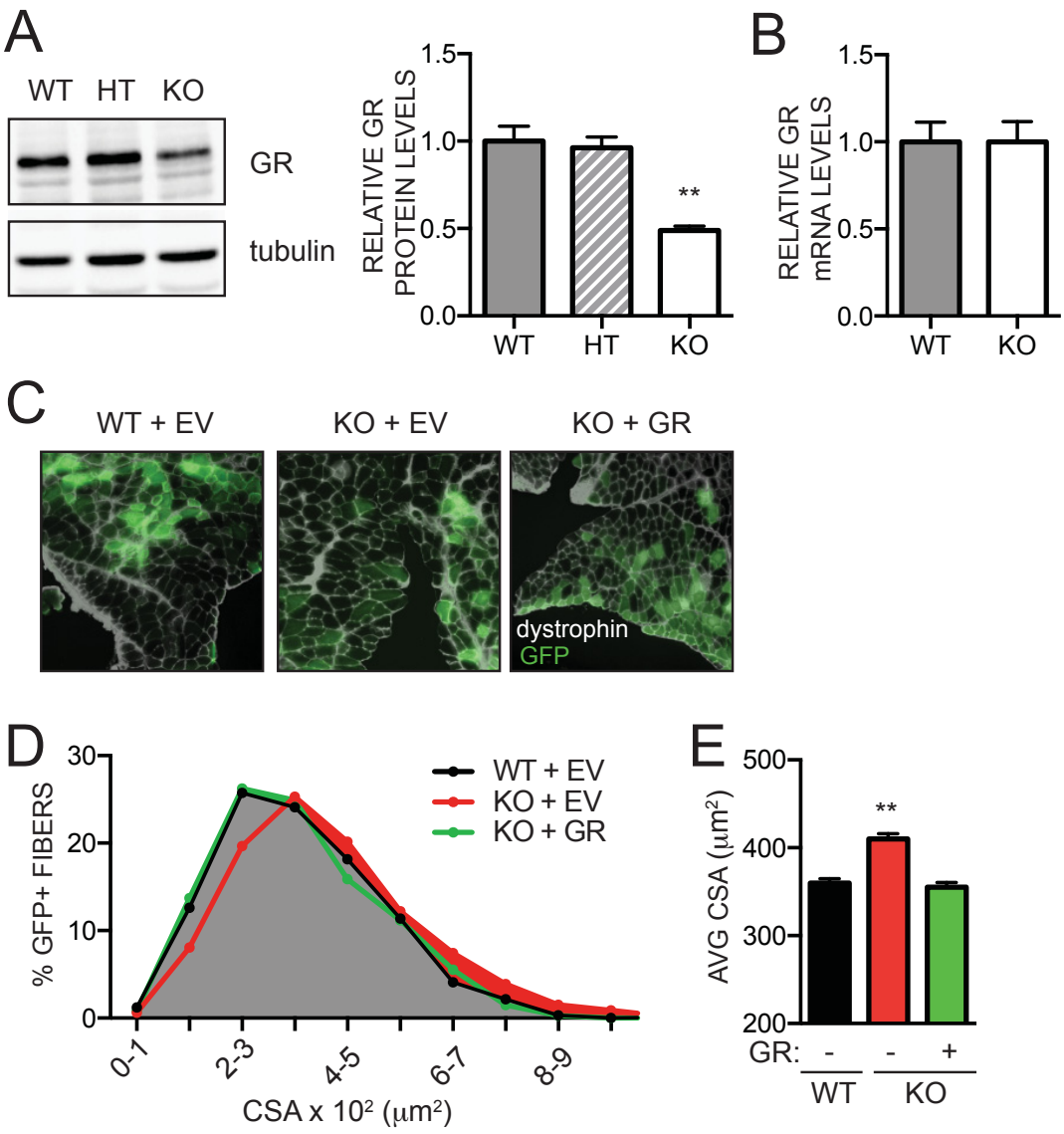

Figure 3.7: Restoring GR levels in USP19 KO muscle reverses the protection from muscle atrophy

(A) GR protein levels in WT, HT, and KO muscle. (B) GR mRNA levels in WT and KO muscle tissue. (C) Muscle sections from WT and KO mice with an empty vector (EV) or GR plasmid electroporated. Dystrophin delineates the muscle fibers and GFP marks fibers that have been efficiently electroporated. (D) GFP+ muscle fiber size distribution (E) Average muscle fiber cross-sectional area. **p<0.01

3.3 – Discussion

In this chapter, we describe for the first-time mechanistic insights into the regulation of muscle mass by USP19. This deubiquitinating enzyme regulates insulin and glucocorticoid signaling, two critical pathways that modulate protein turnover. Insulin and the related hormone IGF-1 promote protein synthesis and suppress protein degradation through activation of the Akt-mTOR and the Akt-FoxO pathways respectively. Here, we show that inactivation of USP19 results in increased insulin-stimulated phosphorylation of Akt and $p70^{S6K}$, with no effect on phosphorylated FoxO. Consistent with the role of $p70^{S6K}$ in the activation of translation, we observed increased rates of synthesis of both sarcoplasmic and myofibrillar fractions in the KO muscle, suggesting that USP19 regulates a global protein synthesis pathway, rather than the synthesis of specific proteins. FoxO1, 3 activate transcription of the key ubiquitin ligases MuRF1, atrogin-1/MafBx as well as genes in the autophagic system. The lack of evident differences in insulin-stimulated phosphorylation of FoxO can explain the lack of change in levels of these two ligases and of multiple markers of autophagy including levels of lipidated LC3 in the fasted KO muscle. This is in contrast to what is observed in glucocorticoid-induced muscle atrophy where USP19 inactivation reduces the upregulation of the atrogenes but has no effect on the rates of protein synthesis (305). These differences could be due to USP19 influencing multiple signaling pathways, the relative importance of each being different in different forms of atrophy. USP19 could also act on both protein synthesis and degradation pathways, but at different times during

the course of atrophy. The latter is plausible since fasting induced atrophy is acute, while other atrophy models (glucocorticoid and denervation) are significantly more chronic.

In addition to insulin signaling, we show that USP19 modulates glucocorticoid signaling (Fig 3.6). The production of glucocorticoids is increased in many illnesses, and this class of hormones is also frequently used therapeutically for suppression of immunity or inflammation and so excess glucocorticoids play an essential role in many forms of muscle wasting (311,312). Indeed, the activation of muscle protein breakdown by a number of diverse catabolic stimuli (sepsis, renal failure, cytokines) can be blocked or blunted by interfering with the production of the action of glucocorticoids (313-315). Glucocorticoids suppress muscle protein synthesis and also have a permissive effect on activation of protein degradation (173,316). Thus, the decreased expression of glucocorticoid target genes in the fasted KO muscle is highly consistent with improved muscle mass from decreased glucocorticoid action. Interestingly, we found that mRNA levels of the GR target gene Ddit4 (REDD1) are lower in our KO mice. REDD1 acts by sequestering 14-3-3 proteins thereby increasing the activity of TSC1/2 that act to inhibit mTOR (184,185). Also, upstream of mTOR is Akt, a kinase responsible for its activation. The GR target gene Pi3kr1 (p85α) is the regulatory subunit of PI3K which, when expressed at high levels, acts as a dominant negative thereby inhibiting PI3K activity and decreasing Akt activation (317). In our system, we see a decreased expression of Pi3kr1, increased phosphorylation of Akt and decreased Ddit4 (REDD1) mRNA expression consistent with overall mTORC1 activation. These

two pathways converging at mTOR could explain the increased protein synthesis observed in the KO mice.

The improvement in insulin signaling in our KO mice extended beyond effects on muscle protein turnover. Muscle is the major site of insulin-stimulated glucose uptake, and we observed enhanced glucose lowering when insulin was administered to the KO mice. Glucose tolerance was significantly better in the KO mice consistent with improved glucose disposal. Fasting insulin levels were also markedly lower in the KO mice in the presence of near identical glucose levels indicating whole body improvement in insulin sensitivity. Increased insulin sensitivity is consistent with decreased hepatic glucose output that we observed in the KO. Additionally, the gluconeogenic enzyme Pepck is regulated at the expression level by insulin (inhibitory) and glucocorticoids (activating) and thus, decreased Pepck expression is consistent with USP19 KO mice having increased insulin sensitivity and decreased GR signaling in the liver. The overall improvement in insulin sensitivity and glucose tolerance also suggests potential roles for USP19 in modulating insulin resistance and the development of diabetes respectively. These questions will be explored in chapter 4.

Insulin and glucocorticoids play essential roles in the metabolic response to fasting, particularly in the regulation of the breakdown of muscle proteins to supply amino acids to the liver for gluconeogenesis (309). The altered signaling in these pathways that we observed would predict a less negative protein balance upon fasting. Indeed, we demonstrated that the inactivation

of USP19 offers protection from fasting-induced decreases in muscle mass and function. Loss of appetite or anorexia is associated with many chronic conditions as well as aging, and so likely contributes significantly to the overall burden of muscle wasting (318). It has also been shown that loss of USP19 protects from muscle wasting induced by denervation and glucocorticoid treatment (305). Thus, this work provides further evidence that pharmacological inhibition of USP19 could be a beneficial approach in the treatment of muscle wasting disorders

CHAPTER 4

RESULTS

The deubiquitinating enzyme USP19 modulates adipogenesis and potentiates high-fat diet-induced obesity

4.1 Preface to Chapter 4

In chapter 3, we showed that USP19 KO mice are protected from fasting-induced muscle atrophy due to increased levels of protein synthesis in muscle compared to WT mice. These KO mice also have improved insulin sensitivity, enhanced insulin signaling and decreased glucocorticoid signaling in muscle. We next asked whether USP19 modulates other insulin and glucocorticoid-regulated processes such as fat development, obesity, and diabetes.

In this chapter, we show that USP19 KO mice have significantly less fat than their WT littermates due to fewer and smaller adipocytes. We show that USP19 is required for normal fat development and that USP19 KO mice are protected from high-fat diet-induced obesity. USP19 KO mice are also protected from the development of diabetes during diet-induced obesity and have enhanced insulin signaling in the muscle and the liver. Finally, we show that USP19 expression is correlated to the expression of important adipogenic genes in human visceral adipose tissue, not subcutaneous adipose tissue, suggesting a possible role for USP19 in the function of adipose tissue highly associated with metabolic disease in humans.

4.2 Results

4.2.1 USP19 KO mice have smaller fat pads as a result of fewer and smaller adipocytes

On a normal diet (ND), male USP19 KO mice had significantly smaller epididymal fat pads compared to WT mice after normalization to body weight (**Figure 4.1 A and 4.1 B**). Normalization was done as USP19 KO mice are ~10% smaller than WT mice. This decrease in fat mass is consistent throughout the lifespan from as early as 21 days to as late as 24 months of age. Fat tissue expansion is the result of two processes – adipocyte hypertrophy and/or adipocyte hyperplasia. To determine if USP19 KO mice have a defect in adipocyte hypertrophy or hyperplasia, we assessed the size of the adipocytes in the fat pads of WT and KO mice. The adipocytes in USP19 KO mice had significantly smaller cross-sectional areas starting at six months of age (**Figure 4.1 C and 4.1 D**). Interestingly, the adipocyte size was similar between WT and KO mice at an early age of two months (**Figure 4.1 C and 4.1 D**), yet the fat pad is significantly smaller (**Figure 4.1 B**), an indication that fewer adipocytes were present.

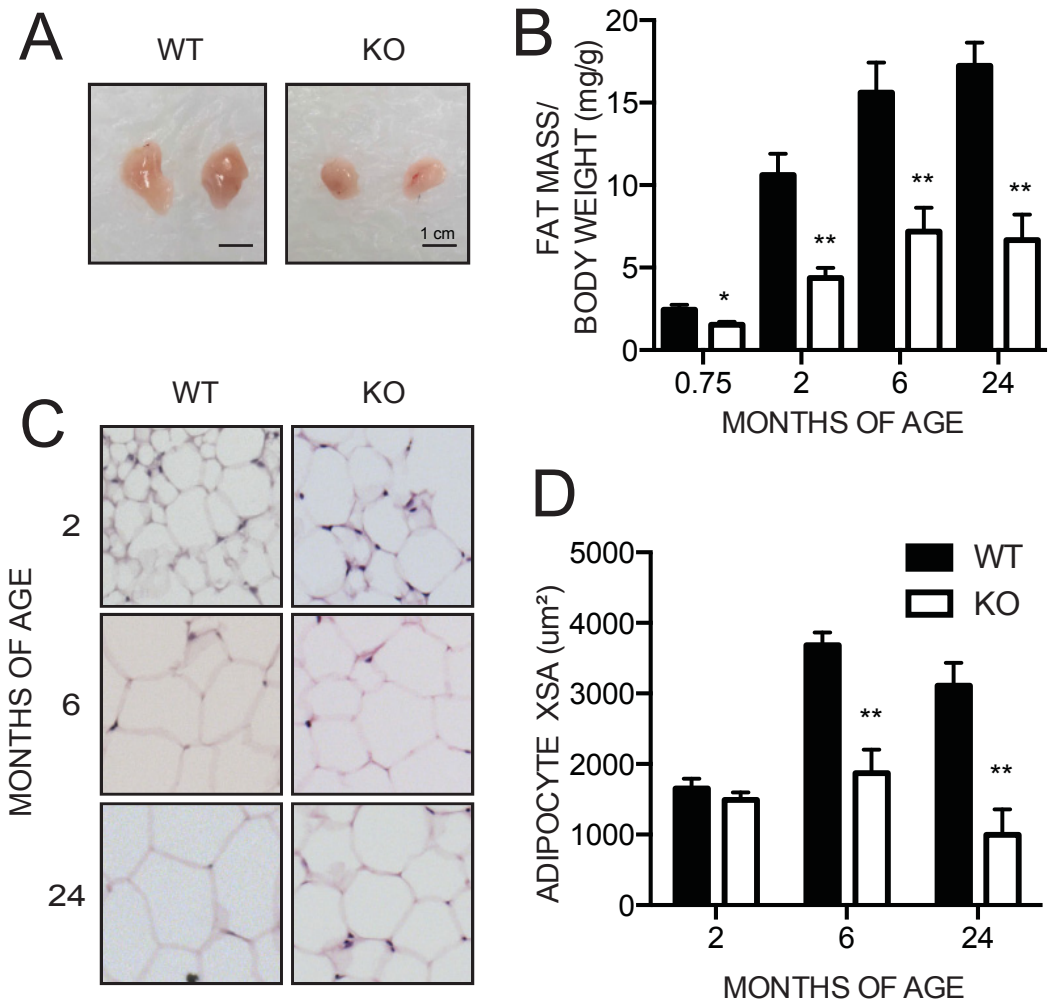

Figure 4.1: USP19 KO mice have smaller fat pads as a result of fewer and smaller adipocytes

(A) Representative images of epididymal fat pads from male USP19 WT and KO mice at 2 months of age. (B) Epididymal fat mass normalized to body weight at 0.75, 2, 6, and 24 months of age of USP19 WT and KO mice. n=8-15 (C) Representative images of epididymal fat sections from WT and KO mice at 2, 6, and 24 months of age. (D) Cross-sectional area of adipocytes in the epididymal fat pad n=3-6 mice per genotype and n >250 adipocytes per animal from 5 different fields. *p<0.05, **p<0.01.

4.2.2 Young USP19 KO mice have fewer proliferating adipocytes than WT mice

Since USP19 KO mice have fewer adipocytes and USP19 has been implicated in the regulation of proliferation by regulating KPC1, the ligase for cell cycle regulator p27 (295), we asked whether USP19 KO mice had fewer proliferating cells compared to WT mice. We administered bromodeoxyuridine (BrdU) to young (21 days post-partum) mice and allowed incorporation for 24 hours to label actively proliferating cells. After staining for BrdU and perilipin (an adipocyte marker) 24 hours after injection, we found that USP19 KO mice had 50% fewer BrdU+/Perilipin+ cells in the epididymal fat pad compared to WT mice suggesting a proliferation defect in KO cells (**Figure 4.2 A and 4.2 B**).

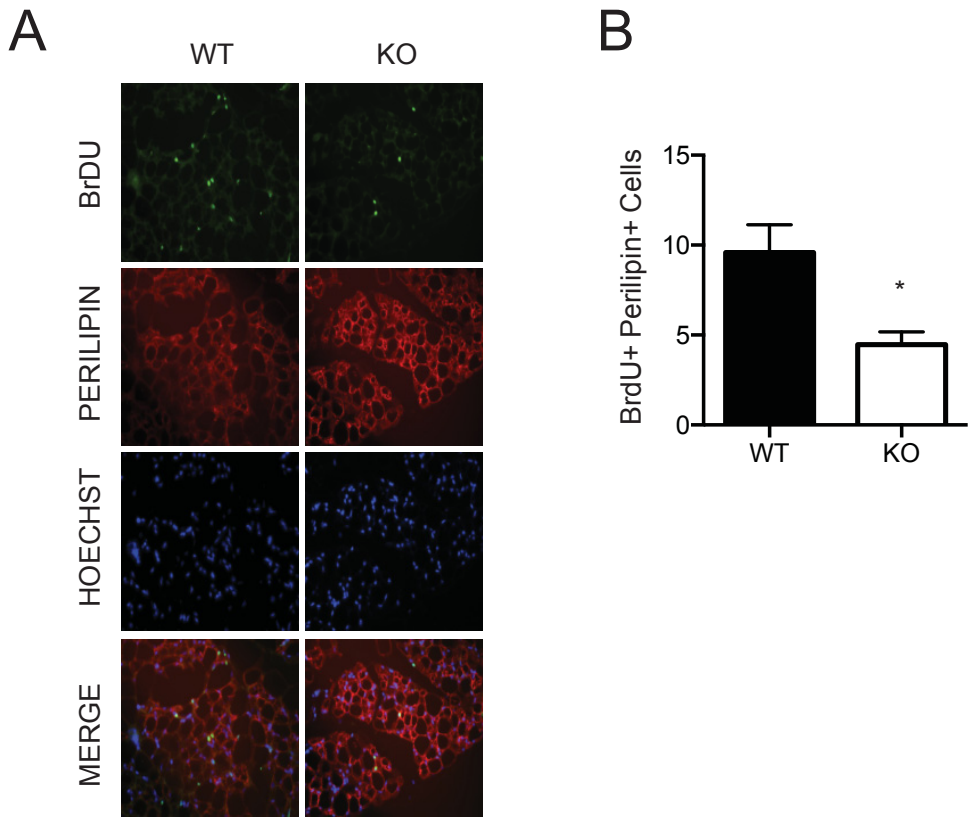

Figure 4.2: USP19 KO mice have fewer proliferating cells in the epididymal fat pad

(A) Representative images of epididymal fat pads from male USP19 WT and KO mice at 21 days of age injected with BrdU 24 hours before sacrifice. Green is BrdU, red is perilipin (an adipocyte marker) and blue is Hoechst (staining the nuclei). (B) Quantification of average BrdU+/perilipin+ cells per field. Five random fields per animal were selected and 50+ adipocytes per field were measured.

4.2.3 USP19 is upregulated during adipogenesis

In the previous sections, we showed that USP19 KO mice have fewer and smaller adipocytes suggesting that there may be a defect in fat cell development in these mice. To address this, we first asked whether USP19 is regulated during cellular differentiation into adipocytes. In mouse 3T3-L1 cells induced to differentiate into adipocytes in culture, USP19 is upregulated ~8 fold at the mRNA level (**Figure 4.3 A**) and ~3 fold at the protein level (**Figure 4.3 B**) on day 11 of differentiation.

4.2.4 USP19 is required for normal adipogenesis

Since USP19 is upregulated during adipogenesis, we next asked whether USP19 is required for this process to proceed normally. To dissect the role of USP19 in adipogenesis, we isolated the stromal vascular fraction from the inguinal fat pads of WT and USP19 KO mice and differentiated them into adipocytes *in vitro*. USP19 KO cells failed to accumulate lipid like WT cells as shown by marked reductions in staining by Oil Red O that labels neutral lipids (**Figure 4.4 A**). The differentiated cells isolated from KO mice expressed significantly lower levels of the critical regulator of adipogenesis, Pparg, as well as genes necessary for adipocyte function such as Fabp4, Adipoq, and Leptin (**Figure 4.4 B**). Additionally, the cells isolated from the KO mice expressed lower levels of PPARg protein (**Figure 4.4 C**). Therefore, USP19 is required for robust adipogenic differentiation of the SVF.

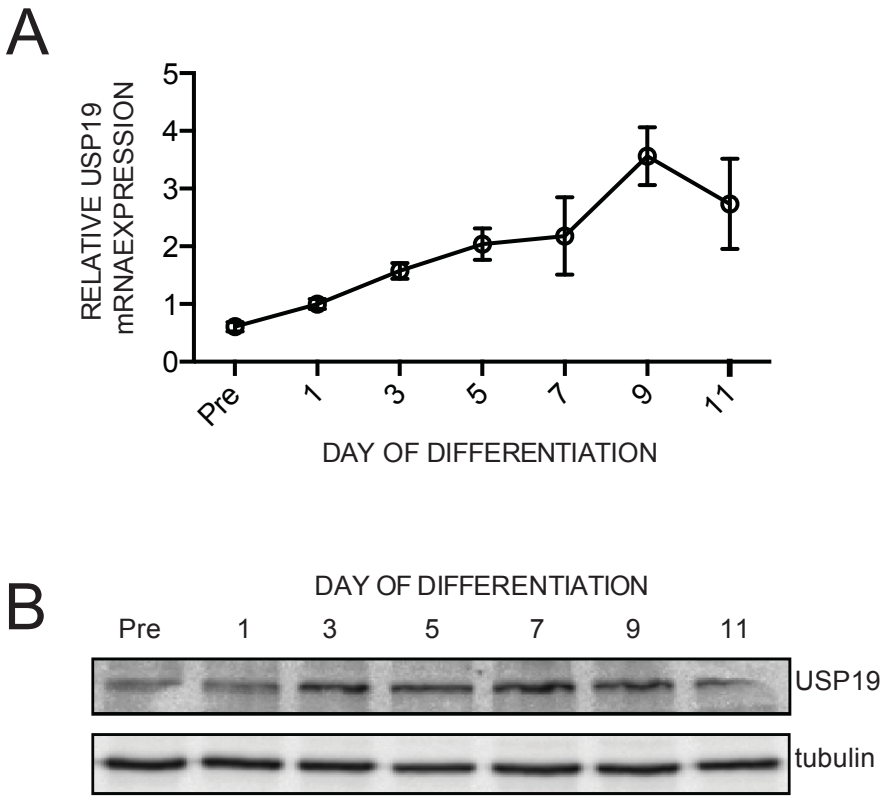

Figure 4.3: USP19 is upregulated during 3T3-L1 adipogenesis

(A) USP19 mRNA expression at multiple time points of adipogenic differentiation. (B) USP19 and tubulin protein levels at multiple time points of adipogenic differentiation. n=4-6

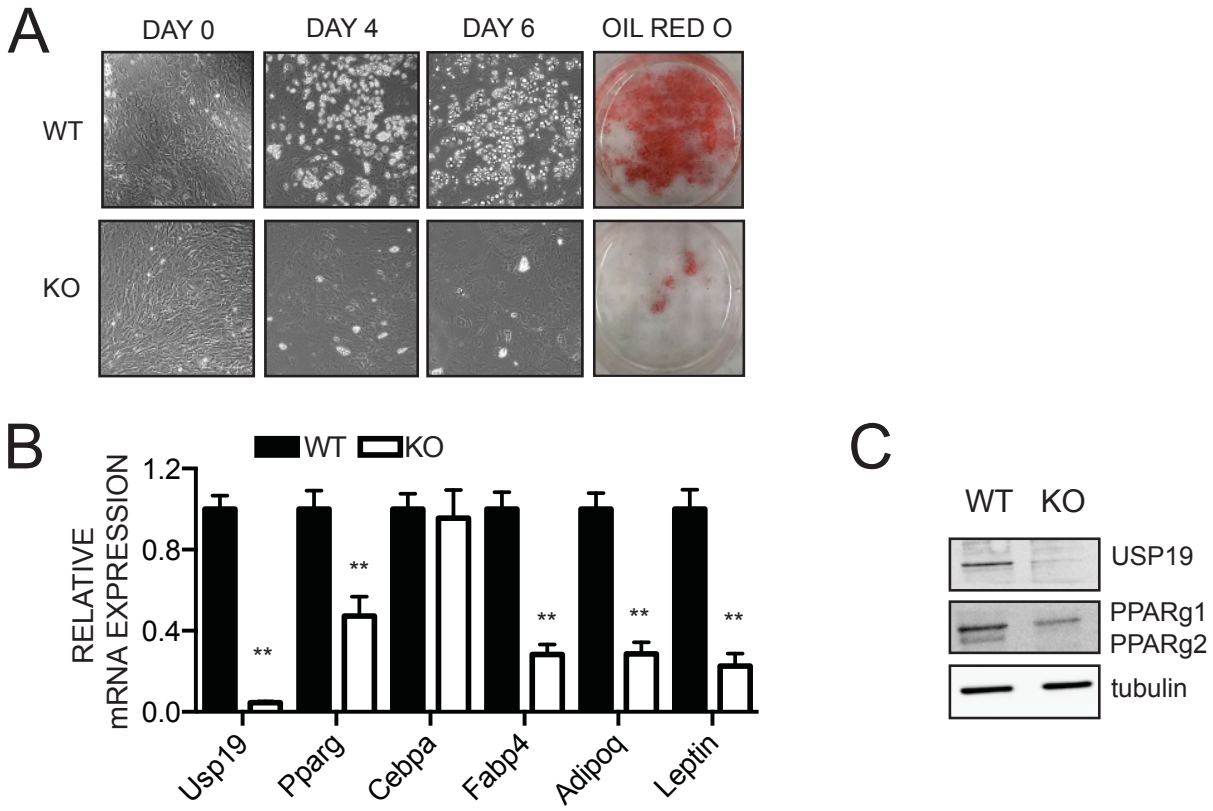

Figure 4.4: USP19 is required for normal adipogenesis

Stromal vascular fraction cells from USP19 WT and KO inguinal fat pads were isolated and differentiated in culture. (A) Representative brightfield images of differentiation of USP19 WT and KO cells and Oil red O stain on Day 9 of differentiation. (B) Gene expression of adipogenic genes on Day 9 of SVF differentiation from USP19 WT and KO cells. (C) Cells were harvested at Day 9 of differentiation and blotted for USP19, PPARg, and tubulin. n=3 *p<0.05, **p<0.05

4.2.5 USP19 KO mice remain leaner on a high-fat diet

To test whether this defect in adipogenesis would prevent the mice from developing obesity, we challenged the mice with a high-fat diet (HFD) where 60% of the calories come from fat. We found that USP19 KO mice weigh less than WT mice after 18 weeks on HFD (**Figure 4.5 A**). To assess the body composition of the mice, they were subjected to MRI. Interestingly, the KO mice had significantly lower levels of fat mass and higher levels of lean mass before and during high-fat feeding (**Figure 4.5 B and 4.5 C**).

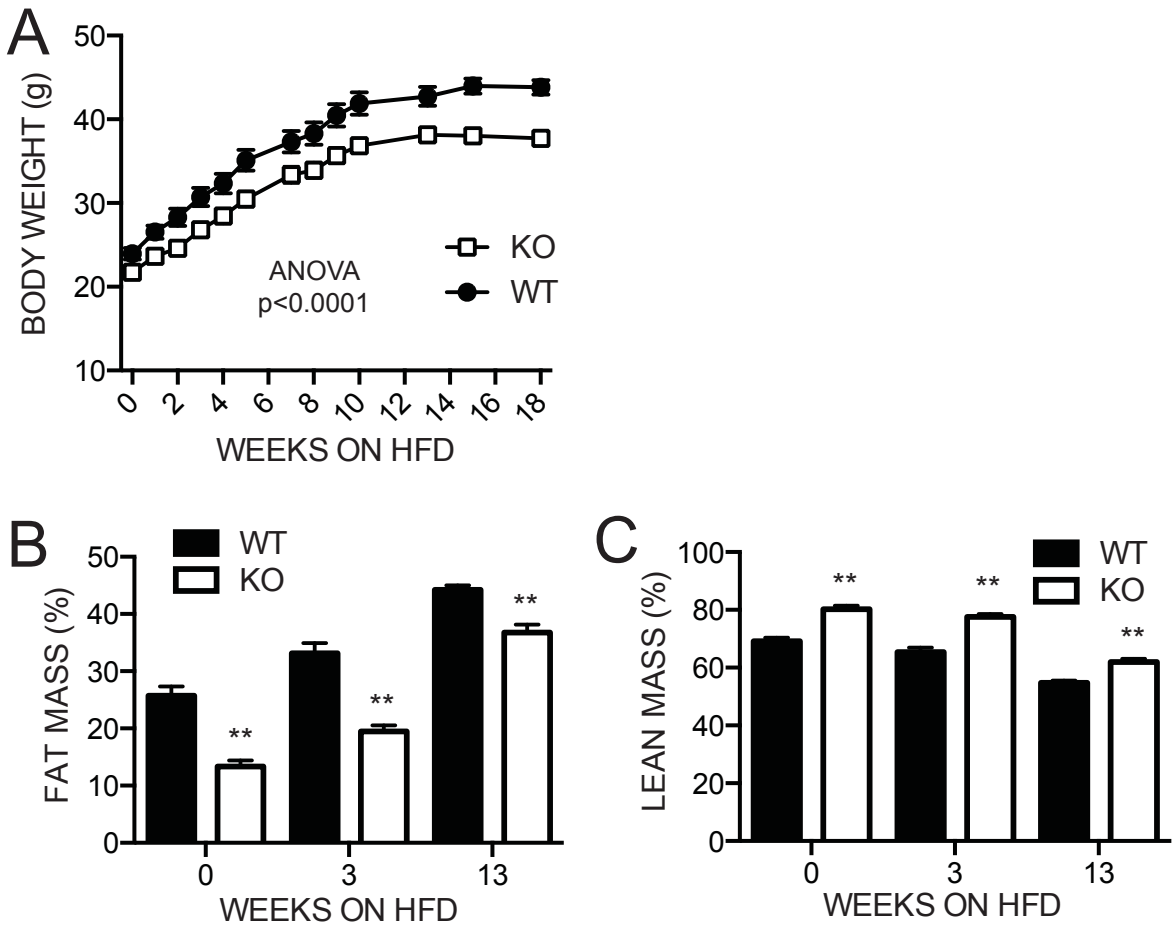

Figure 4.5: USP19 KO mice remain leaner on a high fat diet

WT and USP19 KO mice were put on a high-fat diet (HFD) for 18 weeks. (A) Body weight change on HFD. (B) Total body fat mass measured by MRI. (C) Total body lean mass measured by MRI. n=17 **p<0.01

4.2.6 USP19 KO mice have smaller livers and adipose tissue depots with larger muscles at the end of a high- fat diet

At sacrifice after HFD, USP19 KO mice had significantly lower body weight than WT mice (**Figure 4.6 A**). All tissue masses were normalized to body length because body weight differences were large (**Figure 4.6 B**). KO mice had smaller subcutaneous and brown adipose tissue fat pads, with a trend towards smaller epididymal fat pads (**Figure 4.6 C**). Consistent with the MRI results and a leaner body composition, USP19 KO mice had larger tibialis anterior and gastrocnemius muscles compared to WT mice (**Figure 4.6 D**). KO mice also had significantly smaller livers and hearts (**Figure 4.6 E**). Therefore, the overall body composition of USP19 KO mice at sacrifice is consistent with a leaner body with larger muscles and less fat compared to WT mice.

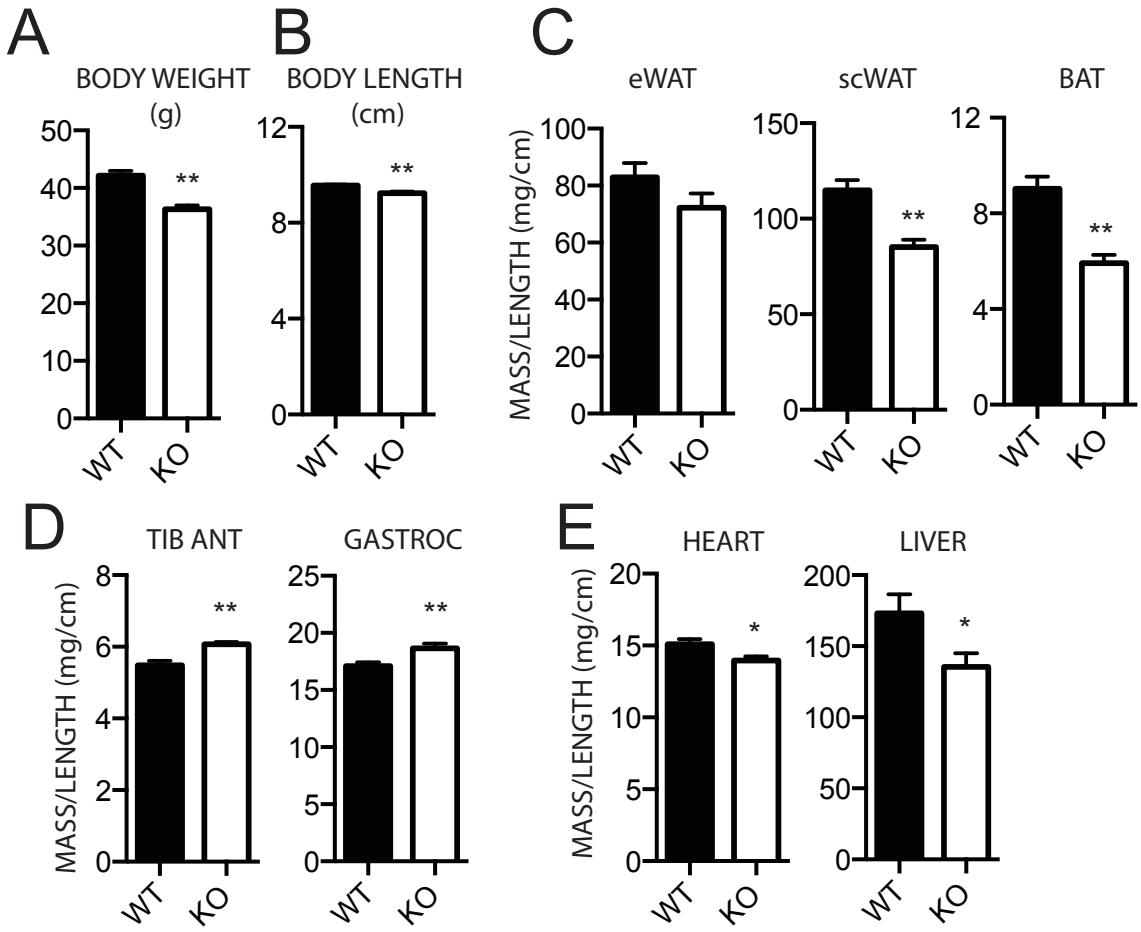

Figure 4.6: USP19 KO mice have smaller fat pads and larger muscles after HFD

USP19 WT and KO mice were put on HFD for 18 weeks. At sacrifice, tissues were collected. (A) Body weight (g) and (B) body length (cm) were measured. (C) Mass of the epididymal (eWAT), subcutaneous (scWAT) and brown (BAT) fat pads normalized to body length. (D) Mass of the tibialis anterior (TIB ANT) and gastrocnemius (GASTROC) muscles normalized to body length. (E) Mass of the heart and liver normalized to body length. n=15-16. *p<0.05, **p<0.01

4.2.7 USP19 KO mice have an altered metabolism on a high- fat diet

To understand what factors may be contributing to the altered body composition, the mice were housed in metabolic cages while indirect calorimetry, activity, and food intake were measured. USP19 KO mice consumed similar amounts of food on HFD (**Figure 4.7 A**) but had significantly increased locomotory activity compared to WT mice (**Figure 4.7 B**). Increased total activity was observed in the KO mice during both the light and the dark cycle (**Figure 4.7 C**). Consistently, USP19 KO mice consumed more O_2 (**Figure 4.7 D**) and produced more CO_2 (**Figure 4.7 E**) than WT mice, but their respiratory exchange ratio (RER) was similar (**Figure 4.7 F**). This suggests that on HFD, USP19 WT and KO mice are using the same dietary source of energy as fuel based on the similar RER, but the KO mice are metabolizing more fuel based on the increased O_2 consumed and CO_2 produced.

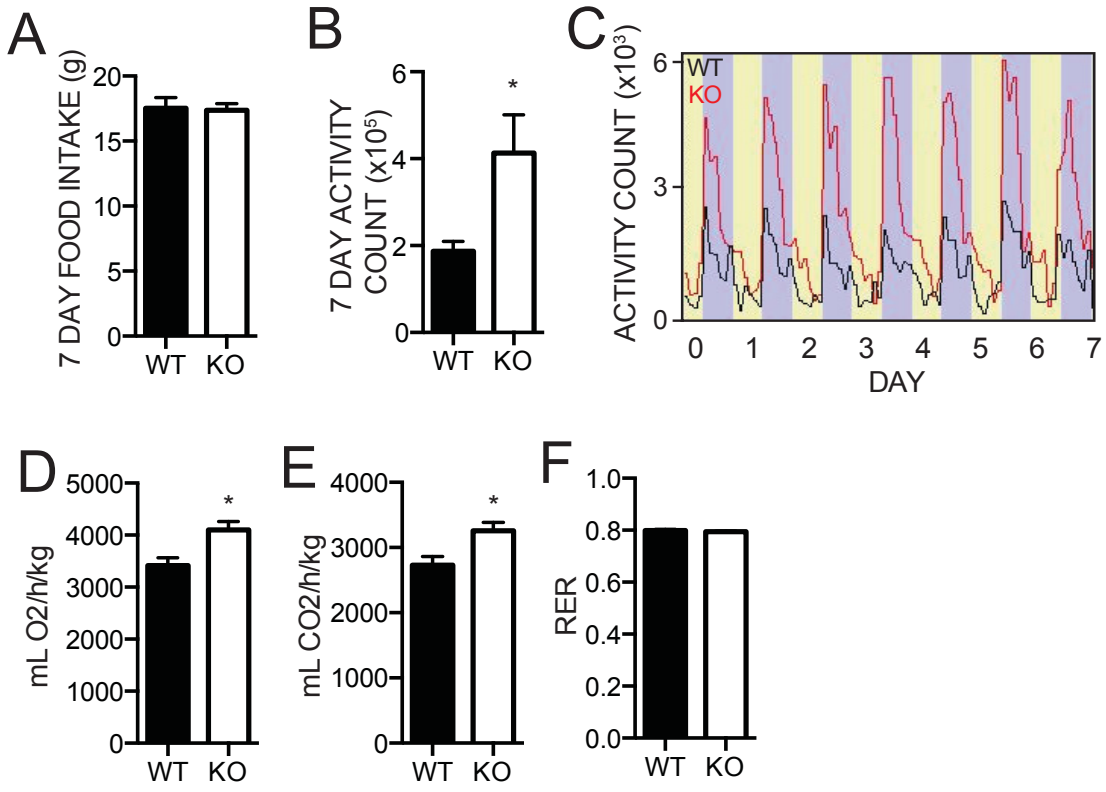

Figure 4.7: USP19 KO mice have altered metabolism on HFD

WT and USP19 KO mice on HFD were housed in metabolic cages for 7 days of acclimatization followed by 7 days of measurement. (A) Total food intake and (B) activity count. (C) Average activity excursions of WT and USP19 KO mice over 7 days in the metabolic cage. (D) Average O_2 consumption and (E) CO_2 production over 7 days on HFD. (F) Respiratory exchange ratio of CO_2 produced to O_2 consumed. n=8 *p<0.05.

4.2.8 USP19 KO mice are more insulin sensitive and glucose tolerant than WT mice

Based on the increased activity levels and leaner body composition of the KO mice, we evaluated the fasting glucose and insulin levels of WT and KO mice on HFD. USP19 KO mice had significantly lower fasting insulin levels despite similar fasting glucose levels (**Figure 4.8 A and 4.8 B**), yielding a lower HOMA index suggesting that they are more insulin sensitive than WT mice (**Figure 4.8 C**). To assess this further, we challenged these mice with an insulin tolerance test. Indeed, upon insulin administration, we saw enhanced blood glucose lowering in our KO mice (**Figure 4.8 D**). Additionally, KO mice were able to lower their blood glucose more effectively than WT mice during a glucose tolerance test (**Figure 4.8 E**). To test whether the KO mice showed effects on glucose metabolism in the liver, pyruvate, a substrate for gluconeogenesis, was administered to the mice and their blood glucose was monitored over time. The KO mice showed a lower level of glucose production compared to the WT mice (**Figure 4.8 F**) consistent with increased insulin sensitivity in the liver. Thus, USP19 KO mice have improved glucose metabolism on HFD.

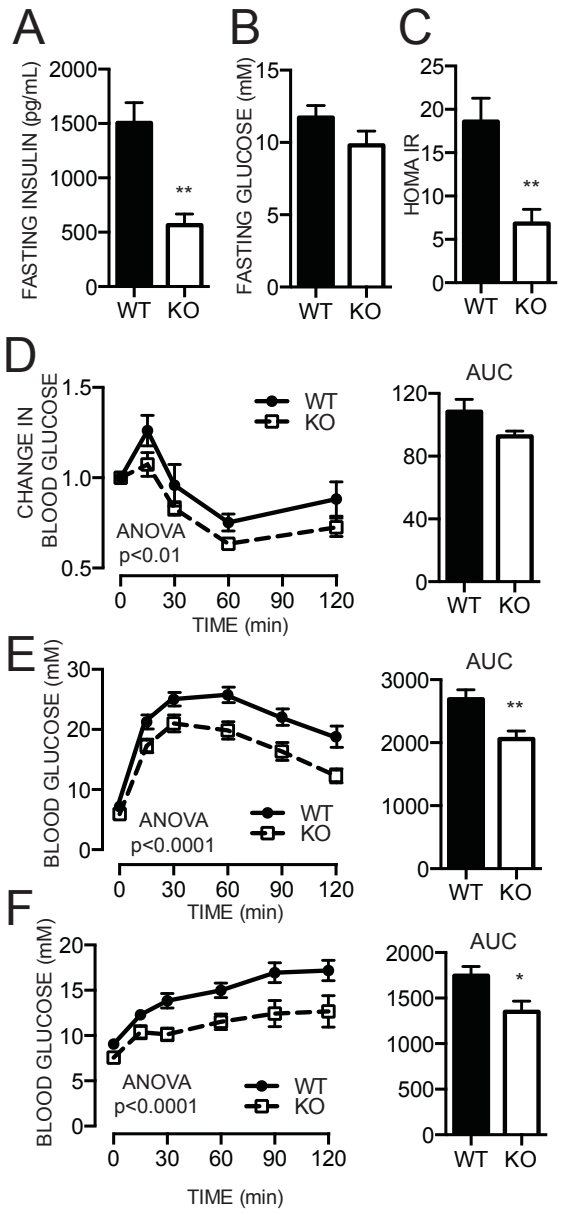

Figure 4.8: USP19 KO mice have improved glucose homeostasis on HFD

USP19 KO mice have improved glucose homeostasis. USP19 WT and KO mice were fasted overnight for 16 hours. (A) Fasting insulin levels and (B) blood glucose levels were assessed. (C) HOMA Index was calculated by multiplying fasting insulin and glucose and dividing by 22.5. (D) Insulin tolerance test was performed by injecting 1 U/kg insulin to the mice intraperitoneally and measuring blood glucose over time. Shown are values normalized to blood glucose at time 0. Area under each curve was calculated. (E) Glucose tolerance test and area under each curve was calculated. (F) Pyruvate tolerance test and area under the curve was calculated. n=10-21. *p<0.05, **p<0.01

4.2.9 USP19 KO mice have enhanced insulin signaling in muscle and liver but not adipose tissue

To explore the cellular physiology of this improved glucose homeostasis seen in section *4.2.8*, we assessed the activation by insulin of the Akt-mTOR signaling pathway in the insulin-sensitive tissues of the muscle, liver and adipose tissue. On a HFD, USP19 KO mice showed increased levels of phosphorylated Akt and $p70^{S6K}$ compared to WT mice in the skeletal muscle (**Figure 4.9 A and 4.9 B**), increased phosphorylated Akt in the liver (**Figure 4.9 C and 4.9 D**), but no increased signaling in the adipose tissue (**Figure 4.9 E and 4.9 F**). No changes were observed in the level of the insulin receptor (IR) or insulin receptor substrate (IRS-1) in these mice. This suggests that the ability of USP19 to maintain better glucose homeostasis is due to increased insulin signaling in the muscle and the liver, but not the adipose tissue.

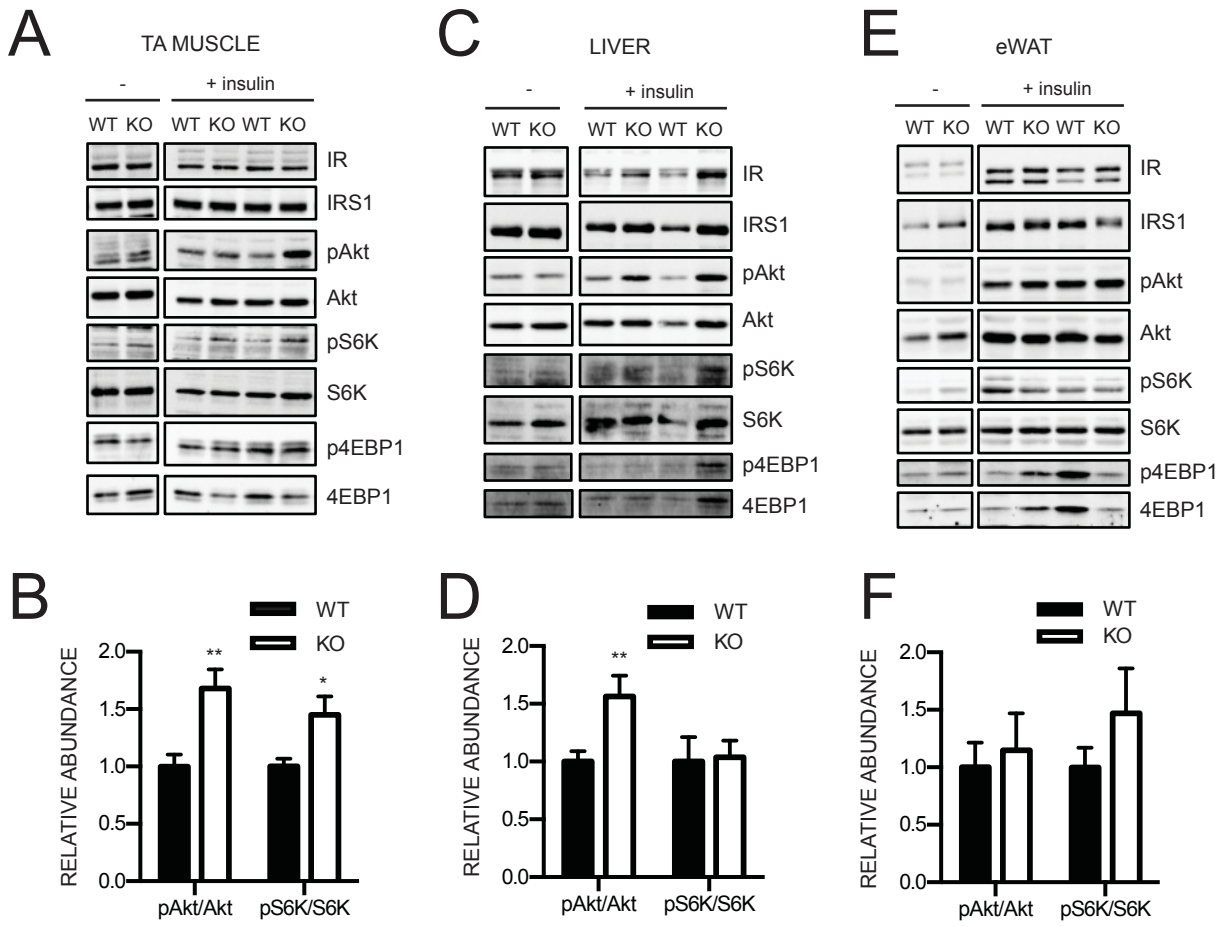

Figure 4.9: USP19 KO mice have enhanced insulin signaling in the muscle and liver

USP19 WT and KO mice were injected with 1 U/kg insulin 20 minutes prior to sacrifice. (A) TA muscle (C) liver and (E) eWAT were homogenized and homogenates were analyzed by western blot for indicated components of the insulin signaling pathway. (B, D, F) Quantification of insulin-stimulated phosphoAkt on the threonine 308 residue normalized to total amount of Akt and of phosphoS6K normalized to the total amount of S6K all relative to WT. n=8-12. *p<0.05, **p<0.01

4.2.10 USP19 KO mice have low levels of the adipokine leptin

To understand why USP19 KO mice have enhanced insulin signaling and improved glucose tolerance, we assessed the adipokine profile of these mice. Many adipokines are known to induce insulin resistance (Tnfa, Il6, Retn, Rbp4, Lcn2) or promote insulin sensitivity (Angptl2, Adipoq, Leptin, Nampt). To assess the adipokine profile of the adipose tissue we looked at the mRNA levels of relevant adipokines in the epididymal white adipose tissue. Leptin was significantly lower at the RNA level in the white adipose tissue of KO mice (**Figure 4.10 A**). Leptin levels were also significantly lower in the serum of male KO mice on normal diet (ND) or HFD and trending towards significantly lower levels in female mice on normal diet (**Figure 4.10 B**). Serum adiponectin, another critical adipokine was no different between WT and USP19 KO mice (**Figure 4.10 C**). Therefore, USP19 KO mice have very similar adipokine profiles compared to WT mice except for decreased Leptin levels, consistent with decreased fat mass in KO mice.

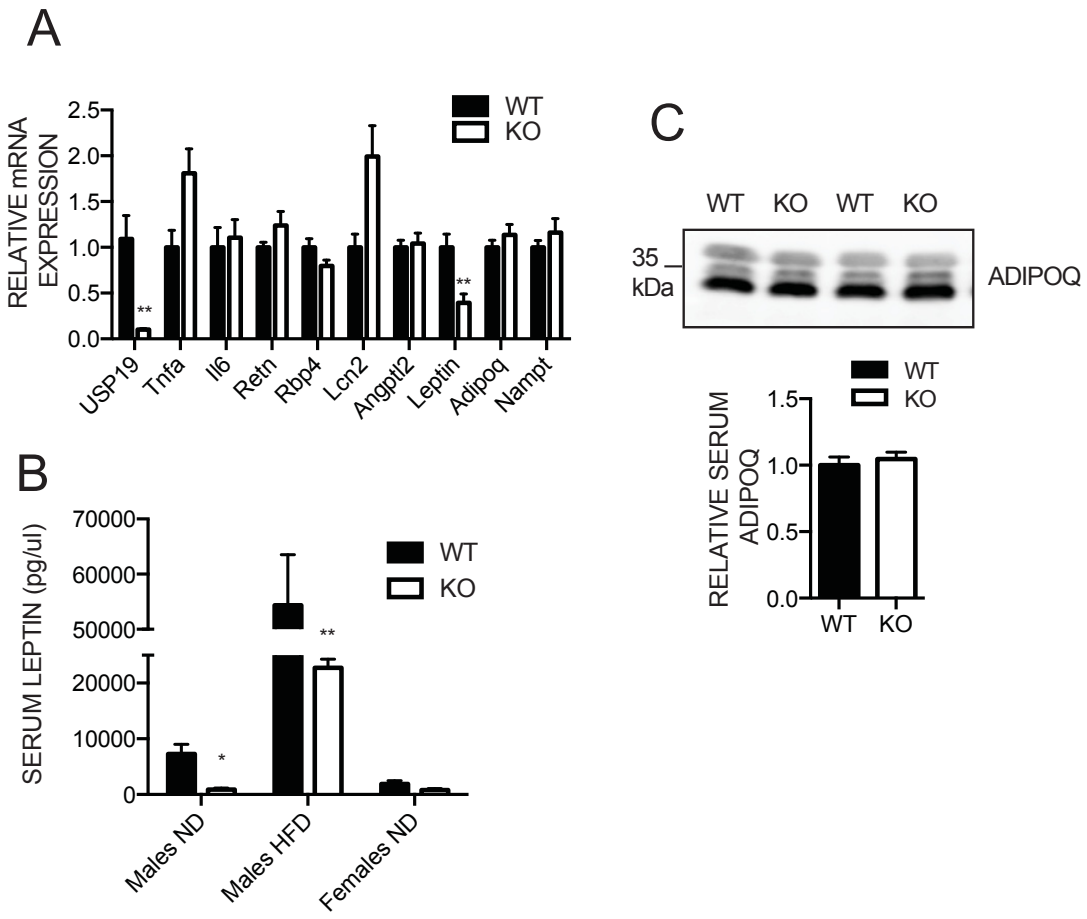

Figure 4.10: USP19 KO mice have lower levels of the adipokine leptin

(A) Adipokine mRNA levels were assessed in WT and USP19 KO epididymal white adipose tissue on a normal diet (ND). (B) Serum leptin was measured in male mice on ND or HFD and in female mice on a ND. (C) Serum adiponectin levels were measured by western blot.

4.2.11 USP19 KO mice do not accumulate fat in the liver on a high-fat diet

Another major contributor to metabolic dysfunction and insulin resistance is the development of non-alcoholic fatty liver disease (NAFLD) during diet-induced obesity. USP19 KO mice had smaller livers at the end of the HFD (**Figure 4.11 A**). To test whether USP19 KO mice had smaller livers because the liver accumulated less fat, we examined the livers of WT and KO mice after high-fat diet by histology. We observed much larger lipid vacuoles in the hepatocytes of WT mice compared to KO mice. Therefore, USP19 KO mice do not accumulate lipid in the liver to the same extent as WT mice (**Figure 4.11 B**).

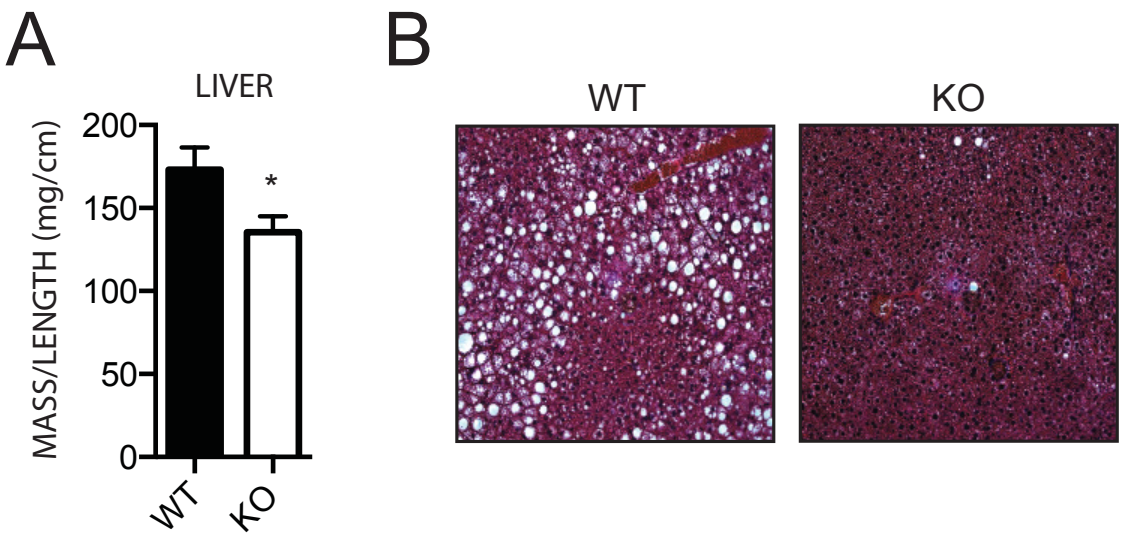

Figure 4.11: USP19 KO mice accumulate less fat in the liver

(A) Mass of livers normalized to body length after 18 weeks on HFD. (B) Representative images of H&E stained liver from WT and USP19 KO mice after 16 weeks on HFD.

4.2.12 USP19 mRNA expression in human adipose tissue is similar in groups with BMI 35-40 **kg/m^2** *or BMI 60-69* **kg/m^2**

Since inactivation of USP19 in mice resulted in a phenotype that is leaner and is protected from much of the metabolic dysfunction associated with obesity. We next asked whether USP19 is important for human adipose tissue function. To explore this, we asked whether USP19 mRNA expression was increased in subjects with higher BMI, so we compared groups with BMI 35-40 kg/m^2 or 60-69 kg/m^2. Samples were obtained as fat biopsies from patients undergoing bariatric surgery, and patients with diabetes were excluded from the analysis. We assessed adipose tissue from the visceral abdominal depot (omental and mesenteric) as well as from a subcutaneous depot. It is suggested in the literature that there is an association between high levels of abdominal obesity and insulin resistance (319). There was no difference in USP19 mRNA expression between the two groups of BMIs in the mesenteric (**Figure 4.12 A**), omental (**Figure 4.12 B**) or subcutaneous (**Figure 4.12 B**) adipose tissue depots. Since BMI may not be accurately representative of body fat distribution, we used the waist to hip ratio (WHR) as a better indicator of fat distribution. The higher the waist to hip ratio, the more visceral adiposity there is. Again, there was no significant correlation between USP19 expression and WHR (**Figure 4.12 A-C**)

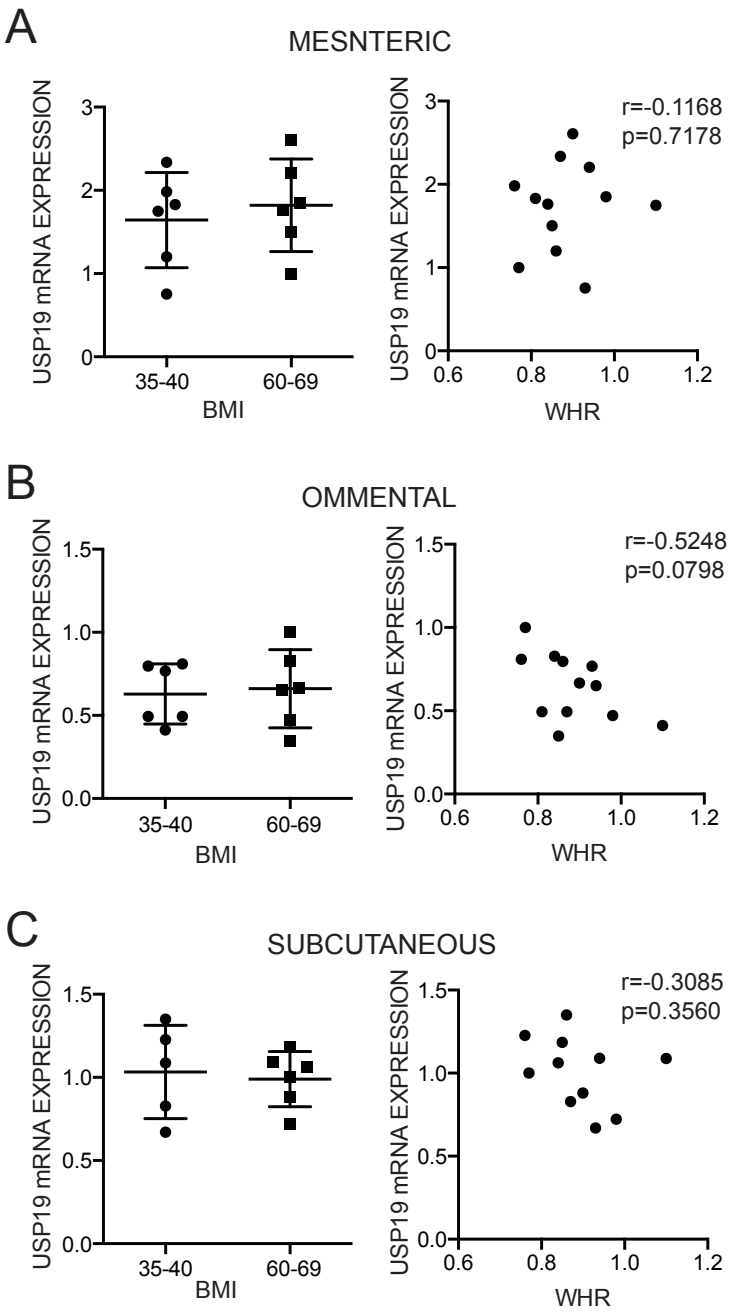

Figure 4.12: No difference in human USP19 expression between high BMI and very high BMI groups

USP19 mRNA expression in (A) mesenteric, (B) omental or (C) subcutaneous adipose tissue biopsies between two groups of subjects one with BMI 35-40 kg/m^2 and the other with BMI 60-69 kg/m^2 as well as correlation to waist to hip ratio (WHR).

4.2.13 USP19 mRNA expression is correlated to adipogenic gene expression only in visceral adipose tissue

Because we did not observe any relationship between USP19 expression in adipose tissue and BMI, we asked whether there was a relationship between USP19 and adipogenic gene expression at the cellular level. To explore this, we tested whether USP19 expression is correlated to the expression of genes involved in critical adipose tissue processes such as PPARg, FABP4, ADIPOQ, and LEPTIN. USP19 expression was significantly correlated to the expression of PPARg, FABP4, and ADIPOQ in the mesenteric and omental adipose tissue (**Figure 4.13 A and 4.13 B**). Interestingly, this correlation was not seen in the more metabolically inert subcutaneous adipose tissue (**Figure 4.13 C**). This suggests that USP19 may play a role in human adipose tissue function.

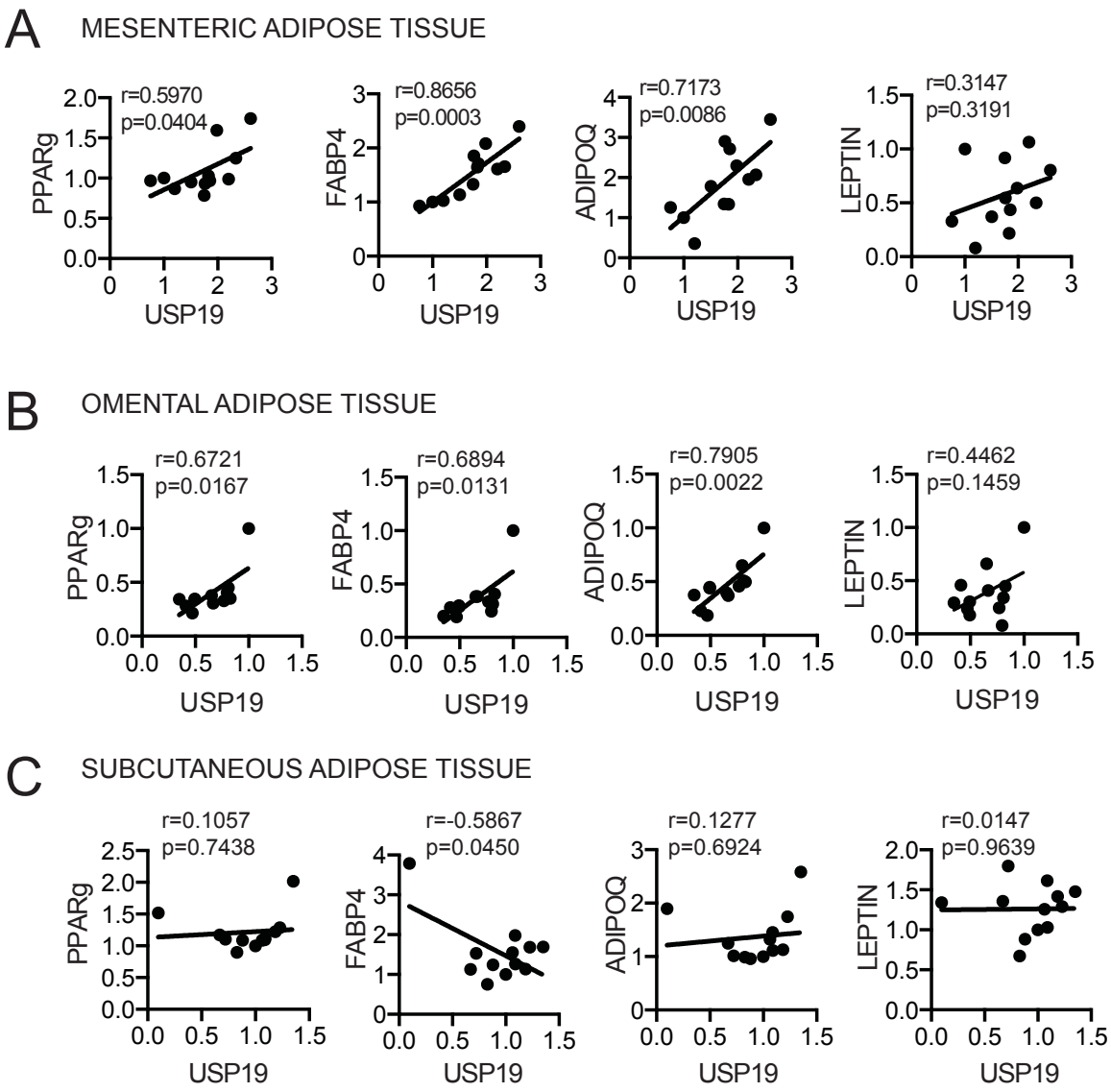

Figure 4.13: Human mesenteric and omental adipose tissue USP19 mRNA expression is positively correlated to adipocyte gene expression

(A) Mesenteric, (B) omental and (C) subcutaneous white adipose tissue RNA expression was analyzed. USP19 expression is plotted against the expression of PPARg, FABP4, ADIPOQ or LEPTIN. Pearson correlation analysis was performed. r and p values are presented in the figure. n=12 subjects.

4.3 Discussion

In this chapter, we show for the first time that USP19 is important in adipose tissue development and that the inactivation of USP19 reduces fat mass and delays the development of the metabolic consequences of high-fat feeding including diabetes and fat accumulation in the liver.

We show that USP19 KO mice have a defect in fat accumulation throughout the lifespan. This effect on fat mass appears to be due in part to an effect on proliferation of early adipocytes, and a defect in adipogenesis as the inactivation of USP19 resulted in the inability to upregulate adipogenic genes and accumulate lipid during this process. A recent publication showed that USP19 is downregulated during adipogenesis in 3T3L1 cells and mouse embryonic fibroblasts but does not further explore the role of USP19 in this process (320). Our data showed that USP19 is upregulated in 3T3-L1 cells at the mRNA and protein level. The reason for the discrepancies between these two observations is currently unknown. Other deubiquitinating enzymes are also important for adipogenesis, namely USP7 regulating the ubiquitination of PPARg as well as the histone acetyltransferase TIP60 15 16 (321,322). Uchl3 has also been implicated in adipogenesis and cells isolated from Uchl3 KO mice fail to undergo adipogenesis (323).

We did not observe any difference in USP19 mRNA expression in human adipose tissue between two groups of subjects with distinct BMIs. However, these samples come from patients who have high BMIs and have been subdivided into high (35-40 kg/m^2) and very high (60-69

kg/m^2) BMI categories. It remains to be seen if USP19 expression might be correlated with BMI if we had a range of BMIs from 20 to 70. We did find that USP19 mRNA expression is positively correlated to some important adipocyte genes including PPARg, FABP4, and ADIPOQ. Intriguingly, this correlation only exists in the omental and mesenteric adipose tissues and not the subcutaneous depot. The amount of intra-abdominal adipose tissue (omental and mesenteric) is associated with increased insulin resistance during obesity (319,324,325). This suggests that higher USP19 expression results in more adipogenic adipose tissue and would follow the results we saw in the mouse where loss of USP19 results in fewer and smaller adipocytes. Interestingly, in the mouse model, we observed decreases in leptin upon loss of USP19, but no changes in adiponectin levels, seemingly the opposite of what we observed in the human samples. This may be due to differences between species or differences in adiposity as the animal studies were performed on chow fed mice, while the human analysis was performed on obese individuals. Additionally, in the mouse model, we saw effects of USP19 inactivation on insulin signaling in both muscle and liver. Thus, it is possible that USP19 may have a broader systemic metabolic effect in humans, but this remains to be explored.

The decreased fat mass observed in the USP19 KO mice was associated with improved glucose homeostasis. On high-fat diet, USP19 KO mice showed better blood glucose lowering capabilities when insulin is administered and improved glucose tolerance. Additionally, hepatic glucose production from the gluconeogenic substrate pyruvate was significantly lower in the KO

mice. In chapter 3 of this thesis, we showed that USP19 KO mice also have improved glucose, insulin and pyruvate tolerance on a normal diet. Taken together, USP19 KO mice on a normal diet or a HFD have improved glucose homeostasis. Interestingly, insulin signaling is only enhanced in the muscle and liver of the KO mice on HFD. This suggests that the main differences in glucose homeostasis may be due to increased glucose disposal in the muscle, not the adipose tissue, and decreased glucose production from the liver. It remains to be explored whether insulin-regulated processes in the adipose tissue, such as lipogenesis and lipolysis, are affected in the KO mice. However, since insulin signaling is similar between WT and KO in the adipose tissue, it is possible that there are no differences in these processes. The exact mechanism through which USP19 is modulating insulin signaling is still elusive. In chapter 3, we showed that USP19 modulated glucocorticoid receptor (GR) protein levels. GR signaling is well known to negatively regulate insulin signaling through the upregulation of a variety of genes such as Pi3kr1 (P85α) or Ddit4 (REDD1) which regulate PI3K and mTOR respectively (309). Thus, it is possible that decreased levels of GR in the KO mice contribute to the increased insulin signaling observed. Additionally, decreased GR levels could contribute to the decreased adipogenesis in USP19 KO mice, as glucocorticoids are an important signal for early adipogenic induction *in vitro* (326).

Finally, we showed that USP19 KO mice are more physically active than WT mice. This increase in activity could potentially explain some of the phenotypes we observed in these mice. Since this is a whole-body KO, USP19 expression may be important in the brain. Lack of USP19

in the brain could lead to altered behaviour that results in increased locomotory activity and therefore results in altered metabolism in these mice. Using the incoming calories for locomotion rather than storing it as triacylglyerol in the adipose tissue could explain the leaner phenotype that we observe. Additionally, increased physical activity is associated with increased insulin sensitivity (327) and so could explain the increased insulin sensitivity and signaling that we observed in the KO mice. However, we do see cell-autonomous effects of USP19 suggesting that physical activity is not the only driver of the phenotype. For example, when the SVF from WT and USP19 KO mice is cultured in vitro, we observe a significant decrease in fat accumulation. In the future, tissue-specific knockouts will help tease out the tissue intrinsic metabolic role of USP19.

Together, these studies yield insights into how a deubiquitinating enzyme, USP19, may modulate fat development and protect from the development of diabetes. The direct substrate or substrates that USP19 acts on in these metabolic processes are still unknown. As stated above, GR is an intriguing candidate that will be explored further in Chapter 5. Identification of these substrates could lead to the development of novel inhibitory molecules with potential in the clinic to protect from the development of obesity and diabetes.

CHAPTER 5

RESULTS

USP19 regulates the level of the glucocorticoid receptor

5.1 Preface to Chapter 5

Identifying the molecular substrates of USP19 deubiquitinating action will be important if USP19 is to become a valuable druggable target. Deubiquitinating enzymes (DUB) likely have multiple substrates and because of this, small molecules that inhibit the enzymatic activity of DUBs may have undesirable downstream effects. Thus, identifying direct substrates of USP19 will allow for the development of molecules that will disrupt the interaction between USP19 and specific substrates.

In chapter 3, we identified two pathways that are modulated by USP19 – the insulin and glucocorticoid signaling pathways. We also showed that USP19 KO mice have lower levels of glucocorticoid receptor (GR) protein. Finally, we showed that restoring the levels of GR in KO mice is sufficient to reverse protection from muscle atrophy observed in these mice. Taken together, this data suggests that GR may be a substrate of USP19 that mediates its important actions in muscle. Additionally, in chapter 4, we showed that USP19 is required for adipogenesis to proceed normally *in vitro*. Glucocorticoid signaling enhances adipogenesis by inducing the expression of transcription factors such as CEBPβ and CEBPδ. In the absence of USP19, and potentially dysregulated GR signaling, adipogenesis would not be able to proceed normally. Thus, GR being a substrate of USP19 could also explain the phenotypes that we observed in chapter 4. This chapter explores whether GR is a genuine substrate of USP19 deubiquitinating action that may be mediating the metabolic phenotypes observed in USP19 KO mice.

5.2 Results

5.2.1 GR protein levels are lower but mRNA levels are similar in USP19 KO mice

In the absence of a deubiquitinating enzyme, the substrate will be more ubiquitinated. This increase in ubiquitination can result in increased proteolysis of the substrate or changes in cellular signaling, depending on the nature of the ubiquitin chain. If the substrate is directed towards proteolysis, steady-state levels of the protein will be decreased while mRNA levels will be similar. To assess if GR is a substrate of USP19, we looked at both the protein and mRNA level of GR in the metabolic tissues of WT and USP19 KO mice. We found that GR protein levels are 50% lower in the muscle (**Figure 5.1 A**), liver (**Figure 5.1 B**) and adipose tissue (**Figure 5.1 C**) of KO mice. Additionally, the mRNA levels of GR are nearly identical between WT and USP19 KO mice in all of these tissues (**Figure 5.1A-C**). Finally, we asked if this effect on GR protein level persists in KO cells *ex vivo*, suggesting a possible cell-autonomous effect of USP19 on GR levels. Indeed, we observed significantly decreased GR protein levels in primary cells isolated from the muscle, liver and adipose tissue of USP19 KO mice (**Figure 5.1 D**). Because the effect of USP19 on GR protein levels persisted in cells cultured *ex vivo*, it was unlikely due to high levels of circulating glucocorticoid in the KO which could down regulate the receptor. Indeed, when we measured circulating levels of corticosterone, they were similar in WT and KO mice (**Figure 5.1 E**). Together, these data suggest that USP19 regulates the level of GR post-transcriptionally.

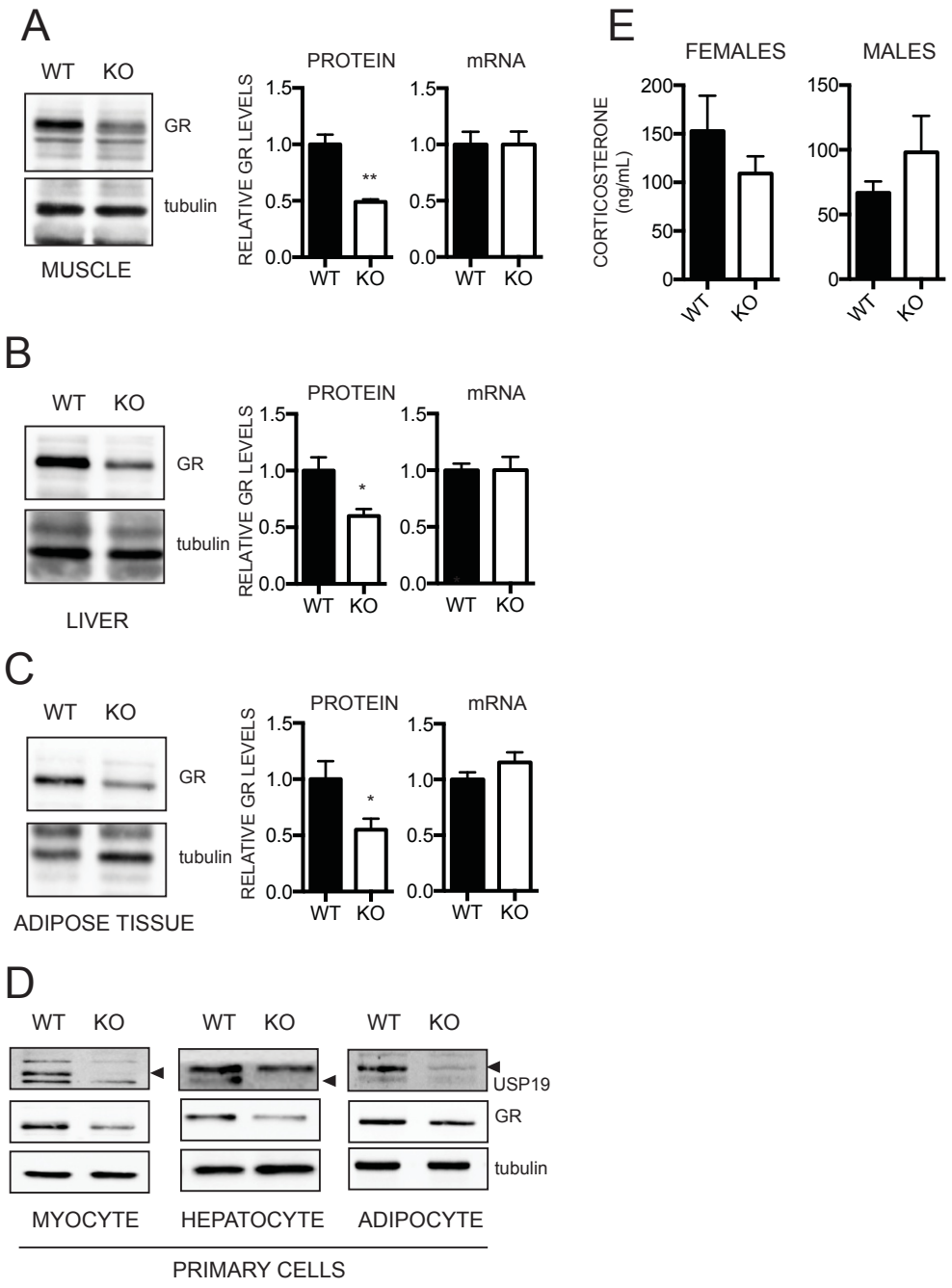

Figure 5.1: GR protein levels are lower but mRNA levels are similar in USP19 KO mice metabolic tissue

(A) GR protein and mRNA level in muscle. (B) GR protein and mRNA level in liver. (C) GR protein and mRNA level in adipose tissue. (D) GR protein levels in primary cells isolated from muscle, liver and adipose tissue. (E) Serum corticosterone levels in overnight fasted mice n=5-8. *p<0.05, **p<0.01

5.2.2 USP19, GR, and HSP90 interact

Because GR protein levels are lower in USP19 KO tissues suggesting that GR might be a substrate of USP19, we next asked if USP19 and GR interact in the cell as would be expected if GR is a substrate of USP19. Interestingly, USP19 has been shown to interact with HSP90 (293,300,328), the cytosolic chaperone for GR. Therefore, we hypothesized that the three proteins might interact in a complex. To test this, we expressed HA-GR and Flag-USP19 in HEK293 cells and immunoprecipitated HA-GR from the lysate and asked if Flag-USP19 and endogenous HSP90 co-immunoprecipitated. We can see that HSP90 and a small fraction of Flag-USP19 can co-immuniprecipitate with a tagged HA-GR (**Figure 5.2 A**). To explore whether this interaction occurs with endogenous proteins *in situ* in C2C12 muscle cells, we used a proximity ligation assay, in which cells are fixed and permeabilized and incubated with antibodies against the potentially interacting proteins. Secondary antibodies are coupled to oligonucleotides which can anneal if the two proteins are in extremely close proximity (less than 40 nm) and therefore are likely to be interacting. Subsequent addition of ligase and polymerase and fluorescently labeled oligo nucleotide results in generation and amplification of a fluorescent signal. We observed that USP19 and GR, USP19 and HSP90, and HSP90 and GR all produce a signal indicating that they interact in a binary fashion (**Figure 5.2 B**). Finally, we asked whether USP19, GR and HSP90 co-localize in the cell and tested this using immunofluorescence analysis. Though these three proteins exist diffusely in the cytoplasm, we show that there is some co-localization between USP19 and GR,

USP19 and HSP90 and GR and HSP90 in C2C12 cells (**Figure 5.2 C**). Together these data suggest that USP19, GR, and HSP90 interact and they may exist in a complex in the cell.

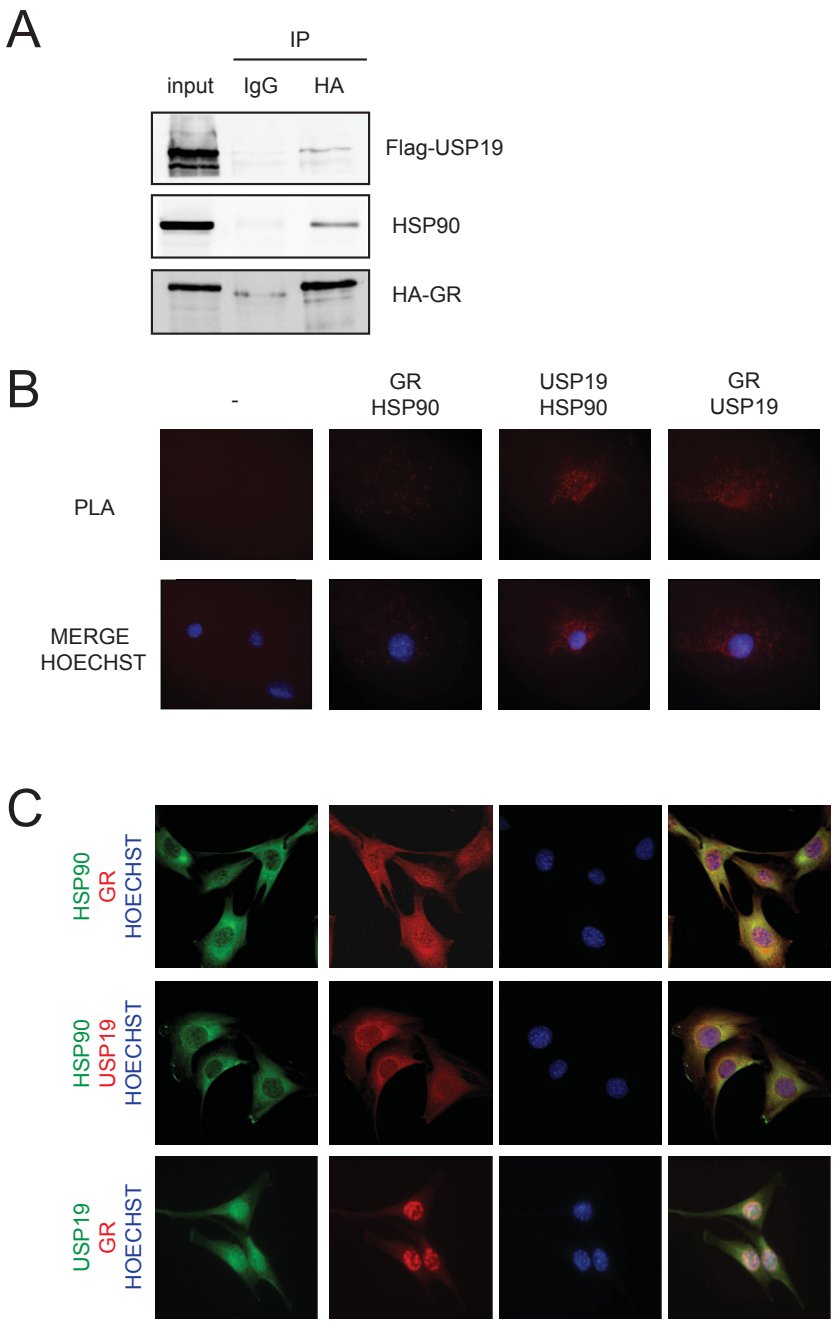

Figure 5.2: GR, USP19, and HSP90 interact

(A) HA-GR and Flag-USP19 were expressed in HEK293 cells and an HA-specific antibody was used to immunoprecipitate GR and any associated proteins. (B) Proximity ligation assay to identify *in situ* interactions between GR and HSP90, USP19 and HSP90, or GR and USP19 in C2C12 muscle cells. (C) Indirect immunofluorescence analysis in C2C12 muscle cells. Cells were fixed and probed with antibodies against HSP90, GR, and USP19 and visualized with a laser scanning confocal microscope.

5.2.3 GR protein is more ubiquitinated and more rapidly degraded in USP19 KO cells

In the previous sections, we established that GR levels are lower in KO mice and that GR and USP19 interact in the cell. These data suggested that GR may be a true substrate of USP19 deubiquitinating action. We next asked whether GR is more ubiquitinated in the absence of USP19. To test this, we treated CTL and USP19 KO HEK293T cells with or without the proteasome inhibitor MG132 to accumulate ubiquitinated proteins destined for proteasomal degradation. We observed an increase in the smear of higher molecular weight, presumably ubiquitinated, GR upon proteasome inhibition in USP19 KO cells (**Figure 5.3 A**). Next, we asked whether this increased ubiquitination of GR in KO cells causes a more rapid degradation of GR. To test this, we inhibited protein synthesis with cycloheximide (CHX), and monitored the degradation of GR in CTL and KO cells over time. We observed significantly more rapid degradation of GR in KO cells compared to WT cells (**Figure 5.3 B**). GR levels appeared to be higher in the KO cells in the basal state. This was likely due to increased transfection efficiency of the KO cell line as GR mRNA levels following transfection of the GR expressing plasmid were higher than in the WT parental cell line similarly transfected.

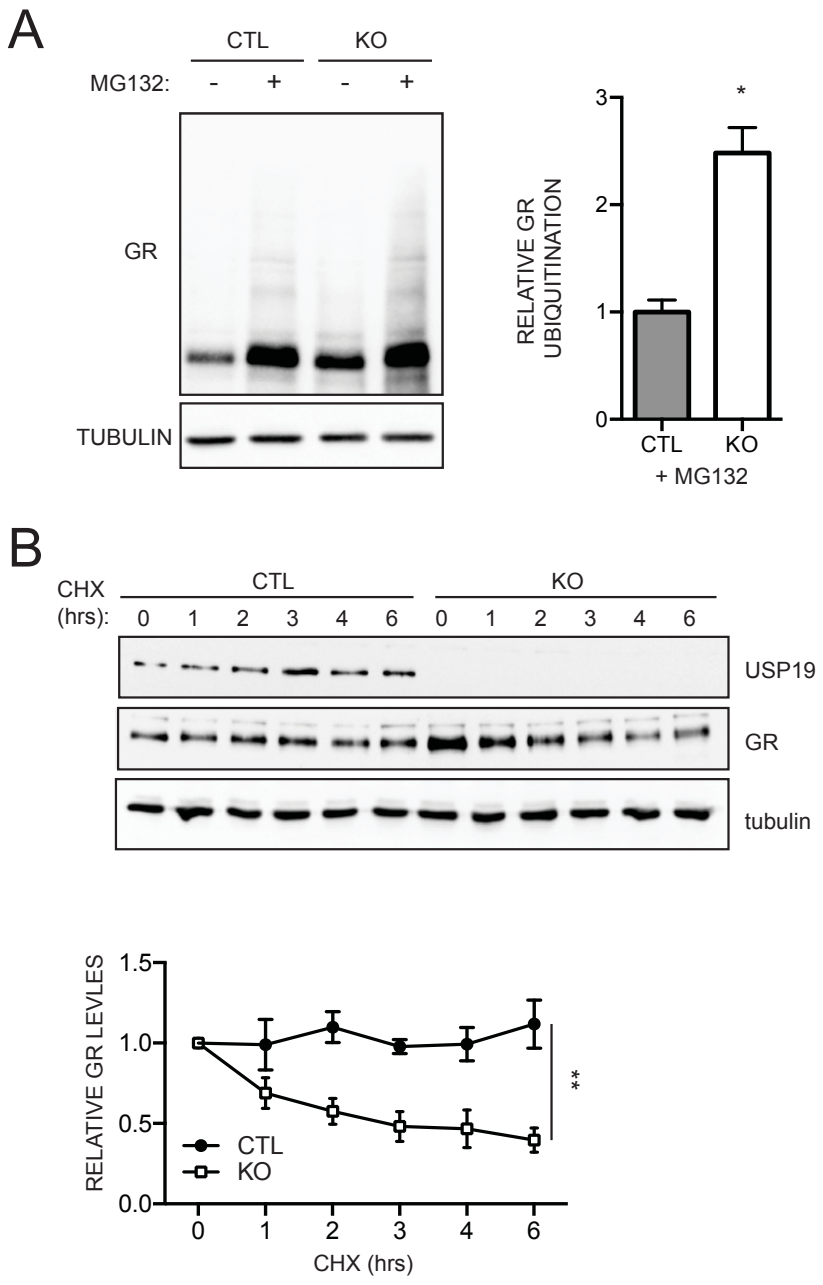

Figure 5.3: GR is more ubiquitinated and more rapidly degraded in USP19 KO cells

(A) 293T CTL and KO cells were transfected with plasmid expressing HA tagged GR and exposed to proteasome inhibitor MG132 for 6 hours. GR levels and higher molecular weight species of GR were observed and quantified by Western blot with anti-GR. (B) 293T CTL and KO cells were transfected with plasmid expressing HA tagged GR treated with protein synthesis inhibitor cycloheximide (CHX) for 6 hours. GR levels were monitored. n=4 *p<0.05, **p<0.01

5.2.4 The CS domains of USP19 are necessary but not sufficient to increase GR levels

In the previous sections, we showed that USP19 and GR interact and that GR is more ubiquitinated and more rapidly degraded in the absence of USP19. We next asked which domains of USP19 are important for the regulation of GR protein levels. To address this, we expressed a variety of USP19 constructs (**Figure 5.4 A**) in cells and observed the effect on GR protein levels. These constructs included the USP19 isoform with a transmembrane domain localized to the endoplasmic reticulum (ER) (294), the USP19 isoform with no transmembrane domain localized to the cytosol (CYT), a catalytically inactive mutant of USP19 where the active cysteine has been mutated to an alanine (CA), various N-terminal deletions (ΔN) that lack one or both of the CS/p23 like domains, and the N-terminus of USP19 containing only the CS domains (CS). All of these constructs have a 3 x Flag tag in the N-terminus. We observed that overexpression of ER USP19 or CYT USP19 resulted in increased protein levels of GR (**Figure 5.4 B**). Interestingly, there is no difference in the ability of these differentially localized isoforms of USP19 to increase the levels of GR protein perhaps because the catalytic and CS domains of the ER isoform face the cytoplasm. Surprisingly, the catalytically inactive version of USP19 also resulted in increased levels of USP19 (**Figure 5.4 C**), suggesting that the effect on GR protein levels is potentially independent of the catalytic activity of USP19. Finally, we observed that the N-terminal deletions, lacking both CS domains of USP19, no longer resulted in increased GR levels suggesting that the CS domains are necessary for the effect of USP19 on GR stability (**Figure 5.4 C**). Finally, we asked whether the

CS domains were sufficient to increase the levels of GR. We did not observe any increase in GR protein levels when only the N-terminal CS domains were expressed suggesting that the catalytic domain of USP19 is also important for increasing GR protein levels (**Figure 5.4 D**). Taken together, these results indicate that expression of ER or CYT USP19 can increase the levels of GR protein and both CS and catalytic domains of USP19 are necessary but not sufficient for GR stability.

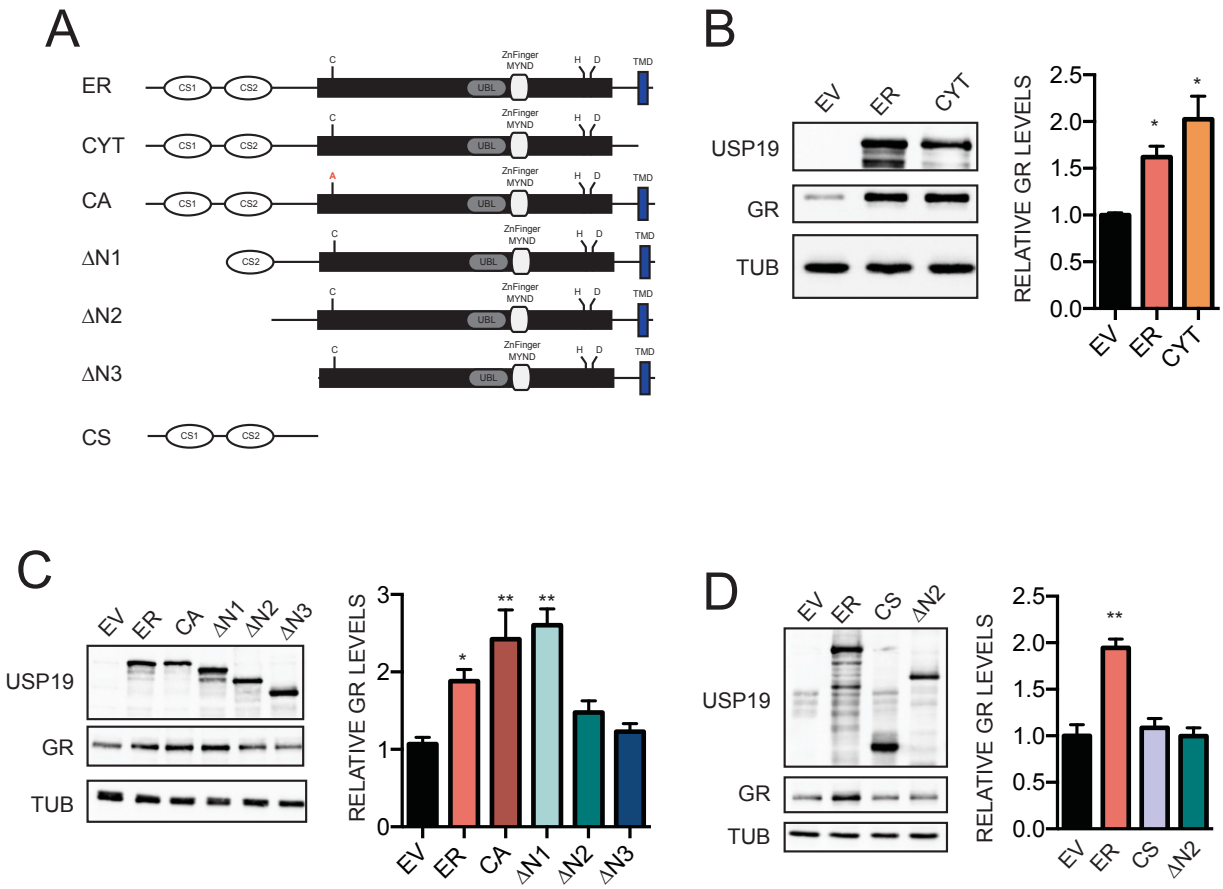

Figure 5.4: Overexpression of USP19 increases GR protein levels

(A) Schematic representation of USP19 expression plasmids. HEK293T cells were co-transfected with HA-tagged GR and various Flag-tagged USP19 expressing plasmids. After 48 hours of expression lysates were subjected to western blot using antibodies against USP19, GR, and tubulin. (B) Co-transfection of HA-GR and an empty vector (EV) or ER-localized or cytosolic-localized USP19. (C) Co-transfection of HA-GR and EV, ER-localized, catalytically inactive, or N-terminal deletions of USP19. (D) Co transfection of HA-GR and EV, ER-localized, CS domains only, or N-terminal deletion of USP19.

5.2.5 GR activity is reduced in USP19 KO cells

Since we showed that GR is more rapidly degraded in the absence of USP19, we asked whether this effect on the protein levels of GR also translated into an effect on the transcriptional activity of GR. To test this, we transfected a plasmid encoding luciferase under the control of a promoter containing three glucocorticoid response elements (**Figure 5.5 A**) into CTL or USP19 KO 293T cells. At baseline and upon stimulation of GR activity by dexamethasone, we observed decreased luciferase activity in the KO cells (**Figure 5.5 B**). This is consistent with the data above, indicating that the level of GR and the activity of GR are both decreased in the KO cells.

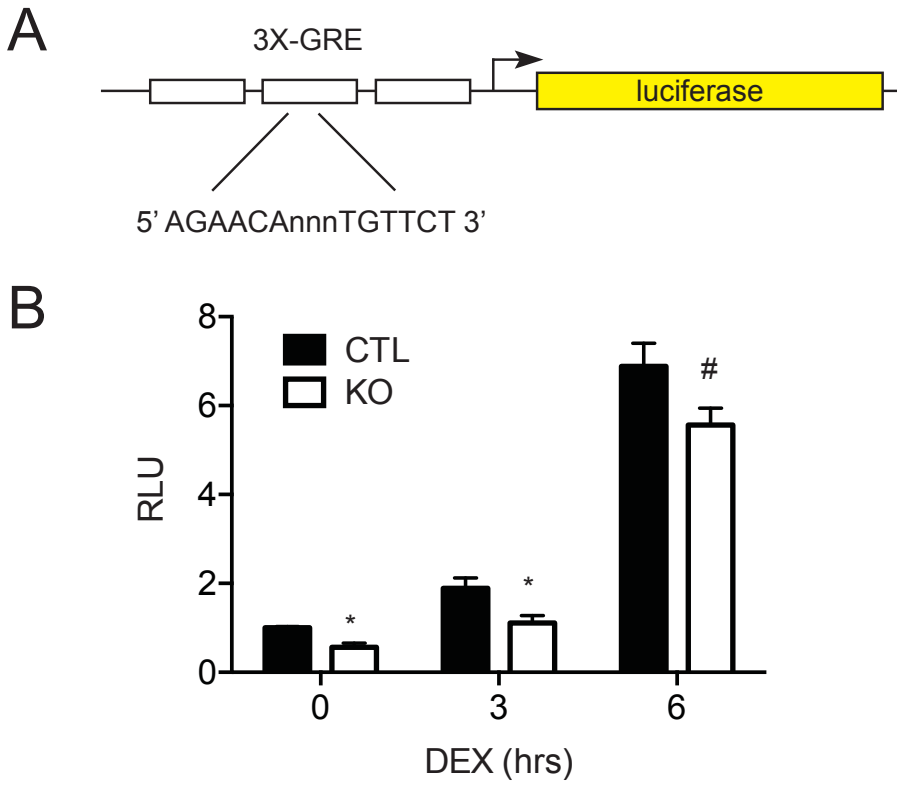

Figure 5.5: GR activity is reduced in USP19 KO cells

(A) Schematic of the 3 x glucocorticoid response element (GRE) luciferase construct with palindromic GRE sequence presented. (B) Relative luciferase units (normalized to Renilla luciferase as a transfection control) in CTL and KO cells before or after 3 or 6 hours of 1uM dexamethasone stimulation. n=6. *p<0.05 #p=0.1.

5.3 Discussion

In this chapter, we begin to uncover mechanistic insight into how USP19 regulates the levels of the glucocorticoid receptor (GR). We show that GR protein levels are 50% lower in the three critical metabolic tissues of the muscle, liver and adipose tissue suggesting that USP19 may mediate its effects on metabolism in those tissues through the regulation of GR.

We show for the first time that USP19 and GR interact, perhaps in complex with the molecular chaperone HSP90. USP19 has been shown to interact with HSP90 in the literature, and thus, it is plausible that USP19 is interacting with GR through HSP90 (284,293,300,328). USP19 also has protein domains and motifs that hint towards importance in the chaperone system. In its N-terminus, USP19 has two CS/p23 domains with high homology to HSP90 co-chaperones. Additionally, the cytosolic isoform of USP19 has a C-terminal EEVD motif similar to the C-terminal domains of the chaperones HSP90 and HSP70 and thus could also be recruited to the chaperone system via this domain. In the literature, it is still unclear which domains of USP19 are important for interaction with HSP90 as one paper suggests that the CS/p23 domains are important while another suggests that only the catalytic domain is required for interaction (293,300).

Intriguingly, the catalytically inactive mutant of USP19 (CA) can still increase GR protein levels, suggesting that the effect of USP19 on GR may be independent of its catalytic activity. There are non-enzymatic ways that USP19 may be able to decrease the ubiquitination of a substrate and decrease its degradation rate. For example, when USP19 interacts with a target protein, it could

mask important lysine residues that become ubiquitinated and target the protein for degradation. Thus, with USP19 present, the ligase cannot access the lysine residue to ubiquitinate the substrate, and therefore it does not get degraded. Similarly, USP19 could bind to the same region of the substrate protein as the ligase does, and thus in the presence of USP19, the ligase cannot bind to the substrate. In fact, it has been shown that the catalytic activity of USP19 is dispensable for the regulation of other target substrates including hypoxia-inducible factor 1α (HIF1α) (329) and the cellular inhibitors of apoptosis (cIAPs) (297). Thus, it is not unprecedented that the catalytic activity of USP19 is not required for the regulation of the stability of a substrate protein. The caveat to this is that these experiments were all done by overexpressing the catalytically inactive version of USP19 and thus, the overexpression of USP19 alone may prevent the substrate from being acted on by the ligase. Therefore, it is possible that the observations suggesting non-catalytic roles of USP19 are an artifact of the overexpression system. To avoid these artifacts of overexpression, the best approach to determining whether the catalytic activity is required would be to generate CRISPR mutant cells where the catalytic cysteine of endogenous USP19 has been mutated to alanine.

USP19 may be recruited to HSP90 and GR via its CS domains and this is why we no longer observe increased levels of GR protein with loss of those domains and why those domains alone are not sufficient to increase GR protein levels. Thus, both the CS domains and the catalytic

domain (though perhaps not the catalytic activity itself) are required for USP19 regulation of GR protein levels.

Together, the data in this chapter shows that GR protein levels are regulated by USP19. Our working model for how this might function is as follows: USP19 is recruited to and interacts with HSP90 via its N-terminal CS domains and thus has access to GR as it matures in the chaperone system. Increased levels of USP19 results in decreased levels of GR ubiquitination (by direct deubiquitination or by blocking access of the ubiquitin ligase), and thus the steady state level of GR protein is increased. Increased GR protein levels could result in downstream metabolic effects including decreased insulin signaling, increased protein degradation, and decreased protein synthesis in the skeletal muscle as well as increased adipogenesis and fat accumulation in the adipose tissue, and increased gluconeogenesis in the liver.

More studies need to be done to confirm our working model. First, we need to demonstrate that HSP90, GR, and USP19 are in a single complex. Purification of each of these three proteins, followed by identification of the other two proteins in the purified fraction would help confirm that they are indeed in a complex. Additionally, a sequential co-purification where HSP90 and interacting proteins are immunoprecipitated, then GR is immunoprecipitated from the purified fraction, followed by western blot for USP19 in the purified fraction would further confirm the presence of a complex. Second, the importance of the CS domains of USP19 needs to be confirmed. This will require modeling of the three-dimensional structures of the USP19 CS

domains on the structures of p23 or Sgt1 in complex with HSP90 (330,331) to identify residues in USP19 that would likely mediate its interaction with HSP90. Creating point mutations that could disrupt the interaction between USP19 and HSP90/GR will confirm if the CS domains are necessary for the interaction with HSP90 and the regulation of GR protein levels.

CHAPTER 6

GENERAL DISCUSSION

6.1 Summary of Thesis

In this thesis, I show for the first time that the deubiquitinating enzyme USP19 is an important regulator of major metabolic processes involved in the regulation of energy homeostasis. In chapter 3, using a knockout mouse model, I first showed that the inactivation of USP19 protects mice from fasting-induced muscle loss due to increased rates of protein synthesis in the catabolic state compared to WT mice. I also showed that USP19 modulates insulin signaling in muscle resulting in enhanced insulin sensitivity and glucose tolerance in the KO mouse. Importantly, I showed that USP19 may modulate the process of gluconeogenesis by regulating the levels of the gluconeogenic enzyme Pepck. Finally, I showed that USP19 regulates glucocorticoid signaling in both mouse and human skeletal muscle and that the modulation of glucocorticoid receptor protein levels by USP19 is important for the regulation of muscle mass.

In chapter 4, I investigated the role of USP19 in fat development and showed that USP19 is required for normal proliferation and differentiation of adipocytes. I also showed that the inactivation of USP19 is protective against the development of high fat diet (HFD) induced obesity, as well as the metabolic complications of obesity such as diabetes and fatty liver disease. Finally, I showed that USP19 mRNA expression is positively correlated to the expression of important adipocyte genes in human adipose tissue, suggesting a role for USP19 in human adipose tissue function.

Lastly, in chapter 5, I identified the glucocorticoid receptor (GR) as a target substrate of USP19 deubiquitinating action that mediates the above metabolic processes. Upon loss of USP19, I observed significantly lower levels of GR in the metabolic tissues of the muscle, liver and adipose tissue and showed that GR appears to be more ubiquitinated and more rapidly degraded in USP19 KO cells. I also showed that the N-terminal CS/p23-like domains of USP19 are necessary but not sufficient to modulate GR protein levels.

Taken together, I have provided evidence for the regulation of the glucocorticoid receptor by USP19 which may mediate metabolic processes including the regulation of muscle mass, glucose homeostasis, and fat development. Our working model is as follows: in the absence of USP19, GR is more ubiquitinated and therefore, more rapidly degraded and less abundant, and this results in decreased glucocorticoid signaling. In the muscle, upon fasting, decreased GR levels results in increased insulin signaling as well as decreased levels of protein degradation and increased rates of protein synthesis during fasting. In the liver, decreased levels of GR results in increased insulin signaling and decreased hepatic glucose output. Finally, in the adipose tissue, decreased GR levels results in decreased levels adipogenesis (**Figure 6.1**).

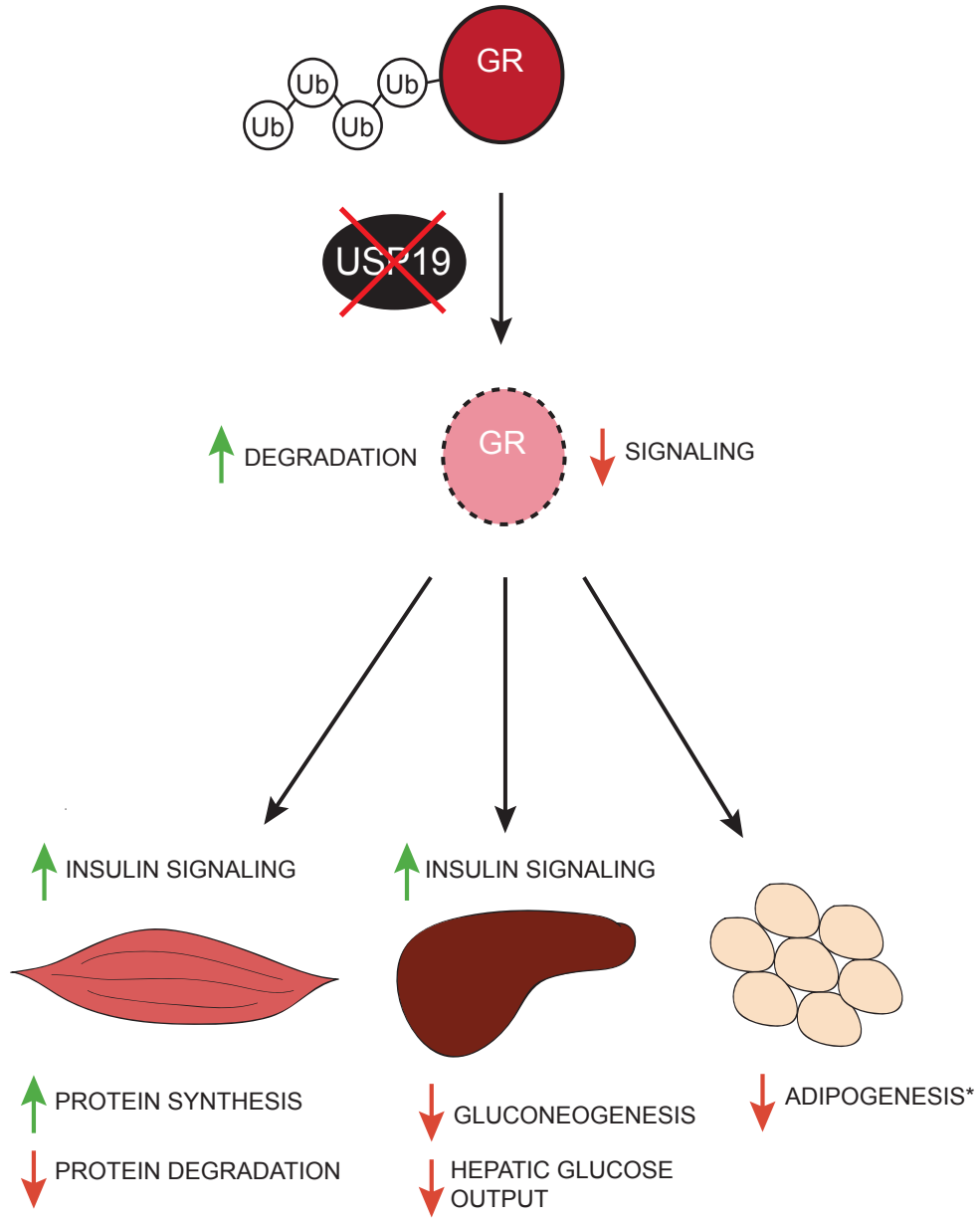

Figure 6.1 – Working model for USP19 action in metabolic tissues

Loss of USP19 results in increased ubiquitination of glucocorticoid receptor (GR) and thus decreased levels of GR protein in muscle, liver, and adipose tissue. Decreased GR in these tissues alters cellular metabolic processes including insulin signaling, glucose uptake and production, and protein synthesis. Asterisk indicates a plausible mechanism that has not been directly confirmed by experiment.

6.2 General Discussion

6.2.1 Metabolic Processes Regulated by USP19

In this thesis, we show that USP19 KO mice have a metabolic phenotype consisting of increased muscle mass, decreased fat mass, improved insulin sensitivity and glucose tolerance, and also, increased physical activity. To assess how the inactivation of USP19 might be causing this phenotype we assessed whether USP19 regulates metabolic processes in the three tissues important for the storage and mobilization of macronutrients – skeletal muscle, adipose tissue and liver.

We and others have shown that USP19 plays a role in the modulation of muscle mass (303-305). USP19 was first identified and characterized in a screen for deubiquitinating enzymes that were downregulated in catabolic conditions and could, therefore, result in increased ubiquitination and degradation of muscle proteins. This screening did not reveal any DUBs that were downregulated but did reveal a single DUB that was upregulated during catabolic conditions, identified as USP19 (278). In this thesis, we have shown that USP19 modulates muscle mass during nutrient deprivation, through the regulation of protein synthesis rates of both sarcoplasmic and myofibrillar proteins but it has no apparent effect on proteolytic pathways. Previously, it has been shown that in other catabolic states (such as denervation or dexamethasone treatment) USP19 does not modulate muscle mass through the regulation of protein synthesis, but rather through the activation of proteolytic pathways such as the ubiquitin-proteasome system and the autophagy-

lysosomal system (305). The different actions of USP19 in different catabolic states may reflect the inherent differences between these catabolic conditions. For example, muscle fiber types respond differently to various catabolic stimuli. Oxidative fibers are more resistant to fasting induced atrophy than glycolytic fibers while the reverse is true for denervation-induced atrophy (332). In addition to different effects in different fiber types, the differences between the effects of loss of USP19 in different catabolic states may be due to differences in systemic versus local atrophy or acute versus chronic atrophy. Denervation is a locally induced atrophy while fasting and glucocorticoids are systemic models of atrophy suggesting that USP19 may play different roles depending on the systemic state of the organism and the different hormonal signals received by the muscle. Additionally, between fasting and glucocorticoid treatment, atrophy induced by fasting is much more acute, while atrophy induced by glucocorticoids is more chronic. Perhaps the effects of USP19 on protein synthesis and degradation are timing dependent such that in the early acute phase of atrophy USP19 plays a substantial role in the regulation of protein synthesis, but as atrophy progresses more chronically, the degradative role of USP19 is more apparent. Analysis of detailed time courses of these effects will be required to test this possible explanation.

In the adipose tissue, we have shown that USP19 inactivation results in mice that have smaller fat pads due to fewer and smaller adipocytes indicating that USP19 is important for adipose tissue expansion and adipocyte development. Although the smaller fat pads of USP19 KO mice can be partially explained by decreased proliferation and differentiation of adipocytes, these mice

are not entirely devoid of adipocytes and fat depots. In fact, at an early age, USP19 KO adipocytes are similar in size to WT adipocytes but as they age, the adipocytes in the WT mice expand in size while those in the KO do not. Adipocytes store and mobilize lipids through the processes of lipogenesis and lipolysis, respectively. Since the KO adipocytes do not expand, it is possible that they may have a defect in lipogenesis, or they may have enhanced lipolysis. We have not fully characterized the lipogenic and lipolytic capacity of the adipose tissue USP19 KO mice with detailed measurements of flux in each of the pathways, but our data to date do not suggest any defects. We have preliminary data to suggest that circulating non-esterified fatty acid levels are similar between WT and KO mice. However, circulating cholesterol and triacylglycerol levels remain to be measured. Additionally, the steady-state mRNA levels of lipogenic and lipolytic enzymes are similar between WT and KO mice (data not shown). An alternative explanation as to why USP19 KO mice have smaller adipocytes than WT mice may be because they do not store lipid but rather oxidize it as an energy source and thus the adipocyte never expands. We see increased levels of O_2 consumed in our KO mice, consistent with increased metabolism. However the respiratory exchange ratio (RER) is similar between WT and KO mice, on both normal and high-fat diet, suggesting that they are using a similar fuel source for energy (333) and thus, the KO mice are not oxidizing lipids more readily than the WT mice. Beyond the white adipose tissue, it is possible that USP19 KO mice have a phenotype in the thermogenic brown adipose tissue (BAT). Instead of storing energy in the form of triacylglycerol in the adipocyte, the energy is converted to

heat in the BAT (334). Preliminary data suggest that KO mice have smaller brown adipose tissue fat pads after a high fat diet and have increased expression of the uncoupling protein UCP-1 (data not shown) suggesting that the tissue may indeed be more thermogenic compared to WT BAT.

In the liver, we have shown that USP19 regulates the process of gluconeogenesis and hepatic glucose output. The maintenance of blood glucose levels during periods of fasting is accomplished by hepatic glucose production through glycogenolysis and gluconeogenesis. USP19 KO mice had decreased hepatic glucose production after a pyruvate challenge, thus decreased gluconeogenic capacity. Additionally, hepatocytes isolated from KO livers had blunted upregulation of the gluconeogenic enzyme Pepck after administration of a gluconeogenic stimulus consistent with USP19 KO mice having a defect in the ability to mount the gluconeogenic response. To date, we have not examined the levels of hepatic glycogen stores or glycogenolysis rates in our KO mice but defects in this process could also contribute to the decreased hepatic glucose production observed.

In addition to modulating metabolic processes in muscle, adipose tissue, and liver, USP19 also modulates activity levels in mice. The inactivation of USP19 results in mice that are much more active than WT littermates. Activity levels and energy demands play a role in the balance between energy storage and mobilization and so the increase in activity levels in USP19 KO mice could explain many of the metabolic phenotypes that we observe. For example, increased activity levels may result in decreased adiposity and increased muscle mass. The reason why USP19 KO

mice are more active than WT mice and whether this differential activity fully explains the metabolic phenotype is not clear. Since this is a global KO, USP19 may have important roles in the brain and thus disrupting USP19 in the brain could cause changes in behaviour and activity levels. This demonstrates the limitations of working with a whole-body KO model as it is difficult to tell whether an observed effect is intrinsic to the tissue of interest or is caused indirectly by an effect in another tissue. There is evidence to suggest that the role of USP19 is cell autonomous as we showed that silencing of USP19 in C2C12 muscle cells has an effect on insulin signaling and that primary cells isolated from muscle, adipose tissue and liver of KO mice and cultured for up to two weeks, exhibit lower levels of GR protein. Additionally, electroporation of shRNA against USP19 or silencing with siRNA in muscle of WT mice results in protection from muscle atrophy arguing strongly that this effect is tissue specific (304,305). In addition, USP19 KO mice are also protected by denervation induced atrophy (305). Since the denervated muscles are inactive, the benefit cannot be due to increased muscle activity in the KO mice. Nonetheless, it will be important to generate tissue-specific KO of USP19 in all three of these tissues to ensure that the effects of USP19 are intrinsic to the tissue itself. Additionally, we could re-express USP19 in specific tissues, and assess whether the phenotype in that tissue is lost. This could be accomplished by electroporation of a USP19 expressing plasmid into the muscle of KO mice or through a tail vein injection of adenovirus with USP19 to re-express USP19 in the liver. However, it is more difficult to re-express a gene in adipose tissue so the tissue-specific KO would be necessary to test this.

6.2.2 Cellular Pathways Modulated by USP19

After characterizing the role of USP19 in physiological processes such as the maintenance of muscle mass, adipocyte development, gluconeogenesis, and glucose homeostasis, it was important to uncover which cellular processes were being modulated by USP19 to result in these effects. Because many metabolic tissues are affected by USP19 inactivation and because we assessed different states of energy balance (either nutrient deprivation or nutrient excess) to characterize the role of USP19 in these processes, we first asked if insulin action was different between WT and KO mice. We showed that USP19 KO mice had significantly lower levels of circulating insulin after overnight fasting either on a normal diet or a high fat diet and that the muscle and the liver of USP19 KO mice showed enhanced insulin signaling. Enhanced insulin signaling will result in increased glucose uptake in muscle and decreased glucose production from the liver, which is consistent with our results from the glucose and pyruvate tolerance tests, respectively. However, we did not directly measure glucose production from the liver or glucose uptake in muscle or adipose tissue, instead measuring changes in blood glucose levels as a surrogate. In future studies, we could test this directly *in vivo*, by measuring glucose production from the liver of WT and KO mice using a labelled glucose tracer and a hyperinsulinemic-euglycemic clamp study to measure insulin sensitivity and glucose uptake in these mice (335-337). In cell culture, we could monitor the secretion of glucose into the media from WT and KO primary hepatocytes treated with a gluconeogenic stimulus as well as measuring the uptake of the non-

metabolizable glucose analog 2-deoxyglucose into insulin-stimulated muscle cells or adipocytes to assess glucose uptake (338,339). Insulin signaling stimulates metabolic processes including carbohydrate, fatty acid and protein anabolism in skeletal muscle, adipose tissue, and liver. While we saw increased activation of Akt and $p70^{S6K}$ in the muscle and liver, this increase in activation was not due to increased levels of the upstream regulators of the pathway such as the insulin receptor or insulin receptor substrate, both of which can be ubiquitinated to regulate their protein levels (108,110,340). This suggests that the regulation of insulin signaling by USP19 is downstream of the receptor, perhaps through crosstalk with other intracellular signaling pathways.

To understand how insulin signaling is modulated by USP19, we examined another hormonal signaling pathway, glucocorticoid signaling through the glucocorticoid receptor (GR). In a microarray analysis, we identified GR target genes as possibly being differentially regulated in USP19 WT and KO muscle. Additionally, GR signaling was of interest because it is a pathway that negatively regulates insulin signaling as well as being an important signaling pathway for metabolic processes in muscle, liver, and adipose tissue. Indeed, we observed decreased levels of glucocorticoid signaling concomitant with decreased levels of glucocorticoid receptor (GR) protein while GR mRNA levels were similar between WT and KO mice. This suggests that the effects of loss of USP19 on GR levels are post-transcriptional in nature and thus, GR is a possible target for a DUB like USP19. GR protein levels can be regulated at the level of expression, or by post-translational modifications such as phosphorylation (141,341), acetylation (342),

sumoylation (145,343,344), or ubiquitination (144,345) thus it is plausible that USP19 acts to remove post-translationally conjugated ubiquitin from GR. Additionally, decreased GR signaling was not due to decreased circulating ligand as the levels of serum corticosterone were similar between WT and KO mice.

Other hormones beyond insulin and glucocorticoids are also important for the regulation of energy storage and mobilization in these tissues including glucagon and epinephrine. Epinephrine increases blood glucose levels, induces lipolysis in the adipose tissue as well as glycogenolysis in the muscle, and the depletion of epinephrine by adrenomedullation exacerbates fasting induced muscle atrophy (87-89,346). The role of glucagon is to increase hepatic glucose production thus increasing blood glucose levels (91). However, the effects of these hormones cannot completely explain the phenotype we observed in the USP19 KO mice. Therefore, they are unlikely to play important roles in USP19 regulation of energy homeostasis, but can be explored in future studies.

6.2.3 Molecular Mechanisms of USP19 Action

Having characterized the metabolic phenotypes of USP19 KO mice, we wanted to gain a greater understanding of the molecular mechanisms of USP19 action in these processes. To this end, we identified the glucocorticoid receptor (GR) as a target of GR deubiquitinating action. We showed that GR, USP19 and HSP90 interact in cells. Additionally, GR levels are lower in KO mice and GR is more ubiquitinated and more rapidly degraded in KO cells. Taken together, it

suggests that in normal cells, USP19 will act on GR to promote its deubiquitination and decrease its degradation and thus, GR can exert its transcriptional activity in cells. In conditions of stress (cancer, fasting, diabetes), USP19 is upregulated in muscle (278). This induction of USP19 may serve to increase the levels of GR to enhance the action of glucocorticoids which serve as a critical part of the organismal response to many stress stimuli such as infection or injury. However, prolonged exposure to or elevated levels of glucocorticoids will result in increased levels of GR signaling that can lead to detrimental metabolic effects such as muscle wasting and obesity (312,347).

The fact that USP19 interacts with both GR and HSP90, and that the CS/p23 domains of USP19 are important for USP19 regulation of GR stability is intriguing. There are four possibilities of how USP19 might be mediating its effects on GR with respect to HSP90: 1) HSP90 is not necessary and USP19 deubiquitinates GR independent of HSP90 activity, perhaps after it dissociates from the chaperone complexes; 2) HSP90 is not necessary and USP19 acts as a chaperone, rather than a deubiquitinating enzyme to increase GR stability; 3) HSP90 is necessary and USP19 acts as a co-chaperone to assist in the maturation and ligand binding of GR; 4) HSP90 is necessary and USP19 is recruited to the chaperone machinery to deubiquitinate client proteins like GR. To address the possibilities above, it will be important to determine if USP19 has chaperone or co-chaperone activity. Our data to date suggest that USP19 acts as a deubiquitinating enzyme for GR (possibility 1 and 4) rather than a chaperone or co-chaperone. We still need to test

whether HSP90 is necessary for the effect of USP19 on GR protein levels by repeating experiments in conditions where HSP90 activity is inhibited or HSP90 is silenced.

HSP90 is an important chaperone in the cell with many client proteins including nuclear receptors and many kinases. A deubiquitinating enzyme that acts on HSP90 client substrates has not been identified to date. However, USP19 was shown to be an HSP90 co-factor in a large proteomic screen and was the only DUB identified (328). Since HSP90 client substrates can be ubiquitinated and degraded (348-350), it is logical that they should be able to be deubiquitinated and rescued from that degradation. This is intriguing and suggests that USP19 may regulate more than just GR in terms of HSP90 client substrates. Many important kinases are also HSP90 client substrates (351) so it would be interesting to see if USP19 can regulate those as well. In future studies, we could screen various HSP90 clients in a system with perturbed USP19 expression and determine if there is a preference for the regulation of a certain class of client proteins such as the nuclear hormone receptors. We have some preliminary data suggesting that USP19 KO mice may also have lower levels of the nuclear receptor ERα in skeletal muscle. Additionally, USP19 has been shown to regulate the levels of poly-glutamate expanded huntingtin (Htt) and ataxin-3 (Atx3) through HSP90 (300,352) suggesting a role of USP19 in regulating another class of HSP90 client protein. If USP19 has a preference for a certain class of client protein, it would be interesting to understand how that specificity occurs. Multiple studies have demonstrated that USP19 interacts with HSP90 and we have confirmed these observations (unpublished data). The nature of the

interaction between USP19 and HSP90 is still controversial as one study suggests that the CS domains of USP19 are important for the interaction, while another study suggests that only the catalytic domain is required for interaction with HSP90 (293,300). Additionally, the cytoplasmic isoform of USP19 has a C-terminal EEVD motif, the same motif that HSP90 and HSP70 have in their C-termini that recruit co-chaperones. This is intriguing as one paper has suggested that USP19 may have intrinsic chaperone activity (284) and so the role of USP19 may be even more complex if it also functions to recruit co-chaperones.

6.2.4 Role of USP19 in Pathological States and Translational Potential

Since USP19 can modulate many metabolic processes and regulates both insulin and glucocorticoid signaling, it may be of interest to explore whether the inhibition of USP19 would be protective from the variety of metabolic diseases prevalent in patients today. We have shown in this thesis that the genetic inactivation of USP19 in mice is protective from the development of muscle wasting as well as obesity and its complications. Importantly, the inactivation of USP19 results in mice that are grossly normal except for being slightly smaller and males being subfertile compared to WT mice suggesting that any off-target effects of molecules inhibiting USP19 would be minimal (305).

Muscle wasting is an extremely burdensome complication of many common diseases including many cancers, AIDS, chronic obstructive pulmonary disorder, kidney failure as well as a systemic response to fasting and excessive glucocorticoids, and finally as a consequence of aging

(197). Because of its prevalence and extreme cost to a patient's quality of life (weakness, immobility, loss of independence, increased risk of mortality), successful prevention or treatment of muscle wasting would greatly improve patient outcomes. Unfortunately, to date, no pharmaceutical has been approved for use in the clinic to treat muscle wasting and thus, the identification and characterization of novel mediators of muscle wasting, such as USP19, is important to develop novel, effective therapies. In addition to protection from fasting induced muscle atrophy (shown in this thesis), the inactivation of USP19 protects against atrophy in conditions such as denervation and glucocorticoid treatment (305). Since the mechanisms underlying these various atrophy processes are different, this suggests a broad role for USP19 in regulating muscle catabolic programs and suggests that targeting USP19 for the treatment of muscle wasting may apply to many conditions.

In addition to protection from muscle wasting, we have shown that USP19 inactivation protects from the metabolic consequences of high fat diet-induced obesity including protection from the development of diabetes and fatty liver disease. Thus, inhibition of USP19 in these conditions may also be protective. These diseases are extremely prevalent and put an enormous burden on healthcare systems. In addition to protection from diabetes and fatty liver, it would be interesting to see if the inactivation of USP19 has any protective effects on the cardiovascular system. Since we observe a beneficial phenotype in the skeletal muscle of USP19 KO mice, it is possible that there may be a phenotype in the heart muscle of these mice as well. Under normal

conditions, we have not observed any differences in the mass of the heart between WT and KO mice. After a high fat diet, the hearts of USP19 KO mice were significantly smaller suggesting a protection from high fat diet-induced cardiac hypertrophy (353) but we need to assess the cross-sectional area of cardiomyocytes and fibrosis in the heart to confirm. Additionally, based on the leanness of these mice, the mice may have a better lipid profile and may be protected from the development of atherosclerotic plaques in the vasculature.

Ultimately, the inhibition of USP19 by small molecules may be of interest for the treatment of these diseases in the clinic. We have shown that the inactivation of USP19 in mice is protective against some of the pathological metabolic states discussed above, but for USP19 to have therapeutic translational potential, it must also modulate these processes in human patients. Previously, it was shown that USP19 mRNA expression correlates with the expression of atrogenes MuRF1 and atrogin-1 in two cohorts of patients with cancers that cause muscle atrophy (305). In this thesis, we have shown that USP19 may regulate metabolic processes in human muscle as well as in human adipose tissue. In human skeletal muscle from patients with abdominal cancers (various grades of atrophying muscle), we found that USP19 expression is correlated to GR target gene expression, suggesting that USP19 may regulate GR signaling in human muscle as it does in mouse muscle. This is interesting as we showed that the mechanism of USP19 action in modulating muscle mass is through the regulation of GR protein levels. What we have not yet assessed is whether USP19 also modulates insulin signaling in human muscle. This is difficult to

assess as there are currently no USP19 specific inhibitors available, but when they do become available we could treat patients with the inhibitors and do euglycemic clamp studies to assess insulin sensitivity as well as take muscle biopsies and assess the activation of the insulin signaling pathway. In the adipose tissue, we have shown that USP19 expression is correlated to adipogenic gene expression but only in visceral adipose tissue depots. This is an intriguing observation as central obesity has recently been associated with increased risk of insulin resistance and other metabolic complications (319) and thus USP19 may be protective from the metabolic consequences of obesity by preventing the development of central obesity.

Finally, the translational potential of USP19 will depend on the design of small molecules that inhibit its actions. Small molecules that inhibit only the catalytic activity of USP19 may have undesirable effects downstream of DUB activity as DUBs likely have multiple target substrates that are often condition and cell-type specific. In addition to the possible downstream effects, some DUBs (including USP19) exert effects that are independent of catalytic activity (297,354,355), and thus, inhibiting the activity of the DUB will have no effect. Therefore, disrupting the interaction between the DUB and a specific target substrate that is mediating the effect of interest may be a more suitable strategy. The identification of the glucocorticoid receptor as a target substrate of USP19 is an important step forward toward this end. The development of molecules that may disrupt this interaction could eventually lead to the generation of a novel drug that will prevent muscle wasting in patients with cancers, COPD, or kidney failure, or improve blood

glucose levels in diabetic patients. First, more studies into the nature of the interaction between USP19 and GR are needed including defining which domains of USP19 are important for this interaction, which conditions are permissive for this interaction, and whether this is a direct interaction or if USP19 and GR interact in a complex with other proteins such as HSP90.

6.3 Original Contributions

This thesis describes both physiological and biochemical functions of the deubiquitinating enzyme USP19 in the regulation of energy homeostasis. Specifically, we show for the first time that:

Chapter 3

1. USP19 inactivation protects against fasting induced muscle loss as a result of increased muscle protein synthesis rates without changes in degradation.

2. USP19 inactivation results in mice that are more insulin sensitive, glucose tolerant and have enhanced insulin signaling in the muscle as well as decreased capacity for gluconeogenesis in the liver.

3. USP19 is important for glucocorticoid receptor (GR) signaling in skeletal muscle of mice and gene expression analysis in muscle of human subjects is consistent with this.

Chapter 4

4. USP19 inactivation results in mice that have significantly less fat mass due to fewer and smaller adipocytes and USP19 is required for normal fat cell proliferation and adipogenesis.

5. USP19 inactivation results in mice that are resistant to high fat diet induced obesity and its complications such as diabetes and fatty liver disease.

6. USP19 mRNA expression is positively correlated to the expression of adipogenic genes in human visceral adipose tissue but not in human subcutaneous adipose tissue.

Chapter 5

7. GR protein levels are lower in muscle, liver, and adipose tissue of USP19 KO mice while mRNA levels are the same and GR activity is lower in USP19 KO cells.

8. GR, USP19, and HSP90 interact with each other and GR appears to be more ubiquitinated and more rapidly degraded in USP19 KO cells.

9. GR stability is dependent on the CS/p23 domains of USP19.

REFERENCES

1. Hall KD, Heymsfield SB, Kemnitz JW, Klein S, Schoeller DA, Speakman JR. Energy balance and its components: implications for body weight regulation. Am J Clin Nutr 2012; 95:989-994

2. Galgani J, Ravussin E. Energy metabolism, fuel selection and body weight regulation. Int J Obes (Lond) 2008; 32 Suppl 7:S109-119

3. Eaton SB. Humans, lipids and evolution. Lipids 1992; 27:814-820

4. Bjorndal B, Burri L, Staalesen V, Skorve J, Berge RK. Different adipose depots: their role in the development of metabolic syndrome and mitochondrial response to hypolipidemic agents. J Obes 2011; 2011:490650

5. Velloso CP. Regulation of muscle mass by growth hormone and IGF-I. Br J Pharmacol 2008; 154:557-568

6. Konopka AR, Harber MP. Skeletal muscle hypertrophy after aerobic exercise training. Exerc Sport Sci Rev 2014; 42:53-61

7. Sainsbury A, Cooney GJ, Herzog H. Hypothalamic regulation of energy homeostasis. Best Pract Res Clin Endocrinol Metab 2002; 16:623-637

8. Murphy KG, Bloom SR. Gut hormones and the regulation of energy homeostasis. Nature 2006; 444:854-859

9. Ehler E, Gautel M. The sarcomere and sarcomerogenesis. Adv Exp Med Biol 2008; 642:1-14

10. Burke RE, Levine DN, Zajac FE, 3rd. Mammalian motor units: physiological-histochemical correlation in three types in cat gastrocnemius. Science 1971; 174:709-712

11. Larsson L, Edstrom L, Lindegren B, Gorza L, Schiaffino S. MHC composition and enzyme-histochemical and physiological properties of a novel fast-twitch motor unit type. Am J Physiol 1991; 261:C93-101

12. Scott W, Stevens J, Binder-Macleod SA. Human skeletal muscle fiber type classifications. Phys Ther 2001; 81:1810-1816

13. Bobinac D, Malnar-Dragojevic D, Bajek S, Soic-Vranic T, Jerkovic R. Muscle fiber type composition and morphometric properties of denervated rat extensor digitorum longus muscle. Croat Med J 2000; 41:294-297

14. Soukup T, Zacharova G, Smerdu V. Fibre type composition of soleus and extensor digitorum longus muscles in normal female inbred Lewis rats. Acta Histochem 2002; 104:399-405

15. Lexell J, Jarvis JC, Currie J, Downham DY, Salmons S. Fibre type composition of rabbit tibialis anterior and extensor digitorum longus muscles. J Anat 1994; 185 (Pt 1):95-101

16. Jensen J, Rustad PI, Kolnes AJ, Lai YC. The role of skeletal muscle glycogen breakdown for regulation of insulin sensitivity by exercise. Front Physiol 2011; 2:112

17. Esbjornsson-Liljedahl M, Sundberg CJ, Norman B, Jansson E. Metabolic response in type I and type II muscle fibers during a 30-s cycle sprint in men and women. J Appl Physiol (1985) 1999; 87:1326-1332

18. Helge JW, Biba TO, Galbo H, Gaster M, Donsmark M. Muscle triacylglycerol and hormone-sensitive lipase activity in untrained and trained human muscles. Eur J Appl Physiol 2006; 97:566-572

19. Koopman R, Manders RJ, Jonkers RA, Hul GB, Kuipers H, van Loon LJ. Intramyocellular lipid and glycogen content are reduced following resistance exercise in untrained healthy males. Eur J Appl Physiol 2006; 96:525-534

20. Lauritzen HP, Schertzer JD. Measuring GLUT4 translocation in mature muscle fibers. Am J Physiol Endocrinol Metab 2010; 299:E169-179
21. Adeva-Andany MM, Gonzalez-Lucan M, Donapetry-Garcia C, Fernandez-Fernandez C, Ameneiros-Rodriguez E. Glycogen metabolism in humans. BBA Clin 2016; 5:85-100
22. Bergstrom J, Hultman E, Roch-Norlund AE. Muscle glycogen synthetase in normal subjects. Basal values, effect of glycogen depletion by exercise and of a carbohydrate-rich diet following exercise. Scand J Clin Lab Invest 1972; 29:231-236
23. Kochan RG, Lamb DR, Lutz SA, Perrill CV, Reimann EM, Schlender KK. Glycogen synthase activation in human skeletal muscle: effects of diet and exercise. Am J Physiol 1979; 236:E660-666
24. Berg J, Tymoczko J, Stryer L. Biochemistry: Section 21.5 Glycogen Breakdown and Synthesis are Reciprocally Regulatedtry. Vol 5th Edition. New York: W H Freeman.
25. Ruderman NB. Muscle amino acid metabolism and gluconeogenesis. Annu Rev Med 1975; 26:245-258
26. Egerman MA, Glass DJ. Signaling pathways controlling skeletal muscle mass. Crit Rev Biochem Mol Biol 2014; 49:59-68
27. Cai D, Frantz JD, Tawa NE, Jr., Melendez PA, Oh BC, Lidov HG, Hasselgren PO, Frontera WR, Lee J, Glass DJ, Shoelson SE. IKKbeta/NF-kappaB activation causes severe muscle wasting in mice. Cell 2004; 119:285-298
28. Dogra C, Changotra H, Wedhas N, Qin X, Wergedal JE, Kumar A. TNF-related weak inducer of apoptosis (TWEAK) is a potent skeletal muscle-wasting cytokine. FASEB J 2007; 21:1857-1869
29. Ogawa M, Yamaji R, Higashimura Y, Harada N, Ashida H, Nakano Y, Inui H. 17beta-estradiol represses myogenic differentiation by increasing ubiquitin-specific peptidase 19 through estrogen receptor alpha. J Biol Chem 2011; 286:41455-41465
30. Clarke BA, Drujan D, Willis MS, Murphy LO, Corpina RA, Burova E, Rakhilin SV, Stitt TN, Patterson C, Latres E, Glass DJ. The E3 Ligase MuRF1 degrades myosin heavy chain protein in dexamethasone-treated skeletal muscle. Cell Metab 2007; 6:376-385
31. Shimizu N, Yoshikawa N, Ito N, Maruyama T, Suzuki Y, Takeda S, Nakae J, Tagata Y, Nishitani S, Takehana K, Sano M, Fukuda K, Suematsu M, Morimoto C, Tanaka H. Crosstalk between glucocorticoid receptor and nutritional sensor mTOR in skeletal muscle. Cell Metab 2011; 13:170-182
32. Zimmers TA, Davies MV, Koniaris LG, Haynes P, Esquela AF, Tomkinson KN, McPherron AC, Wolfman NM, Lee SJ. Induction of cachexia in mice by systemically administered myostatin. Science 2002; 296:1486-1488
33. McFarlane C, Plummer E, Thomas M, Hennebry A, Ashby M, Ling N, Smith H, Sharma M, Kambadur R. Myostatin induces cachexia by activating the ubiquitin proteolytic system through an NF-kappaB-independent, FoxO1-dependent mechanism. J Cell Physiol 2006; 209:501-514
34. Song YH, Li Y, Du J, Mitch WE, Rosenthal N, Delafontaine P. Muscle-specific expression of IGF-1 blocks angiotensin II-induced skeletal muscle wasting. J Clin Invest 2005; 115:451-458
35. Bilodeau PA, Coyne ES, Wing SS. The ubiquitin proteasome system in atrophying skeletal muscle: roles and regulation. Am J Physiol Cell Physiol 2016; 311:C392-403

36. Denton RM, Randle PJ. Concentrations of glycerides and phospholipids in rat heart and gastrocnemius muscles. Effects of alloxan-diabetes and perfusion. Biochem J 1967; 104:416-422
37. Itani SI, Zhou Q, Pories WJ, MacDonald KG, Dohm GL. Involvement of protein kinase C in human skeletal muscle insulin resistance and obesity. Diabetes 2000; 49:1353-1358
38. Schmitz-Peiffer C. Signalling aspects of insulin resistance in skeletal muscle: mechanisms induced by lipid oversupply. Cell Signal 2000; 12:583-594
39. Dube JJ, Amati F, Stefanovic-Racic M, Toledo FG, Sauers SE, Goodpaster BH. Exercise-induced alterations in intramyocellular lipids and insulin resistance: the athlete's paradox revisited. Am J Physiol Endocrinol Metab 2008; 294:E882-888
40. Goodpaster BH, He J, Watkins S, Kelley DE. Skeletal muscle lipid content and insulin resistance: evidence for a paradox in endurance-trained athletes. J Clin Endocrinol Metab 2001; 86:5755-5761
41. Gimble JM, Bunnell BA, Frazier T, Rowan B, Shah F, Thomas-Porch C, Wu X. Adipose-derived stromal/stem cells: a primer. Organogenesis 2013; 9:3-10
42. Diaz MB, Herzig S, Vegiopoulos A. Thermogenic adipocytes: from cells to physiology and medicine. Metabolism 2014; 63:1238-1249
43. Galic S, Oakhill JS, Steinberg GR. Adipose tissue as an endocrine organ. Mol Cell Endocrinol 2010; 316:129-139
44. Grundy SM, Cleeman JI, Daniels SR, Donato KA, Eckel RH, Franklin BA, Gordon DJ, Krauss RM, Savage PJ, Smith SC, Jr., Spertus JA, Costa F. Diagnosis and management of the metabolic syndrome: an American Heart Association/National Heart, Lung, and Blood Institute scientific statement. Curr Opin Cardiol 2006; 21:1-6
45. Wang QA, Tao C, Gupta RK, Scherer PE. Tracking adipogenesis during white adipose tissue development, expansion and regeneration. Nat Med 2013; 19:1338-1344
46. Rosen ED, Walkey CJ, Puigserver P, Spiegelman BM. Transcriptional regulation of adipogenesis. Genes Dev 2000; 14:1293-1307
47. Rosen ED, Sarraf P, Troy AE, Bradwin G, Moore K, Milstone DS, Spiegelman BM, Mortensen RM. PPAR gamma is required for the differentiation of adipose tissue in vivo and in vitro. Mol Cell 1999; 4:611-617
48. Tontonoz P, Hu E, Spiegelman BM. Stimulation of adipogenesis in fibroblasts by PPAR gamma 2, a lipid-activated transcription factor. Cell 1994; 79:1147-1156
49. Farmer SR. Transcriptional control of adipocyte formation. Cell Metab 2006; 4:263-273
50. Diraison F, Beylot M. Role of human liver lipogenesis and reesterification in triglycerides secretion and in FFA reesterification. Am J Physiol 1998; 274:E321-327
51. Swierczynski J, Goyke E, Wach L, Pankiewicz A, Kochan Z, Adamonis W, Sledzinski Z, Aleksandrowicz Z. Comparative study of the lipogenic potential of human and rat adipose tissue. Metabolism 2000; 49:594-599
52. Letexier D, Pinteur C, Large V, Frering V, Beylot M. Comparison of the expression and activity of the lipogenic pathway in human and rat adipose tissue. J Lipid Res 2003; 44:2127-2134
53. Herman MA, Peroni OD, Villoria J, Schon MR, Abumrad NA, Bluher M, Klein S, Kahn BB. A novel ChREBP isoform in adipose tissue regulates systemic glucose metabolism. Nature 2012; 484:333-338
54. Kersten S. Physiological regulation of lipoprotein lipase. Biochim Biophys Acta 2014; 1841:919-933

55. Nye CK, Hanson RW, Kalhan SC. Glyceroneogenesis is the dominant pathway for triglyceride glycerol synthesis in vivo in the rat. J Biol Chem 2008; 283:27565-27574
56. Smith SJ, Cases S, Jensen DR, Chen HC, Sande E, Tow B, Sanan DA, Raber J, Eckel RH, Farese RV, Jr. Obesity resistance and multiple mechanisms of triglyceride synthesis in mice lacking Dgat. Nat Genet 2000; 25:87-90
57. Langin D. Adipose tissue lipolysis as a metabolic pathway to define pharmacological strategies against obesity and the metabolic syndrome. Pharmacol Res 2006; 53:482-491
58. Zechner R, Strauss JG, Haemmerle G, Lass A, Zimmermann R. Lipolysis: pathway under construction. Curr Opin Lipidol 2005; 16:333-340
59. Haemmerle G, Lass A, Zimmermann R, Gorkiewicz G, Meyer C, Rozman J, Heldmaier G, Maier R, Theussl C, Eder S, Kratky D, Wagner EF, Klingenspor M, Hoefler G, Zechner R. Defective lipolysis and altered energy metabolism in mice lacking adipose triglyceride lipase. Science 2006; 312:734-737
60. Zimmermann R, Strauss JG, Haemmerle G, Schoiswohl G, Birner-Gruenberger R, Riederer M, Lass A, Neuberger G, Eisenhaber F, Hermetter A, Zechner R. Fat mobilization in adipose tissue is promoted by adipose triglyceride lipase. Science 2004; 306:1383-1386
61. Zhang Y, Proenca R, Maffei M, Barone M, Leopold L, Friedman JM. Positional cloning of the mouse obese gene and its human homologue. Nature 1994; 372:425-432
62. Scherer PE, Williams S, Fogliano M, Baldini G, Lodish HF. A novel serum protein similar to C1q, produced exclusively in adipocytes. J Biol Chem 1995; 270:26746-26749
63. Stern JH, Rutkowski JM, Scherer PE. Adiponectin, Leptin, and Fatty Acids in the Maintenance of Metabolic Homeostasis through Adipose Tissue Crosstalk. Cell Metab 2016; 23:770-784
64. Rabe K, Lehrke M, Parhofer KG, Broedl UC. Adipokines and insulin resistance. Mol Med 2008; 14:741-751
65. Rui L. Energy metabolism in the liver. Compr Physiol 2014; 4:177-197
66. Agius L. Glucokinase and molecular aspects of liver glycogen metabolism. Biochem J 2008; 414:1-18
67. Woerle HJ, Meyer C, Dostou JM, Gosmanov NR, Islam N, Popa E, Wittlin SD, Welle SL, Gerich JE. Pathways for glucose disposal after meal ingestion in humans. Am J Physiol Endocrinol Metab 2003; 284:E716-725
68. Burgess SC, Hausler N, Merritt M, Jeffrey FM, Storey C, Milde A, Koshy S, Lindner J, Magnuson MA, Malloy CR, Sherry AD. Impaired tricarboxylic acid cycle activity in mouse livers lacking cytosolic phosphoenolpyruvate carboxykinase. J Biol Chem 2004; 279:48941-48949
69. Mutel E, Abdul-Wahed A, Ramamonjisoa N, Stefanutti A, Houberdon I, Cavassila S, Pilleul F, Beuf O, Gautier-Stein A, Penhoat A, Mithieux G, Rajas F. Targeted deletion of liver glucose-6 phosphatase mimics glycogen storage disease type 1a including development of multiple adenomas. J Hepatol 2011; 54:529-537
70. Michael MD, Kulkarni RN, Postic C, Previs SF, Shulman GI, Magnuson MA, Kahn CR. Loss of insulin signaling in hepatocytes leads to severe insulin resistance and progressive hepatic dysfunction. Mol Cell 2000; 6:87-97
71. Opherk C, Tronche F, Kellendonk C, Kohlmuller D, Schulze A, Schmid W, Schutz G. Inactivation of the glucocorticoid receptor in hepatocytes leads to fasting hypoglycemia

and ameliorates hyperglycemia in streptozotocin-induced diabetes mellitus. Mol Endocrinol 2004; 18:1346-1353
72. Waterhouse C, Keilson J. Cori cycle activity in man. J Clin Invest 1969; 48:2359-2366
73. Felig P, Pozefsky T, Marliss E, Cahill GF, Jr. Alanine: key role in gluconeogenesis. Science 1970; 167:1003-1004
74. Combs TP, Marliss EB. Adiponectin signaling in the liver. Rev Endocr Metab Disord 2014; 15:137-147
75. Liu Y, Sweeney G. Adiponectin action in skeletal muscle. Best Pract Res Clin Endocrinol Metab 2014; 28:33-41
76. Bostrom P, Wu J, Jedrychowski MP, Korde A, Ye L, Lo JC, Rasbach KA, Bostrom EA, Choi JH, Long JZ, Kajimura S, Zingaretti MC, Vind BF, Tu H, Cinti S, Hojlund K, Gygi SP, Spiegelman BM. A PGC1-alpha-dependent myokine that drives brown-fat-like development of white fat and thermogenesis. Nature 2012; 481:463-468
77. Markan KR, Naber MC, Ameka MK, Anderegg MD, Mangelsdorf DJ, Kliewer SA, Mohammadi M, Potthoff MJ. Circulating FGF21 is liver derived and enhances glucose uptake during refeeding and overfeeding. Diabetes 2014; 63:4057-4063
78. Lan F, Misu H, Chikamoto K, Takayama H, Kikuchi A, Mohri K, Takata N, Hayashi H, Matsuzawa-Nagata N, Takeshita Y, Noda H, Matsumoto Y, Ota T, Nagano T, Nakagen M, Miyamoto K, Takatsuki K, Seo T, Iwayama K, Tokuyama K, Matsugo S, Tang H, Saito Y, Yamagoe S, Kaneko S, Takamura T. LECT2 functions as a hepatokine that links obesity to skeletal muscle insulin resistance. Diabetes 2014; 63:1649-1664
79. Filippi BM, Abraham MA, Yue JT, Lam TK. Insulin and glucagon signaling in the central nervous system. Rev Endocr Metab Disord 2013; 14:365-375
80. Morton GJ, Schwartz MW. Leptin and the central nervous system control of glucose metabolism. Physiol Rev 2011; 91:389-411
81. Thundyil J, Pavlovski D, Sobey CG, Arumugam TV. Adiponectin receptor signalling in the brain. Br J Pharmacol 2012; 165:313-327
82. Fry M, Ferguson AV. Ghrelin: central nervous system sites of action in regulation of energy balance. Int J Pept 2010; 2010
83. Sherwin RS, Sacca L. Effect of epinephrine on glucose metabolism in humans: contribution of the liver. Am J Physiol 1984; 247:E157-165
84. Jiang G, Zhang BB. Glucagon and regulation of glucose metabolism. Am J Physiol Endocrinol Metab 2003; 284:E671-678
85. Wilcox G. Insulin and insulin resistance. Clin Biochem Rev 2005; 26:19-39
86. Kuo T, McQueen A, Chen TC, Wang JC. Regulation of Glucose Homeostasis by Glucocorticoids. Adv Exp Med Biol 2015; 872:99-126
87. Arnall DA, Marker JC, Conlee RK, Winder WW. Effect of infusing epinephrine on liver and muscle glycogenolysis during exercise in rats. Am J Physiol 1986; 250:E641-649
88. Wise LS, Jungas RL. Evidence for a dual mechanism of lipolysis activation by epinephrine in rat adipose tissue. J Biol Chem 1978; 253:2624-2627
89. Okuda H, Saito Y, Matsuoka N, Fujii S. Mechanism of adrenaline-induced lipolysis in adipose tissue. J Biochem 1974; 75:131-137
90. Cherrington AD, Lacy WW, Chiasson JL. Effect of glucagon on glucose production during insulin deficiency in the dog. J Clin Invest 1978; 62:664-677
91. Ramnanan CJ, Edgerton DS, Kraft G, Cherrington AD. Physiologic action of glucagon on liver glucose metabolism. Diabetes Obes Metab 2011; 13 Suppl 1:118-125

92. Perea A, Clemente F, Martinell J, Villanueva-Penacarrillo ML, Valverde I. Physiological effect of glucagon in human isolated adipocytes. Horm Metab Res 1995; 27:372-375
93. Heckemeyer CM, Barker J, Duckworth WC, Solomon SS. Studies of the biological effect and degradation of glucagon in the rat perifused isolated adipose cell. Endocrinology 1983; 113:270-276
94. Steiner DF, Oyer PE. The biosynthesis of insulin and a probable precursor of insulin by a human islet cell adenoma. Proc Natl Acad Sci U S A 1967; 57:473-480
95. Patzelt C, Labrecque AD, Duguid JR, Carroll RJ, Keim PS, Heinrikson RL, Steiner DF. Detection and kinetic behavior of preproinsulin in pancreatic islets. Proc Natl Acad Sci U S A 1978; 75:1260-1264
96. Kemmler W, Peterson JD, Rubenstein AH, Steiner DF. On the biosynthesis, intracellular transport and mechanism of conversion of proinsulin to insulin and C-peptide. Diabetes 1972; 21:572-581
97. Daniel S, Noda M, Straub SG, Sharp GW. Identification of the docked granule pool responsible for the first phase of glucose-stimulated insulin secretion. Diabetes 1999; 48:1686-1690
98. Myers MG, Jr., Grammer TC, Wang LM, Sun XJ, Pierce JH, Blenis J, White MF. Insulin receptor substrate-1 mediates phosphatidylinositol 3'-kinase and p70S6k signaling during insulin, insulin-like growth factor-1, and interleukin-4 stimulation. J Biol Chem 1994; 269:28783-28789
99. Yu J, Zhang Y, McIlroy J, Rordorf-Nikolic T, Orr GA, Backer JM. Regulation of the p85/p110 phosphatidylinositol 3'-kinase: stabilization and inhibition of the p110alpha catalytic subunit by the p85 regulatory subunit. Mol Cell Biol 1998; 18:1379-1387
100. Ogg S, Paradis S, Gottlieb S, Patterson GI, Lee L, Tissenbaum HA, Ruvkun G. The Fork head transcription factor DAF-16 transduces insulin-like metabolic and longevity signals in C. elegans. Nature 1997; 389:994-999
101. Kenyon C, Chang J, Gensch E, Rudner A, Tabtiang R. A C. elegans mutant that lives twice as long as wild type. Nature 1993; 366:461-464
102. Brunet A, Bonni A, Zigmond MJ, Lin MZ, Juo P, Hu LS, Anderson MJ, Arden KC, Blenis J, Greenberg ME. Akt promotes cell survival by phosphorylating and inhibiting a Forkhead transcription factor. Cell 1999; 96:857-868
103. Puigserver P, Rhee J, Donovan J, Walkey CJ, Yoon JC, Oriente F, Kitamura Y, Altomonte J, Dong H, Accili D, Spiegelman BM. Insulin-regulated hepatic gluconeogenesis through FOXO1-PGC-1alpha interaction. Nature 2003; 423:550-555
104. Sandri M, Sandri C, Gilbert A, Skurk C, Calabria E, Picard A, Walsh K, Schiaffino S, Lecker SH, Goldberg AL. Foxo transcription factors induce the atrophy-related ubiquitin ligase atrogin-1 and cause skeletal muscle atrophy. Cell 2004; 117:399-412
105. Milan G, Romanello V, Pescatore F, Armani A, Paik JH, Frasson L, Seydel A, Zhao J, Abraham R, Goldberg AL, Blaauw B, DePinho RA, Sandri M. Regulation of autophagy and the ubiquitin-proteasome system by the FoxO transcriptional network during muscle atrophy. Nat Commun 2015; 6:6670
106. Laplante M, Sabatini DM. mTOR signaling at a glance. J Cell Sci 2009; 122:3589-3594
107. Garcia-Cao I, Song MS, Hobbs RM, Laurent G, Giorgi C, de Boer VC, Anastasiou D, Ito K, Sasaki AT, Rameh L, Carracedo A, Vander Heiden MG, Cantley LC, Pinton P, Haigis MC, Pandolfi PP. Systemic elevation of PTEN induces a tumor-suppressive metabolic state. Cell 2012; 149:49-62

108. Yang XD, Xiang DX, Yang YY. Role of E3 ubiquitin ligases in insulin resistance. Diabetes Obes Metab 2016; 18:747-754
109. Bonala S, Lokireddy S, McFarlane C, Patnam S, Sharma M, Kambadur R. Myostatin induces insulin resistance via Casitas B-lineage lymphoma b (Cblb)-mediated degradation of insulin receptor substrate 1 (IRS1) protein in response to high calorie diet intake. J Biol Chem 2014; 289:7654-7670
110. Song R, Peng W, Zhang Y, Lv F, Wu HK, Guo J, Cao Y, Pi Y, Zhang X, Jin L, Zhang M, Jiang P, Liu F, Meng S, Zhang X, Jiang P, Cao CM, Xiao RP. Central role of E3 ubiquitin ligase MG53 in insulin resistance and metabolic disorders. Nature 2013; 494:375-379
111. Yi JS, Park JS, Ham YM, Nguyen N, Lee NR, Hong J, Kim BW, Lee H, Lee CS, Jeong BC, Song HK, Cho H, Kim YK, Lee JS, Park KS, Shin H, Choi I, Lee SH, Park WJ, Park SY, Choi CS, Lin P, Karunasiri M, Tan T, Duann P, Zhu H, Ma J, Ko YG. MG53-induced IRS-1 ubiquitination negatively regulates skeletal myogenesis and insulin signalling. Nat Commun 2013; 4:2354
112. Rui L, Yuan M, Frantz D, Shoelson S, White MF. SOCS-1 and SOCS-3 block insulin signaling by ubiquitin-mediated degradation of IRS1 and IRS2. J Biol Chem 2002; 277:42394-42398
113. Shi J, Luo L, Eash J, Ibebunjo C, Glass DJ. The SCF-Fbxo40 complex induces IRS1 ubiquitination in skeletal muscle, limiting IGF1 signaling. Dev Cell 2011; 21:835-847
114. Cheatham B, Volchuk A, Kahn CR, Wang L, Rhodes CJ, Klip A. Insulin-stimulated translocation of GLUT4 glucose transporters requires SNARE-complex proteins. Proc Natl Acad Sci U S A 1996; 93:15169-15173
115. Bouskila M, Hirshman MF, Jensen J, Goodyear LJ, Sakamoto K. Insulin promotes glycogen synthesis in the absence of GSK3 phosphorylation in skeletal muscle. Am J Physiol Endocrinol Metab 2008; 294:E28-35
116. Liu J, Brautigan DL. Insulin-stimulated phosphorylation of the protein phosphatase-1 striated muscle glycogen-targeting subunit and activation of glycogen synthase. J Biol Chem 2000; 275:15940-15947
117. Lawrence JC, Jr., Roach PJ. New insights into the role and mechanism of glycogen synthase activation by insulin. Diabetes 1997; 46:541-547
118. Assimacopoulos-Jeannet F, Brichard S, Rencurel F, Cusin I, Jeanrenaud B. In vivo effects of hyperinsulinemia on lipogenic enzymes and glucose transporter expression in rat liver and adipose tissues. Metabolism 1995; 44:228-233
119. Kim JB, Sarraf P, Wright M, Yao KM, Mueller E, Solanes G, Lowell BB, Spiegelman BM. Nutritional and insulin regulation of fatty acid synthetase and leptin gene expression through ADD1/SREBP1. J Clin Invest 1998; 101:1-9
120. Dimitriadis G, Mitrou P, Lambadiari V, Maratou E, Raptis SA. Insulin effects in muscle and adipose tissue. Diabetes Res Clin Pract 2011; 93 Suppl 1:S52-59
121. Yecies JL, Zhang HH, Menon S, Liu S, Yecies D, Lipovsky AI, Gorgun C, Kwiatkowski DJ, Hotamisligil GS, Lee CH, Manning BD. Akt stimulates hepatic SREBP1c and lipogenesis through parallel mTORC1-dependent and independent pathways. Cell Metab 2011; 14:21-32
122. Li S, Brown MS, Goldstein JL. Bifurcation of insulin signaling pathway in rat liver: mTORC1 required for stimulation of lipogenesis, but not inhibition of gluconeogenesis. Proc Natl Acad Sci U S A 2010; 107:3441-3446

123. Haeusler RA, Kaestner KH, Accili D. FoxOs function synergistically to promote glucose production. J Biol Chem 2010; 285:35245-35248
124. Matsumoto M, Pocai A, Rossetti L, Depinho RA, Accili D. Impaired regulation of hepatic glucose production in mice lacking the forkhead transcription factor Foxo1 in liver. Cell Metab 2007; 6:208-216
125. Li X, Monks B, Ge Q, Birnbaum MJ. Akt/PKB regulates hepatic metabolism by directly inhibiting PGC-1alpha transcription coactivator. Nature 2007; 447:1012-1016
126. Weinstein RS. Glucocorticoid-induced osteoporosis and osteonecrosis. Endocrinol Metab Clin North Am 2012; 41:595-611
127. Biddie SC, Conway-Campbell BL, Lightman SL. Dynamic regulation of glucocorticoid signalling in health and disease. Rheumatology (Oxford) 2012; 51:403-412
128. Kadmiel M, Cidlowski JA. Glucocorticoid receptor signaling in health and disease. Trends Pharmacol Sci 2013; 34:518-530
129. Draper N, Stewart PM. 11beta-hydroxysteroid dehydrogenase and the pre-receptor regulation of corticosteroid hormone action. J Endocrinol 2005; 186:251-271
130. Oakley RH, Cidlowski JA. Cellular processing of the glucocorticoid receptor gene and protein: new mechanisms for generating tissue-specific actions of glucocorticoids. J Biol Chem 2011; 286:3177-3184
131. Meijsing SH, Pufall MA, So AY, Bates DL, Chen L, Yamamoto KR. DNA binding site sequence directs glucocorticoid receptor structure and activity. Science 2009; 324:407-410
132. Meijsing SH. Mechanisms of Glucocorticoid-Regulated Gene Transcription. Adv Exp Med Biol 2015; 872:59-81
133. Surjit M, Ganti KP, Mukherji A, Ye T, Hua G, Metzger D, Li M, Chambon P. Widespread negative response elements mediate direct repression by agonist-liganded glucocorticoid receptor. Cell 2011; 145:224-241
134. Hudson WH, Youn C, Ortlund EA. The structural basis of direct glucocorticoid-mediated transrepression. Nat Struct Mol Biol 2013; 20:53-58
135. Kassel O, Herrlich P. Crosstalk between the glucocorticoid receptor and other transcription factors: molecular aspects. Mol Cell Endocrinol 2007; 275:13-29
136. Song IH, Buttgereit F. Non-genomic glucocorticoid effects to provide the basis for new drug developments. Mol Cell Endocrinol 2006; 246:142-146
137. Whitesell L, Cook P. Stable and specific binding of heat shock protein 90 by geldanamycin disrupts glucocorticoid receptor function in intact cells. Mol Endocrinol 1996; 10:705-712
138. Pratt WB, Morishima Y, Murphy M, Harrell M. Chaperoning of glucocorticoid receptors. Handb Exp Pharmacol 2006:111-138
139. Galliher-Beckley AJ, Williams JG, Cidlowski JA. Ligand-independent phosphorylation of the glucocorticoid receptor integrates cellular stress pathways with nuclear receptor signaling. Mol Cell Biol 2011; 31:4663-4675
140. Wang Z, Frederick J, Garabedian MJ. Deciphering the phosphorylation "code" of the glucocorticoid receptor in vivo. J Biol Chem 2002; 277:26573-26580
141. Chen W, Dang T, Blind RD, Wang Z, Cavasotto CN, Hittelman AB, Rogatsky I, Logan SK, Garabedian MJ. Glucocorticoid receptor phosphorylation differentially affects target gene expression. Mol Endocrinol 2008; 22:1754-1766

142. Barnes PJ. Histone deacetylase-2 and airway disease. Ther Adv Respir Dis 2009; 3:235-243
143. Deroo BJ, Rentsch C, Sampath S, Young J, DeFranco DB, Archer TK. Proteasomal inhibition enhances glucocorticoid receptor transactivation and alters its subnuclear trafficking. Mol Cell Biol 2002; 22:4113-4123
144. Wallace AD, Cidlowski JA. Proteasome-mediated glucocorticoid receptor degradation restricts transcriptional signaling by glucocorticoids. J Biol Chem 2001; 276:42714-42721
145. Tian S, Poukka H, Palvimo JJ, Janne OA. Small ubiquitin-related modifier-1 (SUMO-1) modification of the glucocorticoid receptor. Biochem J 2002; 367:907-911
146. Davies L, Karthikeyan N, Lynch JT, Sial EA, Gkourtsa A, Demonacos C, Krstic-Demonacos M. Cross talk of signaling pathways in the regulation of the glucocorticoid receptor function. Mol Endocrinol 2008; 22:1331-1344
147. Waddell DS, Baehr LM, van den Brandt J, Johnsen SA, Reichardt HM, Furlow JD, Bodine SC. The glucocorticoid receptor and FOXO1 synergistically activate the skeletal muscle atrophy-associated MuRF1 gene. Am J Physiol Endocrinol Metab 2008; 295:E785-797
148. Kuo T, Lew MJ, Mayba O, Harris CA, Speed TP, Wang JC. Genome-wide analysis of glucocorticoid receptor-binding sites in myotubes identifies gene networks modulating insulin signaling. Proc Natl Acad Sci U S A 2012; 109:11160-11165
149. Pantoja C, Huff JT, Yamamoto KR. Glucocorticoid signaling defines a novel commitment state during adipogenesis in vitro. Mol Biol Cell 2008; 19:4032-4041
150. Lee MJ, Pramyothin P, Karastergiou K, Fried SK. Deconstructing the roles of glucocorticoids in adipose tissue biology and the development of central obesity. Biochim Biophys Acta 2014; 1842:473-481
151. Hauner H, Schmid P, Pfeiffer EF. Glucocorticoids and insulin promote the differentiation of human adipocyte precursor cells into fat cells. J Clin Endocrinol Metab 1987; 64:832-835
152. Campbell JE, Peckett AJ, D'Souza A M, Hawke TJ, Riddell MC. Adipogenic and lipolytic effects of chronic glucocorticoid exposure. Am J Physiol Cell Physiol 2011; 300:C198-209
153. Yu CY, Mayba O, Lee JV, Tran J, Harris C, Speed TP, Wang JC. Genome-wide analysis of glucocorticoid receptor binding regions in adipocytes reveal gene network involved in triglyceride homeostasis. PLoS One 2010; 5:e15188
154. Slavin BG, Ong JM, Kern PA. Hormonal regulation of hormone-sensitive lipase activity and mRNA levels in isolated rat adipocytes. J Lipid Res 1994; 35:1535-1541
155. Wang JC, Gray NE, Kuo T, Harris CA. Regulation of triglyceride metabolism by glucocorticoid receptor. Cell Biosci 2012; 2:19
156. Wang Y, Jones Voy B, Urs S, Kim S, Soltani-Bejnood M, Quigley N, Heo YR, Standridge M, Andersen B, Dhar M, Joshi R, Wortman P, Taylor JW, Chun J, Leuze M, Claycombe K, Saxton AM, Moustaid-Moussa N. The human fatty acid synthase gene and de novo lipogenesis are coordinately regulated in human adipose tissue. J Nutr 2004; 134:1032-1038
157. Gathercole LL, Morgan SA, Bujalska IJ, Hauton D, Stewart PM, Tomlinson JW. Regulation of lipogenesis by glucocorticoids and insulin in human adipose tissue. PLoS One 2011; 6:e26223

158. Tomlinson JJ, Boudreau A, Wu D, Abdou Salem H, Carrigan A, Gagnon A, Mears AJ, Sorisky A, Atlas E, Hache RJ. Insulin sensitization of human preadipocytes through glucocorticoid hormone induction of forkhead transcription factors. Mol Endocrinol 2010; 24:104-113
159. Ebbert JO, Jensen MD. Fat depots, free fatty acids, and dyslipidemia. Nutrients 2013; 5:498-508
160. Vegiopoulos A, Herzig S. Glucocorticoids, metabolism and metabolic diseases. Mol Cell Endocrinol 2007; 275:43-61
161. Exton JH. Regulation of gluconeogenesis by glucocorticoids. Monogr Endocrinol 1979; 12:535-546
162. Lemke U, Krones-Herzig A, Berriel Diaz M, Narvekar P, Ziegler A, Vegiopoulos A, Cato AC, Bohl S, Klingmuller U, Screaton RA, Muller-Decker K, Kersten S, Herzig S. The glucocorticoid receptor controls hepatic dyslipidemia through Hes1. Cell Metab 2008; 8:212-223
163. Stalmans W, Laloux M. Glucocorticoids and hepatic glycogen metabolism. Monogr Endocrinol 1979; 12:517-533
164. Margolis RN, Curnow RT. The role of insulin and glucocorticoids in the regulation of hepatic glycogen metabolism: effect of fasting, refeeding, and adrenalectomy. Endocrinology 1983; 113:2113-2119
165. Vanstapel F, Bollen M, de Wulf H, Stalmans W. Induction of hepatic glycogen synthesis by glucocorticoids is not mediated by insulin. Mol Cell Endocrinol 1982; 27:107-114
166. Amatruda JM, Danahy SA, Chang CL. The effects of glucocorticoids on insulin-stimulated lipogenesis in primary cultures of rat hepatocytes. Biochem J 1983; 212:135-141
167. Martin L, Birdsell L, Macdonald N, Reiman T, Clandinin MT, McCargar LJ, Murphy R, Ghosh S, Sawyer MB, Baracos VE. Cancer cachexia in the age of obesity: skeletal muscle depletion is a powerful prognostic factor, independent of body mass index. J Clin Oncol 2013; 31:1539-1547
168. Anker SD, Coats AJ. Cardiac cachexia: a syndrome with impaired survival and immune and neuroendocrine activation. Chest 1999; 115:836-847
169. Marquis K, Debigare R, Lacasse Y, LeBlanc P, Jobin J, Carrier G, Maltais F. Midthigh muscle cross-sectional area is a better predictor of mortality than body mass index in patients with chronic obstructive pulmonary disease. Am J Respir Crit Care Med 2002; 166:809-813
170. Schiaffino S, Dyar KA, Ciciliot S, Blaauw B, Sandri M. Mechanisms regulating skeletal muscle growth and atrophy. FEBS J 2013; 280:4294-4314
171. Evans WJ. Skeletal muscle loss: cachexia, sarcopenia, and inactivity. Am J Clin Nutr 2010; 91:1123S-1127S
172. Gordon BS, Kelleher AR, Kimball SR. Regulation of muscle protein synthesis and the effects of catabolic states. Int J Biochem Cell Biol 2013; 45:2147-2157
173. Wing SS, Goldberg AL. Glucocorticoids activate the ATP-ubiquitin-dependent proteolytic system in skeletal muscle during fasting. Am J Physiol 1993; 264:E668-676
174. Mitch WE, Medina R, Grieber S, May RC, England BK, Price SR, Bailey JL, Goldberg AL. Metabolic acidosis stimulates muscle protein degradation by activating the adenosine triphosphate-dependent pathway involving ubiquitin and proteasomes. J Clin Invest 1994; 93:2127-2133

175. Price SR, Bailey JL, Wang X, Jurkovitz C, England BK, Ding X, Phillips LS, Mitch WE. Muscle wasting in insulinopenic rats results from activation of the ATP-dependent, ubiquitin-proteasome proteolytic pathway by a mechanism including gene transcription. J Clin Invest 1996; 98:1703-1708
176. Goldberg AL. Protein turnover in skeletal muscle. II. Effects of denervation and cortisone on protein catabolism in skeletal muscle. J Biol Chem 1969; 244:3223-3229
177. Scott RC, Schuldiner O, Neufeld TP. Role and regulation of starvation-induced autophagy in the Drosophila fat body. Dev Cell 2004; 7:167-178
178. Latres E, Amini AR, Amini AA, Griffiths J, Martin FJ, Wei Y, Lin HC, Yancopoulos GD, Glass DJ. Insulin-like growth factor-1 (IGF-1) inversely regulates atrophy-induced genes via the phosphatidylinositol 3-kinase/Akt/mammalian target of rapamycin (PI3K/Akt/mTOR) pathway. J Biol Chem 2005; 280:2737-2744
179. Sacheck JM, Ohtsuka A, McLary SC, Goldberg AL. IGF-I stimulates muscle growth by suppressing protein breakdown and expression of atrophy-related ubiquitin ligases, atrogin-1 and MuRF1. Am J Physiol Endocrinol Metab 2004; 287:E591-601
180. Lai KM, Gonzalez M, Poueymirou WT, Kline WO, Na E, Zlotchenko E, Stitt TN, Economides AN, Yancopoulos GD, Glass DJ. Conditional activation of akt in adult skeletal muscle induces rapid hypertrophy. Mol Cell Biol 2004; 24:9295-9304
181. Lecker SH, Jagoe RT, Gilbert A, Gomes M, Baracos V, Bailey J, Price SR, Mitch WE, Goldberg AL. Multiple types of skeletal muscle atrophy involve a common program of changes in gene expression. FASEB J 2004; 18:39-51
182. Bodine SC, Latres E, Baumhueter S, Lai VK, Nunez L, Clarke BA, Poueymirou WT, Panaro FJ, Na E, Dharmarajan K, Pan ZQ, Valenzuela DM, DeChiara TM, Stitt TN, Yancopoulos GD, Glass DJ. Identification of ubiquitin ligases required for skeletal muscle atrophy. Science 2001; 294:1704-1708
183. Gomes MD, Lecker SH, Jagoe RT, Navon A, Goldberg AL. Atrogin-1, a muscle-specific F-box protein highly expressed during muscle atrophy. Proc Natl Acad Sci U S A 2001; 98:14440-14445
184. DeYoung MP, Horak P, Sofer A, Sgroi D, Ellisen LW. Hypoxia regulates TSC1/2-mTOR signaling and tumor suppression through REDD1-mediated 14-3-3 shuttling. Genes Dev 2008; 22:239-251
185. Wang H, Kubica N, Ellisen LW, Jefferson LS, Kimball SR. Dexamethasone represses signaling through the mammalian target of rapamycin in muscle cells by enhancing expression of REDD1. J Biol Chem 2006; 281:39128-39134
186. Draznin B. Molecular mechanisms of insulin resistance: serine phosphorylation of insulin receptor substrate-1 and increased expression of p85alpha: the two sides of a coin. Diabetes 2006; 55:2392-2397
187. Nakao R, Hirasaka K, Goto J, Ishidoh K, Yamada C, Ohno A, Okumura Y, Nonaka I, Yasutomo K, Baldwin KM, Kominami E, Higashibata A, Nagano K, Tanaka K, Yasui N, Mills EM, Takeda S, Nikawa T. Ubiquitin ligase Cbl-b is a negative regulator for insulin-like growth factor 1 signaling during muscle atrophy caused by unloading. Mol Cell Biol 2009; 29:4798-4811
188. Dobs AS, Boccia RV, Croot CC, Gabrail NY, Dalton JT, Hancock ML, Johnston MA, Steiner MS. Effects of enobosarm on muscle wasting and physical function in patients with cancer: a double-blind, randomised controlled phase 2 trial. Lancet Oncol 2013; 14:335-345

189. Garcia JM, Friend J, Allen S. Therapeutic potential of anamorelin, a novel, oral ghrelin mimetic, in patients with cancer-related cachexia: a multicenter, randomized, double-blind, crossover, pilot study. Support Care Cancer 2013; 21:129-137
190. Gielen S, Sandri M, Kozarez I, Kratzsch J, Teupser D, Thiery J, Erbs S, Mangner N, Lenk K, Hambrecht R, Schuler G, Adams V. Exercise training attenuates MuRF-1 expression in the skeletal muscle of patients with chronic heart failure independent of age: the randomized Leipzig Exercise Intervention in Chronic Heart Failure and Aging catabolism study. Circulation 2012; 125:2716-2727
191. Hollriegel R, Beck EB, Linke A, Adams V, Mobius-Winkler S, Mangner N, Sandri M, Gielen S, Gutberlet M, Hambrecht R, Schuler G, Erbs S. Anabolic effects of exercise training in patients with advanced chronic heart failure (NYHA IIIb): impact on ubiquitin-protein ligases expression and skeletal muscle size. Int J Cardiol 2013; 167:975-980
192. Sandri M, Lin J, Handschin C, Yang W, Arany ZP, Lecker SH, Goldberg AL, Spiegelman BM. PGC-1alpha protects skeletal muscle from atrophy by suppressing FoxO3 action and atrophy-specific gene transcription. Proc Natl Acad Sci U S A 2006; 103:16260-16265
193. Vissing K, Rahbek SK, Lamon S, Farup J, Stefanetti RJ, Wallace MA, Vendelbo MH, Russell A. Effect of resistance exercise contraction mode and protein supplementation on members of the STARS signalling pathway. J Physiol 2013; 591:3749-3763
194. Ferrara N, Rinaldi B, Corbi G, Conti V, Stiuso P, Boccuti S, Rengo G, Rossi F, Filippelli A. Exercise training promotes SIRT1 activity in aged rats. Rejuvenation Res 2008; 11:139-150
195. Lynch GS, Ryall JG. Role of beta-adrenoceptor signaling in skeletal muscle: implications for muscle wasting and disease. Physiol Rev 2008; 88:729-767
196. Sinha-Hikim I, Artaza J, Woodhouse L, Gonzalez-Cadavid N, Singh AB, Lee MI, Storer TW, Casaburi R, Shen R, Bhasin S. Testosterone-induced increase in muscle size in healthy young men is associated with muscle fiber hypertrophy. Am J Physiol Endocrinol Metab 2002; 283:E154-164
197. Cohen S, Nathan JA, Goldberg AL. Muscle wasting in disease: molecular mechanisms and promising therapies. Nat Rev Drug Discov 2015; 14:58-74
198. Katzmarzyk PT, Janssen I. The economic costs associated with physical inactivity and obesity in Canada: an update. Can J Appl Physiol 2004; 29:90-115
199. Despres JP, Lemieux I. Abdominal obesity and metabolic syndrome. Nature 2006; 444:881-887
200. Kopelman PG. Obesity as a medical problem. Nature 2000; 404:635-643
201. Horowitz JF, Coppack SW, Paramore D, Cryer PE, Zhao G, Klein S. Effect of short-term fasting on lipid kinetics in lean and obese women. Am J Physiol 1999; 276:E278-284
202. Horowitz JF, Klein S. Whole body and abdominal lipolytic sensitivity to epinephrine is suppressed in upper body obese women. Am J Physiol Endocrinol Metab 2000; 278:E1144-1152
203. Shulman GI. Cellular mechanisms of insulin resistance. J Clin Invest 2000; 106:171-176
204. Wang Y, Sullivan S, Trujillo M, Lee MJ, Schneider SH, Brolin RE, Kang YH, Werber Y, Greenberg AS, Fried SK. Perilipin expression in human adipose tissues: effects of severe obesity, gender, and depot. Obes Res 2003; 11:930-936

205. Hotamisligil GS, Shargill NS, Spiegelman BM. Adipose expression of tumor necrosis factor-alpha: direct role in obesity-linked insulin resistance. Science 1993; 259:87-91
206. Vgontzas AN, Papanicolaou DA, Bixler EO, Kales A, Tyson K, Chrousos GP. Elevation of plasma cytokines in disorders of excessive daytime sleepiness: role of sleep disturbance and obesity. J Clin Endocrinol Metab 1997; 82:1313-1316
207. Fried SK, Bunkin DA, Greenberg AS. Omental and subcutaneous adipose tissues of obese subjects release interleukin-6: depot difference and regulation by glucocorticoid. J Clin Endocrinol Metab 1998; 83:847-850
208. Papatheodorou K, Banach M, Edmonds M, Papanas N, Papazoglou D. Complications of Diabetes. J Diabetes Res 2015; 2015:189525
209. Marchesini G, Brizi M, Bianchi G, Tomassetti S, Bugianesi E, Lenzi M, McCullough AJ, Natale S, Forlani G, Melchionda N. Nonalcoholic fatty liver disease: a feature of the metabolic syndrome. Diabetes 2001; 50:1844-1850
210. Dixon JB, Bhathal PS, O'Brien PE. Nonalcoholic fatty liver disease: predictors of nonalcoholic steatohepatitis and liver fibrosis in the severely obese. Gastroenterology 2001; 121:91-100
211. Farrell GC, Larter CZ. Nonalcoholic fatty liver disease: from steatosis to cirrhosis. Hepatology 2006; 43:S99-S112
212. Van Gaal LF, Mertens IL, De Block CE. Mechanisms linking obesity with cardiovascular disease. Nature 2006; 444:875-880
213. Peeters A, Barendregt JJ, Willekens F, Mackenbach JP, Al Mamun A, Bonneux L, Nedcom tNE, Demography Compression of Morbidity Research G. Obesity in adulthood and its consequences for life expectancy: a life-table analysis. Ann Intern Med 2003; 138:24-32
214. Lau DC, Douketis JD, Morrison KM, Hramiak IM, Sharma AM, Ur E, Obesity Canada Clinical Practice Guidelines Expert P. 2006 Canadian clinical practice guidelines on the management and prevention of obesity in adults and children [summary]. CMAJ 2007; 176:S1-13
215. Douketis JD, Macie C, Thabane L, Williamson DF. Systematic review of long-term weight loss studies in obese adults: clinical significance and applicability to clinical practice. Int J Obes (Lond) 2005; 29:1153-1167
216. Torgerson JS, Hauptman J, Boldrin MN, Sjostrom L. XENical in the prevention of diabetes in obese subjects (XENDOS) study: a randomized study of orlistat as an adjunct to lifestyle changes for the prevention of type 2 diabetes in obese patients. Diabetes Care 2004; 27:155-161
217. Smith SR, Weissman NJ, Anderson CM, Sanchez M, Chuang E, Stubbe S, Bays H, Shanahan WR, Behavioral M, Lorcaserin for O, Obesity Management Study G. Multicenter, placebo-controlled trial of lorcaserin for weight management. N Engl J Med 2010; 363:245-256
218. Pi-Sunyer X, Astrup A, Fujioka K, Greenway F, Halpern A, Krempf M, Lau DC, le Roux CW, Violante Ortiz R, Jensen CB, Wilding JP, Obesity S, Prediabetes NNSG. A Randomized, Controlled Trial of 3.0 mg of Liraglutide in Weight Management. N Engl J Med 2015; 373:11-22
219. Igel LI, Kumar RB, Saunders KH, Aronne LJ. Practical Use of Pharmacotherapy for Obesity. Gastroenterology 2017; 152:1765-1779

220. Douketis JD, Sharma AM. Obesity and cardiovascular disease: pathogenic mechanisms and potential benefits of weight reduction. Semin Vasc Med 2005; 5:25-33
221. Picot J, Jones J, Colquitt JL, Gospodarevskaya E, Loveman E, Baxter L, Clegg AJ. The clinical effectiveness and cost-effectiveness of bariatric (weight loss) surgery for obesity: a systematic review and economic evaluation. Health Technol Assess 2009; 13:1-190, 215-357, iii-iv
222. Ciehanover A, Hod Y, Hershko A. A heat-stable polypeptide component of an ATP-dependent proteolytic system from reticulocytes. Biochem Biophys Res Commun 1978; 81:1100-1105
223. Goldstein G, Scheid M, Hammerling U, Schlesinger DH, Niall HD, Boyse EA. Isolation of a polypeptide that has lymphocyte-differentiating properties and is probably represented universally in living cells. Proc Natl Acad Sci U S A 1975; 72:11-15
224. Schulman BA, Harper JW. Ubiquitin-like protein activation by E1 enzymes: the apex for downstream signalling pathways. Nat Rev Mol Cell Biol 2009; 10:319-331
225. Siepmann TJ, Bohnsack RN, Tokgoz Z, Baboshina OV, Haas AL. Protein interactions within the N-end rule ubiquitin ligation pathway. J Biol Chem 2003; 278:9448-9457
226. Pickart CM, Rose IA. Functional heterogeneity of ubiquitin carrier proteins. J Biol Chem 1985; 260:1573-1581
227. Metzger MB, Hristova VA, Weissman AM. HECT and RING finger families of E3 ubiquitin ligases at a glance. J Cell Sci 2012; 125:531-537
228. Spratt DE, Walden H, Shaw GS. RBR E3 ubiquitin ligases: new structures, new insights, new questions. Biochem J 2014; 458:421-437
229. Rotin D, Kumar S. Physiological functions of the HECT family of ubiquitin ligases. Nat Rev Mol Cell Biol 2009; 10:398-409
230. Kravtsova-Ivantsiv Y, Ciechanover A. Non-canonical ubiquitin-based signals for proteasomal degradation. J Cell Sci 2012; 125:539-548
231. Komander D, Rape M. The ubiquitin code. Annu Rev Biochem 2012; 81:203-229
232. Peng J, Schwartz D, Elias JE, Thoreen CC, Cheng D, Marsischky G, Roelofs J, Finley D, Gygi SP. A proteomics approach to understanding protein ubiquitination. Nat Biotechnol 2003; 21:921-926
233. Xu P, Duong DM, Seyfried NT, Cheng D, Xie Y, Robert J, Rush J, Hochstrasser M, Finley D, Peng J. Quantitative proteomics reveals the function of unconventional ubiquitin chains in proteasomal degradation. Cell 2009; 137:133-145
234. Rock KL, Gramm C, Rothstein L, Clark K, Stein R, Dick L, Hwang D, Goldberg AL. Inhibitors of the proteasome block the degradation of most cell proteins and the generation of peptides presented on MHC class I molecules. Cell 1994; 78:761-771
235. Finley D. Recognition and processing of ubiquitin-protein conjugates by the proteasome. Annu Rev Biochem 2009; 78:477-513
236. Seemuller E, Lupas A, Stock D, Lowe J, Huber R, Baumeister W. Proteasome from Thermoplasma acidophilum: a threonine protease. Science 1995; 268:579-582
237. Lander GC, Estrin E, Matyskiela ME, Bashore C, Nogales E, Martin A. Complete subunit architecture of the proteasome regulatory particle. Nature 2012; 482:186-191
238. Lee MJ, Lee BH, Hanna J, King RW, Finley D. Trimming of ubiquitin chains by proteasome-associated deubiquitinating enzymes. Mol Cell Proteomics 2011; 10:R110 003871
239. Hicke L. Protein regulation by monoubiquitin. Nat Rev Mol Cell Biol 2001; 2:195-201

240. Dammer EB, Na CH, Xu P, Seyfried NT, Duong DM, Cheng D, Gearing M, Rees H, Lah JJ, Levey AI, Rush J, Peng J. Polyubiquitin linkage profiles in three models of proteolytic stress suggest the etiology of Alzheimer disease. J Biol Chem 2011; 286:10457-10465
241. Hofmann RM, Pickart CM. In vitro assembly and recognition of Lys-63 polyubiquitin chains. J Biol Chem 2001; 276:27936-27943
242. Kirisako T, Kamei K, Murata S, Kato M, Fukumoto H, Kanie M, Sano S, Tokunaga F, Tanaka K, Iwai K. A ubiquitin ligase complex assembles linear polyubiquitin chains. EMBO J 2006; 25:4877-4887
243. Hicke L, Dunn R. Regulation of membrane protein transport by ubiquitin and ubiquitin-binding proteins. Annu Rev Cell Dev Biol 2003; 19:141-172
244. Krappmann D, Scheidereit C. A pervasive role of ubiquitin conjugation in activation and termination of IkappaB kinase pathways. EMBO Rep 2005; 6:321-326
245. Silverman N, Maniatis T. NF-kappaB signaling pathways in mammalian and insect innate immunity. Genes Dev 2001; 15:2321-2342
246. Zhou H, Wertz I, O'Rourke K, Ultsch M, Seshagiri S, Eby M, Xiao W, Dixit VM. Bcl10 activates the NF-kappaB pathway through ubiquitination of NEMO. Nature 2004; 427:167-171
247. Hoege C, Pfander B, Moldovan GL, Pyrowolakis G, Jentsch S. RAD6-dependent DNA repair is linked to modification of PCNA by ubiquitin and SUMO. Nature 2002; 419:135-141
248. Al-Hakim A, Escribano-Diaz C, Landry MC, O'Donnell L, Panier S, Szilard RK, Durocher D. The ubiquitous role of ubiquitin in the DNA damage response. DNA Repair (Amst) 2010; 9:1229-1240
249. Dupont S, Mamidi A, Cordenonsi M, Montagner M, Zacchigna L, Adorno M, Martello G, Stinchfield MJ, Soligo S, Morsut L, Inui M, Moro S, Modena N, Argenton F, Newfeld SJ, Piccolo S. FAM/USP9x, a deubiquitinating enzyme essential for TGFbeta signaling, controls Smad4 monoubiquitination. Cell 2009; 136:123-135
250. Winston JT, Strack P, Beer-Romero P, Chu CY, Elledge SJ, Harper JW. The SCFbeta-TRCP-ubiquitin ligase complex associates specifically with phosphorylated destruction motifs in IkappaBalpha and beta-catenin and stimulates IkappaBalpha ubiquitination in vitro. Genes Dev 1999; 13:270-283
251. Terrell J, Shih S, Dunn R, Hicke L. A function for monoubiquitination in the internalization of a G protein-coupled receptor. Mol Cell 1998; 1:193-202
252. Carter S, Bischof O, Dejean A, Vousden KH. C-terminal modifications regulate MDM2 dissociation and nuclear export of p53. Nat Cell Biol 2007; 9:428-435
253. Nijman SM, Luna-Vargas MP, Velds A, Brummelkamp TR, Dirac AM, Sixma TK, Bernards R. A genomic and functional inventory of deubiquitinating enzymes. Cell 2005; 123:773-786
254. Amerik AY, Hochstrasser M. Mechanism and function of deubiquitinating enzymes. Biochim Biophys Acta 2004; 1695:189-207
255. Kimura Y, Tanaka K. Regulatory mechanisms involved in the control of ubiquitin homeostasis. J Biochem 2010; 147:793-798
256. Newton K, Matsumoto ML, Wertz IE, Kirkpatrick DS, Lill JR, Tan J, Dugger D, Gordon N, Sidhu SS, Fellouse FA, Komuves L, French DM, Ferrando RE, Lam C, Compaan D, Yu C, Bosanac I, Hymowitz SG, Kelley RF, Dixit VM. Ubiquitin chain editing revealed by polyubiquitin linkage-specific antibodies. Cell 2008; 134:668-678

257. Nakada S, Tai I, Panier S, Al-Hakim A, Iemura S, Juang YC, O'Donnell L, Kumakubo A, Munro M, Sicheri F, Gingras AC, Natsume T, Suda T, Durocher D. Non-canonical inhibition of DNA damage-dependent ubiquitination by OTUB1. Nature 2010; 466:941-946
258. Durcan TM, Kontogiannea M, Bedard N, Wing SS, Fon EA. Ataxin-3 deubiquitination is coupled to Parkin ubiquitination via E2 ubiquitin-conjugating enzyme. J Biol Chem 2012; 287:531-541
259. Clague MJ, Barsukov I, Coulson JM, Liu H, Rigden DJ, Urbe S. Deubiquitylases from genes to organism. Physiol Rev 2013; 93:1289-1315
260. Zhu Y, Lambert K, Corless C, Copeland NG, Gilbert DJ, Jenkins NA, D'Andrea AD. DUB-2 is a member of a novel family of cytokine-inducible deubiquitinating enzymes. J Biol Chem 1997; 272:51-57
261. Wu N, Zhang C, Bai C, Han YP, Li Q. MiR-4782-3p inhibited non-small cell lung cancer growth via USP14. Cell Physiol Biochem 2014; 33:457-467
262. Coornaert B, Baens M, Heyninck K, Bekaert T, Haegman M, Staal J, Sun L, Chen ZJ, Marynen P, Beyaert R. T cell antigen receptor stimulation induces MALT1 paracaspase-mediated cleavage of the NF-kappaB inhibitor A20. Nat Immunol 2008; 9:263-271
263. Huang TT, Nijman SM, Mirchandani KD, Galardy PJ, Cohn MA, Haas W, Gygi SP, Ploegh HL, Bernards R, D'Andrea AD. Regulation of monoubiquitinated PCNA by DUB autocleavage. Nat Cell Biol 2006; 8:339-347
264. Hu M, Li P, Li M, Li W, Yao T, Wu JW, Gu W, Cohen RE, Shi Y. Crystal structure of a UBP-family deubiquitinating enzyme in isolation and in complex with ubiquitin aldehyde. Cell 2002; 111:1041-1054
265. Lingaraju GM, Bunker RD, Cavadini S, Hess D, Hassiepen U, Renatus M, Fischer ES, Thoma NH. Crystal structure of the human COP9 signalosome. Nature 2014; 512:161-165
266. Meulmeester E, Kunze M, Hsiao HH, Urlaub H, Melchior F. Mechanism and consequences for paralog-specific sumoylation of ubiquitin-specific protease 25. Mol Cell 2008; 30:610-619
267. Hutti JE, Turk BE, Asara JM, Ma A, Cantley LC, Abbott DW. IkappaB kinase beta phosphorylates the K63 deubiquitinase A20 to cause feedback inhibition of the NF-kappaB pathway. Mol Cell Biol 2007; 27:7451-7461
268. Edelmann MJ, Kramer HB, Altun M, Kessler BM. Post-translational modification of the deubiquitinating enzyme otubain 1 modulates active RhoA levels and susceptibility to Yersinia invasion. FEBS J 2010; 277:2515-2530
269. Fernandez-Montalvan A, Bouwmeester T, Joberty G, Mader R, Mahnke M, Pierrat B, Schlaeppi JM, Worpenberg S, Gerhartz B. Biochemical characterization of USP7 reveals post-translational modification sites and structural requirements for substrate processing and subcellular localization. FEBS J 2007; 274:4256-4270
270. Todi SV, Winborn BJ, Scaglione KM, Blount JR, Travis SM, Paulson HL. Ubiquitination directly enhances activity of the deubiquitinating enzyme ataxin-3. EMBO J 2009; 28:372-382
271. Kulathu Y, Garcia FJ, Mevissen TE, Busch M, Arnaudo N, Carroll KS, Barford D, Komander D. Regulation of A20 and other OTU deubiquitinases by reversible oxidation. Nat Commun 2013; 4:1569

272. Cotto-Rios XM, Bekes M, Chapman J, Ueberheide B, Huang TT. Deubiquitinases as a signaling target of oxidative stress. Cell Rep 2012; 2:1475-1484
273. Faesen AC, Dirac AM, Shanmugham A, Ovaa H, Perrakis A, Sixma TK. Mechanism of USP7/HAUSP activation by its C-terminal ubiquitin-like domain and allosteric regulation by GMP-synthetase. Mol Cell 2011; 44:147-159
274. Cohn MA, Kowal P, Yang K, Haas W, Huang TT, Gygi SP, D'Andrea AD. A UAF1-containing multisubunit protein complex regulates the Fanconi anemia pathway. Mol Cell 2007; 28:786-797
275. Sahtoe DD, van Dijk WJ, El Oualid F, Ekkebus R, Ovaa H, Sixma TK. Mechanism of UCH-L5 activation and inhibition by DEUBAD domains in RPN13 and INO80G. Mol Cell 2015; 57:887-900
276. VanderLinden RT, Hemmis CW, Schmitt B, Ndoja A, Whitby FG, Robinson H, Cohen RE, Yao T, Hill CP. Structural basis for the activation and inhibition of the UCH37 deubiquitylase. Mol Cell 2015; 57:901-911
277. Urbe S, Liu H, Hayes SD, Heride C, Rigden DJ, Clague MJ. Systematic survey of deubiquitinase localization identifies USP21 as a regulator of centrosome- and microtubule-associated functions. Mol Biol Cell 2012; 23:1095-1103
278. Combaret L, Adegoke OA, Bedard N, Baracos V, Attaix D, Wing SS. USP19 is a ubiquitin-specific protease regulated in rat skeletal muscle during catabolic states. Am J Physiol Endocrinol Metab 2005; 288:E693-700
279. Hu M, Li P, Song L, Jeffrey PD, Chenova TA, Wilkinson KD, Cohen RE, Shi Y. Structure and mechanisms of the proteasome-associated deubiquitinating enzyme USP14. EMBO J 2005; 24:3747-3756
280. Avvakumov GV, Walker JR, Xue S, Finerty PJ, Jr., Mackenzie F, Newman EM, Dhe-Paganon S. Amino-terminal dimerization, NRDP1-rhodanese interaction, and inhibited catalytic domain conformation of the ubiquitin-specific protease 8 (USP8). J Biol Chem 2006; 281:38061-38070
281. Renatus M, Parrado SG, D'Arcy A, Eidhoff U, Gerhartz B, Hassiepen U, Pierrat B, Riedl R, Vinzenz D, Worpenberg S, Kroemer M. Structural basis of ubiquitin recognition by the deubiquitinating protease USP2. Structure 2006; 14:1293-1302
282. Ye Y, Akutsu M, Reyes-Turcu F, Enchev RI, Wilkinson KD, Komander D. Polyubiquitin binding and cross-reactivity in the USP domain deubiquitinase USP21. EMBO Rep 2011; 12:350-357
283. Luna-Vargas MP, Faesen AC, van Dijk WJ, Rape M, Fish A, Sixma TK. Ubiquitin-specific protease 4 is inhibited by its ubiquitin-like domain. EMBO Rep 2011; 12:365-372
284. Lee JG, Takahama S, Zhang G, Tomarev SI, Ye Y. Unconventional secretion of misfolded proteins promotes adaptation to proteasome dysfunction in mammalian cells. Nat Cell Biol 2016; 18:765-776
285. Velasco K, Zhao B, Callegari S, Altun M, Liu H, Hassink G, Masucci MG, Lindsten K. An N-terminal SIAH-interacting motif regulates the stability of the ubiquitin specific protease (USP)-19. Biochem Biophys Res Commun 2013; 433:390-395
286. Faesen AC, Luna-Vargas MP, Sixma TK. The role of UBL domains in ubiquitin-specific proteases. Biochem Soc Trans 2012; 40:539-545

287. Scheufler C, Brinker A, Bourenkov G, Pegoraro S, Moroder L, Bartunik H, Hartl FU, Moarefi I. Structure of TPR domain-peptide complexes: critical elements in the assembly of the Hsp70-Hsp90 multichaperone machine. Cell 2000; 101:199-210
288. Freeman BC, Myers MP, Schumacher R, Morimoto RI. Identification of a regulatory motif in Hsp70 that affects ATPase activity, substrate binding and interaction with HDJ-1. EMBO J 1995; 14:2281-2292
289. Ogawa M, Kariya Y, Kitakaze T, Yamaji R, Harada N, Sakamoto T, Hosotani K, Nakano Y, Inui H. The preventive effect of beta-carotene on denervation-induced soleus muscle atrophy in mice. Br J Nutr 2013; 109:1349-1358
290. Liu Q, Xu WG, Luo Y, Han FF, Yao XH, Yang TY, Zhang Y, Pi WF, Guo XJ. Cigarette smoke-induced skeletal muscle atrophy is associated with up-regulation of USP-19 via p38 and ERK MAPKs. J Cell Biochem 2011; 112:2307-2316
291. Hassink GC, Zhao B, Sompallae R, Altun M, Gastaldello S, Zinin NV, Masucci MG, Lindsten K. The ER-resident ubiquitin-specific protease 19 participates in the UPR and rescues ERAD substrates. EMBO Rep 2009; 10:755-761
292. Nakamura N, Harada K, Kato M, Hirose S. Ubiquitin-specific protease 19 regulates the stability of the E3 ubiquitin ligase MARCH6. Exp Cell Res 2014; 328:207-216
293. Lee JG, Kim W, Gygi S, Ye Y. Characterization of the deubiquitinating activity of USP19 and its role in endoplasmic reticulum-associated degradation. J Biol Chem 2014; 289:3510-3517
294. Wiles B, Miao M, Coyne E, Larose L, Cybulsky AV, Wing SS. USP19 deubiquitinating enzyme inhibits muscle cell differentiation by suppressing unfolded-protein response signaling. Mol Biol Cell 2015; 26:913-923
295. Lu Y, Adegoke OA, Nepveu A, Nakayama KI, Bedard N, Cheng D, Peng J, Wing SS. USP19 deubiquitinating enzyme supports cell proliferation by stabilizing KPC1, a ubiquitin ligase for p27Kip1. Mol Cell Biol 2009; 29:547-558
296. Wu M, Tu HQ, Chang Y, Tan B, Wang G, Zhou J, Wang L, Mu R, Zhang WN. USP19 deubiquitinates HDAC1/2 to regulate DNA damage repair and control chromosomal stability. Oncotarget 2017; 8:2197-2208
297. Mei Y, Hahn AA, Hu S, Yang X. The USP19 deubiquitinase regulates the stability of c-IAP1 and c-IAP2. J Biol Chem 2011; 286:35380-35387
298. Harada K, Kato M, Nakamura N. USP19-Mediated Deubiquitination Facilitates the Stabilization of HRD1 Ubiquitin Ligase. Int J Mol Sci 2016; 17
299. Jin S, Tian S, Chen Y, Zhang C, Xie W, Xia X, Cui J, Wang RF. USP19 modulates autophagy and antiviral immune responses by deubiquitinating Beclin-1. EMBO J 2016; 35:866-880
300. He WT, Zheng XM, Zhang YH, Gao YG, Song AX, van der Goot FG, Hu HY. Cytoplasmic Ubiquitin-Specific Protease 19 (USP19) Modulates Aggregation of Polyglutamine-Expanded Ataxin-3 and Huntingtin through the HSP90 Chaperone. PLoS One 2016; 11:e0147515
301. Filatova EV, Shadrina MI, Alieva A, Kolacheva AA, Slominsky PA, Ugrumov MV. Expression analysis of genes of ubiquitin-proteasome protein degradation system in MPTP-induced mice models of early stages of Parkinson's disease. Dokl Biochem Biophys 2014; 456:116-118
302. Jagoe RT, Lecker SH, Gomes M, Goldberg AL. Patterns of gene expression in atrophying skeletal muscles: response to food deprivation. FASEB J 2002; 16:1697-1712

303. Sundaram P, Pang Z, Miao M, Yu L, Wing SS. USP19-deubiquitinating enzyme regulates levels of major myofibrillar proteins in L6 muscle cells. Am J Physiol Endocrinol Metab 2009; 297:E1283-1290
304. Ogawa M, Kitakaze T, Harada N, Yamaji R. Female-specific regulation of skeletal muscle mass by USP19 in young mice. J Endocrinol 2015; 225:135-145
305. Bedard N, Jammoul S, Moore T, Wykes L, Hallauer PL, Hastings KE, Stretch C, Baracos V, Chevalier S, Plourde M, Coyne E, Wing SS. Inactivation of the ubiquitin-specific protease 19 deubiquitinating enzyme protects against muscle wasting. FASEB J 2015; 29:3889-3898
306. Pettersson US, Walden TB, Carlsson PO, Jansson L, Phillipson M. Female mice are protected against high-fat diet induced metabolic syndrome and increase the regulatory T cell population in adipose tissue. PLoS One 2012; 7:e46057
307. Welle S, Bhatt K, Pinkert CA. Myofibrillar protein synthesis in myostatin-deficient mice. Am J Physiol Endocrinol Metab 2006; 290:E409-415
308. Stretch C, Khan S, Asgarian N, Eisner R, Vaisipour S, Damaraju S, Graham K, Bathe OF, Steed H, Greiner R, Baracos VE. Effects of sample size on differential gene expression, rank order and prediction accuracy of a gene signature. PLoS One 2013; 8:e65380
309. Kuo T, Harris CA, Wang JC. Metabolic functions of glucocorticoid receptor in skeletal muscle. Mol Cell Endocrinol 2013; 380:79-88
310. Lin HV, Accili D. Hormonal regulation of hepatic glucose production in health and disease. Cell Metab 2011; 14:9-19
311. Bodine SC, Furlow JD. Glucocorticoids and Skeletal Muscle. Adv Exp Med Biol 2015; 872:145-176
312. Schakman O, Kalista S, Barbe C, Loumaye A, Thissen JP. Glucocorticoid-induced skeletal muscle atrophy. Int J Biochem Cell Biol 2013; 45:2163-2172
313. Braun TP, Zhu X, Szumowski M, Scott GD, Grossberg AJ, Levasseur PR, Graham K, Khan S, Damaraju S, Colmers WF, Baracos VE, Marks DL. Central nervous system inflammation induces muscle atrophy via activation of the hypothalamic-pituitary-adrenal axis. J Exp Med 2011; 208:2449-2463
314. May RC, Kelly RA, Mitch WE. Metabolic acidosis stimulates protein degradation in rat muscle by a glucocorticoid-dependent mechanism. J Clin Invest 1986; 77:614-621
315. Hu Z, Wang H, Lee IH, Du J, Mitch WE. Endogenous glucocorticoids and impaired insulin signaling are both required to stimulate muscle wasting under pathophysiological conditions in mice. J Clin Invest 2009; 119:3059-3069
316. Shah OJ, Kimball SR, Jefferson LS. Acute attenuation of translation initiation and protein synthesis by glucocorticoids in skeletal muscle. Am J Physiol Endocrinol Metab 2000; 278:E76-82
317. Cuevas BD, Lu Y, Mao M, Zhang J, LaPushin R, Siminovitch K, Mills GB. Tyrosine phosphorylation of p85 relieves its inhibitory activity on phosphatidylinositol 3-kinase. J Biol Chem 2001; 276:27455-27461
318. Landi F, Calvani R, Tosato M, Martone AM, Ortolani E, Savera G, Sisto A, Marzetti E. Anorexia of Aging: Risk Factors, Consequences, and Potential Treatments. Nutrients 2016; 8:69
319. Tchernof A, Despres JP. Pathophysiology of human visceral obesity: an update. Physiol Rev 2013; 93:359-404

320. Lim KH, Choi JH, Park JH, Cho HJ, Park JJ, Lee EJ, Li L, Choi YK, Baek KH. Ubiquitin specific protease 19 involved in transcriptional repression of retinoic acid receptor by stabilizing CORO2A. Oncotarget 2016; 7:34759-34772
321. Lee KW, Cho JG, Kim CM, Kang AY, Kim M, Ahn BY, Chung SS, Lim KH, Baek KH, Sung JH, Park KS, Park SG. Herpesvirus-associated ubiquitin-specific protease (HAUSP) modulates peroxisome proliferator-activated receptor gamma (PPARgamma) stability through its deubiquitinating activity. J Biol Chem 2013; 288:32886-32896
322. Gao Y, Koppen A, Rakhshandehroo M, Tasdelen I, van de Graaf SF, van Loosdregt J, van Beekum O, Hamers N, van Leenen D, Berkers CR, Berger R, Holstege FC, Coffer PJ, Brenkman AB, Ovaa H, Kalkhoven E. Early adipogenesis is regulated through USP7-mediated deubiquitination of the histone acetyltransferase TIP60. Nat Commun 2013; 4:2656
323. Suzuki M, Setsuie R, Wada K. Ubiquitin carboxyl-terminal hydrolase l3 promotes insulin signaling and adipogenesis. Endocrinology 2009; 150:5230-5239
324. Preis SR, Massaro JM, Robins SJ, Hoffmann U, Vasan RS, Irlbeck T, Meigs JB, Sutherland P, D'Agostino RB, Sr., O'Donnell CJ, Fox CS. Abdominal subcutaneous and visceral adipose tissue and insulin resistance in the Framingham heart study. Obesity (Silver Spring) 2010; 18:2191-2198
325. Wajchenberg BL, Giannella-Neto D, da Silva ME, Santos RF. Depot-specific hormonal characteristics of subcutaneous and visceral adipose tissue and their relation to the metabolic syndrome. Horm Metab Res 2002; 34:616-621
326. Rubin CS, Hirsch A, Fung C, Rosen OM. Development of hormone receptors and hormonal responsiveness in vitro. Insulin receptors and insulin sensitivity in the preadipocyte and adipocyte forms of 3T3-L1 cells. J Biol Chem 1978; 253:7570-7578
327. Balkau B, Mhamdi L, Oppert JM, Nolan J, Golay A, Porcellati F, Laakso M, Ferrannini E, Group E-RS. Physical activity and insulin sensitivity: the RISC study. Diabetes 2008; 57:2613-2618
328. Taipale M, Tucker G, Peng J, Krykbaeva I, Lin ZY, Larsen B, Choi H, Berger B, Gingras AC, Lindquist S. A quantitative chaperone interaction network reveals the architecture of cellular protein homeostasis pathways. Cell 2014; 158:434-448
329. Altun M, Zhao B, Velasco K, Liu H, Hassink G, Paschke J, Pereira T, Lindsten K. Ubiquitin-specific protease 19 (USP19) regulates hypoxia-inducible factor 1alpha (HIF-1alpha) during hypoxia. J Biol Chem 2012; 287:1962-1969
330. Ali MM, Roe SM, Vaughan CK, Meyer P, Panaretou B, Piper PW, Prodromou C, Pearl LH. Crystal structure of an Hsp90-nucleotide-p23/Sba1 closed chaperone complex. Nature 2006; 440:1013-1017
331. Zhang M, Kadota Y, Prodromou C, Shirasu K, Pearl LH. Structural basis for assembly of Hsp90-Sgt1-CHORD protein complexes: implications for chaperoning of NLR innate immunity receptors. Mol Cell 2010; 39:269-281
332. Ciciliot S, Rossi AC, Dyar KA, Blaauw B, Schiaffino S. Muscle type and fiber type specificity in muscle wasting. Int J Biochem Cell Biol 2013; 45:2191-2199
333. Richardson HB. The respiratory quotient. Physiological Reviews 1929; 9:61-125
334. Townsend KL, Tseng YH. Brown fat fuel utilization and thermogenesis. Trends Endocrinol Metab 2014; 25:168-177
335. Kiefer FW, Neschen S, Pfau B, Legerer B, Neuhofer A, Kahle M, Hrabe de Angelis M, Schlederer M, Mair M, Kenner L, Plutzky J, Zeyda M, Stulnig TM. Osteopontin

deficiency protects against obesity-induced hepatic steatosis and attenuates glucose production in mice. Diabetologia 2011; 54:2132-2142
336. Liu S, Liu Q, Sun S, Jiang Q, Peng J, Shen Z. The application of 2-NBDG as a fluorescent tracer for assessing hepatic glucose production in mice during hyperinsulinemic euglycemic clamp. Acta Pharmaceutica Sinica B 2012; 2:403-410
337. DeFronzo RA, Tobin JD, Andres R. Glucose clamp technique: a method for quantifying insulin secretion and resistance. Am J Physiol 1979; 237:E214-223
338. Liu HY, Collins QF, Xiong Y, Moukdar F, Lupo EG, Jr., Liu Z, Cao W. Prolonged treatment of primary hepatocytes with oleate induces insulin resistance through p38 mitogen-activated protein kinase. J Biol Chem 2007; 282:14205-14212
339. Yamamoto N, Ueda M, Sato T, Kawasaki K, Sawada K, Kawabata K, Ashida H. Measurement of glucose uptake in cultured cells. Curr Protoc Pharmacol 2011; Chapter 12:Unit 12 14 11-22
340. Xu X, Keshwani M, Meyer K, Sarikas A, Taylor S, Pan ZQ. Identification of the degradation determinants of insulin receptor substrate 1 for signaling cullin-RING E3 ubiquitin ligase 7-mediated ubiquitination. J Biol Chem 2012; 287:40758-40766
341. Webster JC, Jewell CM, Bodwell JE, Munck A, Sar M, Cidlowski JA. Mouse glucocorticoid receptor phosphorylation status influences multiple functions of the receptor protein. J Biol Chem 1997; 272:9287-9293
342. Ito K, Yamamura S, Essilfie-Quaye S, Cosio B, Ito M, Barnes PJ, Adcock IM. Histone deacetylase 2-mediated deacetylation of the glucocorticoid receptor enables NF-kappaB suppression. J Exp Med 2006; 203:7-13
343. Le Drean Y, Mincheneau N, Le Goff P, Michel D. Potentiation of glucocorticoid receptor transcriptional activity by sumoylation. Endocrinology 2002; 143:3482-3489
344. Druker J, Liberman AC, Antunica-Noguerol M, Gerez J, Paez-Pereda M, Rein T, Iniguez-Lluhi JA, Holsboer F, Arzt E. RSUME enhances glucocorticoid receptor SUMOylation and transcriptional activity. Mol Cell Biol 2013; 33:2116-2127
345. Wang X, DeFranco DB. Alternative effects of the ubiquitin-proteasome pathway on glucocorticoid receptor down-regulation and transactivation are mediated by CHIP, an E3 ligase. Mol Endocrinol 2005; 19:1474-1482
346. Graca FA, Goncalves DA, Silveira WA, Lira EC, Chaves VE, Zanon NM, Garofalo MA, Kettelhut IC, Navegantes LC. Epinephrine depletion exacerbates the fasting-induced protein breakdown in fast-twitch skeletal muscles. Am J Physiol Endocrinol Metab 2013; 305:E1483-1494
347. John K, Marino JS, Sanchez ER, Hinds TD, Jr. The glucocorticoid receptor: cause of or cure for obesity? Am J Physiol Endocrinol Metab 2016; 310:E249-257
348. Ehrlich ES, Wang T, Luo K, Xiao Z, Niewiadomska AM, Martinez T, Xu W, Neckers L, Yu XF. Regulation of Hsp90 client proteins by a Cullin5-RING E3 ubiquitin ligase. Proc Natl Acad Sci U S A 2009; 106:20330-20335
349. Dickey CA, Kamal A, Lundgren K, Klosak N, Bailey RM, Dunmore J, Ash P, Shoraka S, Zlatkovic J, Eckman CB, Patterson C, Dickson DW, Nahman NS, Jr., Hutton M, Burrows F, Petrucelli L. The high-affinity HSP90-CHIP complex recognizes and selectively degrades phosphorylated tau client proteins. J Clin Invest 2007; 117:648-658
350. Connell P, Ballinger CA, Jiang J, Wu Y, Thompson LJ, Hohfeld J, Patterson C. The co-chaperone CHIP regulates protein triage decisions mediated by heat-shock proteins. Nat Cell Biol 2001; 3:93-96

351. Taipale M, Krykbaeva I, Koeva M, Kayatekin C, Westover KD, Karras GI, Lindquist S. Quantitative analysis of HSP90-client interactions reveals principles of substrate recognition. Cell 2012; 150:987-1001
352. He WT, Xue W, Gao YG, Hong JY, Yue HW, Jiang LL, Hu HY. HSP90 recognizes the N-terminus of huntingtin involved in regulation of huntingtin aggregation by USP19. Sci Rep 2017; 7:14797
353. Wang Z, Li L, Zhao H, Peng S, Zuo Z. Chronic high fat diet induces cardiac hypertrophy and fibrosis in mice. Metabolism 2015; 64:917-925
354. Walters BJ, Hallengren JJ, Theile CS, Ploegh HL, Wilson SM, Dobrunz LE. A catalytic independent function of the deubiquitinating enzyme USP14 regulates hippocampal synaptic short-term plasticity and vesicle number. J Physiol 2014; 592:571-586
355. Hanna J, Hathaway NA, Tone Y, Crosas B, Elsasser S, Kirkpatrick DS, Leggett DS, Gygi SP, King RW, Finley D. Deubiquitinating enzyme Ubp6 functions noncatalytically to delay proteasomal degradation. Cell 2006; 127:99-111